UC San Diego

UC San Diego Electronic Theses and Dissertations

Title

A Desmosomal Protein Interaction Screen Uncovers a Novel Mechanism Underlying Cardiac Rhythm Disorders

Permalink

https://escholarship.org/uc/item/6jm2q2jn

Author

Pellman, Jason

Publication Date

2017

Peer reviewed|Thesis/dissertation

eScholarship.org Powered by the California Digital Library
University of California

UNIVERSITY OF CALIFORNIA, SAN DIEGO

A Desmosomal Protein Interaction Screen Uncovers a Novel Mechanism Underlying Cardiac Rhythm Disorders

A dissertation submitted in partial satisfaction of the requirements for the degree Doctor of Philosophy

in

Biomedical Sciences

by

Jason Pellman

Committee in Charge:

Professor Farah Sheikh, Chair
Professor Robert Ross, Co-Chair
Professor Ju Chen
Professor Asa Gustafsson
Professor Hemal Patel

2017

The Dissertation of Jason Pellman is approved, and it is acceptable in quality and form for publication on microfilm and electronically:

_____

_____

_____

_____

Co-Chair

_____

Chair

University of California, San Diego

2017

DEDICATION

To my husband, who knows how to be present regardless of the distance; to my family, who remind me of the virtues of food and sleep; and to my friends, who weather my complaints and radio silence with equal ease. I dedicate this dissertation to my unwavering supporters, without whom nothing would be possible.

TABLE OF CONTENTS

Signature Page iii

Dedication iv

Table of Contents v

List of Abbreviations ix

List of Figures xiii

List of Tables xv

Acknowledgements xvi

Vita xvii

Abstract of the Dissertation xviii

Chapter 1 Introduction 1

1.1 Genetic-based heart disease 2

1.2 Arrhythmogenic Right Ventricular Cardiomyopathy (ARVC) 3

1.2.1 Clinical features of ARVC 3

1.2.2 Genetics of ARVC 4

1.3 The Cardiac Desmosome 11

1.3.1 The cardiac intercalated disc 11

1.3.2 Mouse models of ARVC: Insight into Mechanisms 14

1.4 Protein Degradation Mechanisms at the ICD 23

1.4.1 Protein degradation pathways in the heart 23

1.4.2 Protein degradation plays an important role in cardiac disease 25

1.4.3 Compartmentalization of protein degradation in cardiac muscle 28

1.4.4 ICD as a site of protein degradation that may have importance in cardiac disease 29

1.5 Rationale, Hypothesis, and Specific Aims 32

Chapter 2 Materials and Methods 37

2.1 Yeast-2-hybrid 38
2.2 Protein expression analysis 38
2.2.1 Western blot 38
2.2.2 Immunostaining 39
2.3 Mouse Models 40
2.4 Generation of hiPSC-derived cardiomyocytes 40
2.5 *In vitro* knockout of SNAP29 41
2.6 *In vitro* contractility and electrophysiology measurement 42
2.7 *In vitro* autophagic flux measurement 43
2.8 Cardiac physiology measurement 43
2.8.1 Echocardiography 43
2.8.2 Surface electrocardiography 43
2.8.3 Telemetry ECG 44
2.8.4 Ventricular tachycardia induction 45
2.9 Cardiac histological analysis 46
2.10 Ultrastructural Analysis 46
2.11 Statistical analysis 46
Chapter 3 Discovery of SNAP29 as a Novel Desmosomal Protein in the Heart 48
3.1 SNAP29 is a novel DSP interacting protein 49
3.2 SNAP29 expression is reduced in DSP deficient models 49
3.2.1 SNAP29 expression is reduced in a desmoplakin-deficient mouse model 50
3.2.2 SNAP29 expression is reduced in ARVC hiPSC derived cardiomyocytes 50
Chapter 4 The Effects of Cardiomyocyte-Specific Loss of SNAP29 in Mouse in vivo 55
4.1 Cardiac Characterization of a Cardiac-Specific SNAP29 Knockout (SNAP29-cKO) Mouse 56
4.1.1 SNAP29 expression is reduced in adult SNAP29-cKO mouse hearts 56
4.1.2 SNAP29-cKO mice exhibit baseline and inducible ventricular arrhythmias 56

4.1.3 SNAP29-cKO mice exhibit lipid accumulation in right ventricle 57

4.1.4 Cardiac morphology, fibrosis, and function are not affected by cardiomyocyte loss of SNAP29 57

4.1.5 SNAP29-cKO mice have selectively reduced desmosomal and gap junction protein levels 58

4.2 Protein Degradation Defects in SNAP29-cKO Heart 58

4.2.1 Markers of autophagy accumulate in SNAP29-cKO hearts 58

4.2.2 Characterization of protein degradation in a model of ARVC 59

4.2.3 Characterization of heart and skin disease-associated DSP mutations 59

Chapter 5 Loss of SNAP29 in Neonatal Mouse Cardiomyocytes *in vitro* 69

5.1 Characterization of Cardiomyocyte Function following loss of SNAP29 70

5.1.1 Desmosomal and gap junction proteins are specifically reduced in SNAP29 KO CMs 70

5.1.2 SNAP29 knockout CMs exhibit baseline arrhythmias 70

5.1.3 Autophagic flux is maintained in SNAP29 KO CMs 71

5.1.4 Autophagy inhibition is sufficient to reverse desmosomal protein loss in SNAP29 KO CMs 71

Chapter 6 The Cardiac Features of a SNAP29-Null Mouse Model of CEDNIK Syndrome 77

6.1 Cardiac Characterization of Global Loss of SNAP29 *in vivo* 78

6.1.1 SNAP29 expression is lost in SNAP29 global knockout (SNAP29-gKO) hearts 78

6.1.2 SNAP29-gKO mice exhibit perinatal lethality, growth retardation, and skin peeling 78

6.1.3 SNAP29-gKO mouse hearts have normal morphology 78

6.1.4 Cardiomyocytes from SNAP29-gKO mouse hearts exhibit arrhythmias in vitro 79

6.1.5 Desmosomal proteins are specifically reduced in SNAP29-gKO hearts 79

6.1.6 Markers of autophagy accumulate in SNAP29-gKO hearts 80

Chapter 7 Discussion of the Dissertation 86

7.1 SNAP29 is a novel desmosomal interacting protein 87

7.2 SNAP29 is a negative regulator of autophagy 87

7.3 Desmosomal proteins are targeted by SNAP29-mediated autophagy 88

7.4 SNAP29-mediated autophagy protects cardiomyocytes from arrhythmias 90

7.5 SNAP29-mediated autophagy is required for cardiomyocyte lipid droplet homeostasis 91

7.6 SNAP29-mediated autophagy defects may underlie a subset of early ARVC disease features 92

7.7 Cardiac desmosomal and autophagy defects underlie a SNAP29-deficient mouse model of CEDNIK syndrome 93

7.8 Conclusions 96

7.9 Future Studies 96

References 100

LIST OF ABBREVIATIONS

αMHC	α myosin heavy chain
AAV	Adeno-associated Virus
ALFY	Autophagy Linked FYVE Protein)
ANOVA	Analysis of Variance
ARVC	Arrhythmogenic Right Ventricular Cardiomyopathy
ATG	Autophagy Protein
ATP	Adenosine Triphosphate
β5T1A	β5 proteasome subunit
BAmp	Beating Amplitude
BP	Beating Period
BR	Beating Rate
c-Cbl	Casitas b-Lineage Lymphoma
C-MSC	Cardiac Mesenchymal Stem Cells
Ca2+	Calcium Ion
CAR	Coxsackievirus and Adenovirus Receptor
CARP	Cardiac Ankyrin Repeat Protein
cDNA	Complimentary Deoxyribonucleic Acid
CEDNIK	Cerebral Dysgenesis, Neuropathy, Ichthyosis, and Keratoderma
CI	Cell Index
CPC	Cardiomyocyte Progenitor Cell
CPVT	Catecholaminergic Polymorphic Ventricular Tachycardia
CQ	Chloroquine
CTNNA3	α-catenin
Cx	Connexin

DCM	Dilated Cardiomyopathy
DES	Desmin
DN-RhoK	Dominant Negative Rho Kinase
DSC2	Desmocollin 2
DSG2	Desmoglein 2
DSP	Desmoplakin
DSP-cKO	DSP Conditional Knockout
EC	Extracellular
ECG	Electrocardiogram
ECL	Enhanced Chemiluminescence Substrate
EYFP	Enhanced Yellow Fluorescent Protein
FAJ	Fascia Adherens Junction
FAK	Focal Adhesion Kinase
FHL2	Four and a Half Lim Domain 2
FP	Field Potential
FPAmp	Field Potential Spike Amplitude
FPD	Field Potential Duration
GAPDH	Glyceraldehyde 3-Phosphate Dehydrogenase
GSK3β	Glycogen Synthase Kinase 3 β
GTP	Guanosine Triphosphate
HCM	Hypertrophic Cardiomyopathy
hiPSC	Human Induced Pluripotent Stem Cells
iASPP	Inhibitor of Apoptosis-Stimulating Protein of p53
ICD	Intercalated Disc
IMP	Impedance

JUP	Plakoglobin
Kir6.2	Inward Rectifying Potassium Channel Subunit 6.2
LAMP2	Lysosome-associated Membrane Glycoprotein 2
LATS	Large Tumor Suppressor Kinases
LC3	Microtubule-associated Protein 1A/1B-Light Chain 3
LINC	Linker of Nucleoskeleton and Cytoskeleton
LMNA	Lamin A
Mef2C	Myocyte-specific Enhancer Factor 2C
mER	Mutant Murine Estrogen Receptor
MLC2v	Myosin Light Chain 2 Ventricular Isoform
MURF	Muscle Ring Finger
NaCl	Sodium Chloride
NaV1.5	Sodium Voltage-Gated Channel 1.5
NBR1	Neighbor to Brca1
NCAD	N-Cadherin
p62	Sequestome-1
PA28α	Proteasome Activator 28 α
PCR	Polymerase Chain reaction
PKP2	Plakophilin 2
PLN	Phospholamban
PPARγ	Proliferator-Activated Receptor γ
RCM	Restrictive Cardiomyopathy
RYR2	Ryanodine Receptor 2
Sca1	Stem cells antigen-1
SCNA5	Sodium Voltage-Gated Channel α Subunit 5

SEM	Standard Error of the Mean
siRNA	Small Interfering Ribonucleic Acid
SM22α	Smooth Muscle Protein 22 α
SNAP	Synaptosomal Associated Protein
SNAP29-cKO	SNAP29 Conditional Knockout
SNAP29-gKO	SNAP29 Global Knockout
SNARE	Synaptosomal Associated Membrane Protein Receptor
STX	Syntaxin
SUR2A	Sulfonylurea Receptor 2A
TAC	Transaortic Constriction
TFGβ3	Transforming Growth Factor β 3
TMEM43	Transmembrane protein 43
TTN	Titin
UPS	Ubiquitin-Proteasome System
UTR	Untranslated Region
VAMP	Vesicle Associated Membrane Protein
VT	Ventricular Tachycardia
WWP1	WW Domain Containing E3 Ubiquitin Ligase 1
XMLC2	*Xenopus* Myosin Light Chain 2
ZO-1	Zonula Occludens 1

LIST OF FIGURES

Figure 1. Diagram of cardiac intercalated disc proteins and complexes 34

Figure 2. Identification of the novel cardiac desmosomal interacting protein SNAP29 in a yeast-2-hybrid screen using DSP as bait..... 52

Figure 3. SNAP29 colocalizes with DSP at the ICD in adult mouse and human hearts..... 53

Figure 4. SNAP29 expression is reduced in a DSP-deficient mouse model and a hiPSC-derived cardiomyocyte model 54

Figure 5. Generation, expression, and survival of a novel cardiac specific SNAP29 knockout (SNAP29-cKO) mouse line 61

Figure 6. Telemetry electrocardiography analysis of adult SNAP29-cKO mice 62

Figure 7. Lipid droplet accumulation in SNAP29-cKO hearts..... 63

Figure 8. Cardiac morphology, fibrosis, and function of SNAP29-cKO mice..... 64

Figure 9. Expression levels of ICD proteins in SNAP29-cKO mouse hearts..... 65

Figure 10. Autophagy defects in SNAP29-cKO mouse hearts 66

Figure 11. Autophagy markers are elevated in DSP-cKO mouse hearts 67

Figure 12. Disease-associated DSP mutations disrupt their interaction with SNAP29..... 68

Figure 13. Altered expression of ICD and autophagy proteins in SNAP29-deficient neonatal mouse cardiomyocytes..... 73

Figure 14. Electrophysiological function in SNAP29-deficient neonatal mouse cardiomyocytes..... 74

Figure 15. Elevated autophagy in SNAP29-deficient neonatal mouse cardiomyocytes..... 75

Figure 16. Effects of autophagy inhibition on ICD protein expression in SNAP29-deficient neonatal mouse cardiomyocytes 76

Figure 17. SNAP29 is ablated in global SNAP29 knockout (SNAP29-gKO) neonatal mice..... 81

Figure 18. SNAP29-gKO mice exhibit perinatal lethality, growth retardation, and skin peeling without changes in cardiac morphology..... 82

Figure 19. Electrophysiological function in SNAP29-gKO cardiomyocytes 83

Figure 20. Expression levels of ICD proteins in SNAP29-gKO mouse hearts 84

Figure 21. Autophagy defects in SNAP29-gKO mouse hearts 85

LIST OF TABLES

Table 1. Knockout Mouse Models of ARVC 35

Table 2. Knockin and Transgenic Models of ARVC 36

ACKNOWLEDGEMENTS

First and foremost, I would like to acknowledge and thank Professor Farah Sheikh for her continued support throughout my graduate studies. Her mentorship has been invaluable to both my research and to myself as a scientist. I would also like to acknowledge the members, both past and current, of the Sheikh Lab for their constant help, advice, and input, and especially the following members who directly or indirectly contributed to this project: Dr. Robert Lyon, Dr. Yan Liang, Dr. Valeria Mezzano, Dr. Fabian Zanella, Dr. Jing Zhang, Daniel Nguyen, Afomia Mesfin, Kevin Tenerelli, and Patrick Lee. I would also like to acknowledge the collaborators on this project including Dr. Stephan Lange, Dr. Vishal Nigam, Dr. Kirk Peterson, Yusu Gu, and Nancy Dalton.

Chapters 3-6, in part are currently being prepared for submission for publication of the material. Pellman, Jason; Lyon, Robert; Liang, Yan; Mezzano, Valeria; Zanella, Fabian; Zhang, Jing; Nigam, Vishal; Gu, Yusu; Dalton, Nancy; Peterson, Kirk L.; Sheikh, Farah. The dissertation author was the primary investigator and author of this material.

VITA

2010 Bachelor of Sciences, University of California, San Diego

2017 Doctor of Philosophy, University of California, San Diego

PUBLICATIONS

Pellman J, Lyon RC, Sheikh F. “Extracellular matrix remodeling in atrial fibrosis: mechanisms and implications in atrial fibrillation.” J Mol Cell Cardiol. 2010 Mar;48(3):461-7.

Mezzano V, **Pellman J**, Sheikh F. “Cell junctions in the specialized conduction system of the heart.” Cell Commun Adhes. 2014 Jun;21(3):149-59.

Pellman J, Sheikh F. “A new mechanism links preamyloid oligomer formation in the myocyte stress response associated with atrial fibrillation.” J Mol Cell Cardiol. 2015 Mar;80:110-3.

Pellman J, Sheikh F. “Atrial fibrillation: mechanisms, therapeutics, and future directions.” Compr Physiol. 2015 Apr;5(2):649-65.

Pellman J, Zhang J, Sheikh F. “Myocyte-fibroblast communication in cardiac fibrosis and arrhythmias: Mechanisms and model systems.” J Mol Cell Cardiol. 2016 Mar 17.

ABSTRACT OF THE DISSERTATION

A Desmosomal Protein Interaction Screen Uncovers a Novel Mechanism Underlying Cardiac Rhythm Disorders

by

Jason Pellman

Doctor of Philosophy in Biomedical Sciences

University of California, San Diego, 2017

Professor Farah Sheikh, Chair

Professor Robert Ross, Co-Chair

Arrhythmogenic right ventricular cardiomyopathy (ARVC) is a genetic based cardiac disease, which is characterized by ventricular dysfunction, fibrofatty accumulation, and ventricular arrhythmias culminating in sudden death. ARVC has been termed a disease of the desmosome, a type of cell-cell junction, as human genetic studies have identified mutations in components of the desmosome as causal for the

disease. Desmosomal protein loss is considered a molecular hallmark of ARVC, however, the mechanisms controlling desmosomal protein degradation that may impact cardiac disease remain uncharacterized. In this dissertation, I aim to better understand the mechanisms linking desmosomal biology to development of disease features of ARVC.

In my studies, I have identified a novel link between protein degradation defects and cardiac arrhythmias in ARVC through identification of a novel cardiac desmosomal protein. I performed a yeast-2-hybrid screen using the N-terminus of the desmosomal protein, desmoplakin (DSP) and identified a novel interaction with the autophagy associated protein synaptosomal associated protein 29 kDa (SNAP29). To determine the role of SNAP29 in the heart, I generated a novel cardiac specific SNAP29 knockout (SNAP29-cKO) mouse by crossing a SNAP29-floxed mouse line with the cardiac specific XMLC2-Cre mouse line. Characterization of this line revealed spontaneous and inducible ventricular arrhythmias and lipid droplet accumulation. These defects were associated with specific loss of select desmosomal and gap junction proteins and accumulation of autophagosome-like and autolysosome-like structures specifically at the cardiomyocyte cell-cell junctions. *In vitro* studies revealed that autophagy is activated and targets DSP in the absence of SNAP29. In a DSP-deficient (DSP-cKO) mouse model of ARVC, I observed autophagy defects characteristic of SNAP29 deficiency, suggesting that SNAP29-mediated autophagy may underlie ARVC. In a SNAP29-null mouse model of the human brain and skin disease CEDNIK, I observed characteristic desmosomal, gap junction, autophagy, and electrical defects in neonatal hearts as observed in SNAP29-cKO and DSP-cKO mouse hearts, suggesting cardiac desmosomal defects may underlie CEDNIK.

In conclusion, my doctoral studies provide evidence for a novel interaction between SNAP29 and DSP and a new mechanism regulating cardiac rhythm wherein cardiomyocyte SNAP29 protects desmosomes from targeted protein degradation via autophagy to restrict ventricular arrhythmias.

Chapter 1

Introduction

1.1 Genetic-based heart disease

Heart disease remains the most common cause of death worldwide. It is estimated to account for over 17 million deaths per year as of 2015 and is predicted to increase to over 23 million by 2030 (WHO Report). A large number of factors can contribute to development of cardiac disease, however genetic factors are recognized as one of the strongest risk factors (Lusis 2003, Kathiresan and Srivastava 2012). Naturally occurring genetic mutations have the unique potential to reveal biological mechanisms underlying human cardiac disease. A better understanding of these molecular mechanisms could identify potential targets for novel therapies. In addition, genetic screening can be used as a tool to identify individuals at highest risk for development of heart disease and aid in preventive medicine efforts. Causal gene mutations for cardiac disease were originally identified by performing genetic linkage analyses in families with large pedigrees. The first gene linked to heart disease was identified in 1990, when mutations in the sarcomeric protein, β-myosin heavy chain, were discovered as causal for hypertrophic cardiomyopathy (Geisterfer-Lowrance, Kass et al. 1990). Since then, nearly 1500 mutations in sarcomeric proteins have been associated with familial hypertrophic and dilated cardiomyopathy (McNally, Golbus et al. 2013). Many of these sarcomeric genes were shown to impact cardiac contractility, suggesting that drugs regulating cardiac contractility may be useful therapeutic targets. These studies ultimately informed the development of a novel drug class, cardiac myosin activators, which are currently in phase II trials for the potential treatment of chronic heart failure and left ventricular systolic dysfunction (Lim 2017). This class of drug is able to directly bind cardiac myosin to increase its ATPase activity and increase myosin activation speed (Malik, Hartman et al. 2011). Causal disease associated mutations have been identified for a vast spectrum of cardiac diseases affecting cardiac vasculature, function,

and arrhythmias (Curran, Splawski et al. 1995, Garg, Kathiriya et al. 2003, Garg, Muth et al. 2005, Malik, Hartman et al. 2011). Arrhythmogenic right ventricular cardiomyopathy (ARVC) is a genetic based cardiac disease, which encompasses a spectrum of disease manifestations ranging from arrhythmogenic defects to heart failure features, thus has the potential to shed light on mechanisms that can broadly relate to many cardiac diseases (Thiene, Corrado et al. 2007, Sen-Chowdhry, Morgan et al. 2010). ARVC has also been termed a disease of the desmosome, as human genetic studies have identified mutations in components of the desmosomal cell-cell junction as causal for the disease (Sen-Chowdhry, Morgan et al. 2010). Thus, the study of ARVC has the potential to provide new insights on underlying mechanisms regulating cardiac desmosomal biology as well as how defects in desmosomal function can contribute to development of broad cardiac disease features.

1.2 Arrhythmogenic Right Ventricular Cardiomyopathy (ARVC)

1.2.1 Clinical features of ARVC

ARVC is a genetic-based heart disease that was originally described as a right ventricular disease; however, more recent studies have identified patients with left-dominant and bi-ventricular dysfunction (Thiene, Corrado et al. 2007, Sen-Chowdhry, Morgan et al. 2010). In addition to ventricular dysfunction, patients also display fibrofatty replacement, and ventricular arrhythmias leading to sudden death (Thiene, Corrado et al. 2007, Sen-Chowdhry, Morgan et al. 2010). Ventricular arrhythmias and risk of sudden death increases with exercise (Corrado, Basso et al. 2003). There is also evidence of heterogeneity in ARVC disease features as patients are described as exhibiting purely electrical abnormalities (cardiac arrhythmias alone) and others exhibiting overt structural abnormalities (cardiac arrhythmias plus ventricular dysfunction and/or fibrofatty

replacement) (Dalal, Nasir et al. 2005, Thiene, Corrado et al. 2007). The early stages of electrical disease have been referred to as the clinically “concealed” phase during which sudden death may be the first manifestation of the disease (Basso, Thiene et al. 1996, Dalal, Nasir et al. 2005). The disease can also sometimes progress from electrical to structural disease features (Dalal, Nasir et al. 2005). ARVC is responsible for 10% of sudden cardiac deaths in people ≤65 years of age and 24% in people ≤30 years of age (Tabib, Miras et al. 1999, Tabib, Loire et al. 2003). The prevalence of ARVC is 1 in 1000-5000 people depending on the geographical region, though the prevalence may be higher as some patients are undiagnosed or misdiagnosed due to poor diagnostic markers (Peters, Trummel et al. 2004, Thiene, Corrado et al. 2007). Growing evidence also reveals earlier postnatal onset since pediatric populations ranging from infants to children in their teens are also particularly vulnerable to ARVC (Daliento, Turrini et al. 1995, Nishikawa, Ishiyama et al. 1999, Garcia-Gras, Lombardi et al. 2006, Rey, Rodriguez-Nunez et al. 2007, Wong, AbdurRazak et al. 2008), highlighting the critical need for research to help identify early mechanisms driving ARVC and the need for treatment strategies in patients that target the disease at earlier stages.

1.2.2 Genetics of ARVC

Human genetic studies have linked up to 30-60% ARVC cases to mutations in classic genes encoding components of the desmosome, a type of cell-cell junction (Sen-Chowdhry, Syrris et al. 2007, Bhuiyan, Jongbloed et al. 2009, den Haan, Tan et al. 2009, Bao, Wang et al. 2013, Zhou, Chen et al. 2015). Thus, ARVC is termed a cardiac disease of the desmosome (Sen-Chowdhry, Morgan et al. 2010). The cardiac desmosome is made up of five major proteins: desmoplakin, (DSP), plakophilin 2 (PKP2), plakoglobin (JUP), desmocollin 2 (DSC2), and desmoglein 2 (DSG2). ARVC-

associated mutations have been identified in all desmosomal genes (Bhuiyan, Jongbloed et al. 2009, Bao, Wang et al. 2013). Most mutations are thought to be autosomal dominant; however, recessive mutations have also been identified (Norgett, Hatsell et al. 2000, Rampazzo, Nava et al. 2002, Alcalai, Metzger et al. 2003, Uzumcu, Norgett et al. 2006, Al-Owain, Wakil et al. 2011). DSP was the first desmosomal gene linked to autosomal dominant ARVC (Rampazzo, Nava et al. 2002). Interestingly, mutations in DSP have been associated with left-dominant and biventricular forms of ARVC (Norman, Simpson et al. 2005, Corrado and Thiene 2006, Te Riele, Bhonsale et al. 2012). In addition, recessive mutations in DSP have been associated with the cardiocutaneous disease, Carvajal syndrome, which was first described in a population in Ecuador that harbored ARVC as well as skin and hair defects including epidermolytic palmoplantar keratoderma, and wooly hair, respectively (Carvajal-Huerta 1998). Recessive mutations in JUP have also been associated with the cardiocutaneous disease, Naxos disease (Protonotarios, Tsatsopoulou et al. 1986). Naxos disease was first described in a population on the Greek island of Naxos (Protonotarios, Tsatsopoulou et al. 1986). The syndrome features include ARVC in addition to skin and hair defects, which include palmoplantar keratoderma and wooly hair (Protonotarios, Tsatsopoulou et al. 1986). More recently, a novel recessive DSC2 mutation was identified in patients with ARVC that also harbored palmoplantar keratoderma, and woolly hair (Simpson, Mansour et al. 2009). These cardiocutaneous diseases highlight the importance of the desmosome not only in the heart but also the skin.

Non-desmosomal genes have also been implicated in ARVC through linkage analysis of families affected by ARVC or candidate gene sequencing of patient populations. The first locus identified through linkage analysis was transforming growth factor β 3 (TFGβ3) (Rampazzo, Nava et al. 1994, Beffagna, Occhi et al. 2005). Both 5’

UTR and 3' UTR mutations in TGFβ3 mutations have been associated with ARVC and shown to increase expression of TGFβ3 *in vitro* (Beffagna, Occhi et al. 2005). TGFβ3 has established roles as a positive regulator of cardiac fibrosis (Leask and Abraham 2004), suggesting that these activating mutations may increase the fibrotic disease features associated with ARVC. Although the role of TGF-β3 remains to be determined in ARVC, TGFβ signaling was increased in hearts of a cardiac-specific JUP knockout mouse model, that exhibited features of ARVC including, biventricular dysfunction, fibrosis, spontaneous ventricular arrhythmias, and ultrastructural defects (Li, Liu et al. 2011), suggesting that TGFβ signaling pathways may be impacted by ARVC.

The cardiac ryanodine receptor (RYR2) was first associated with familial ARVC (Rampazzo, Nava et al. 1995, Tiso, Stephan et al. 2001); however, independent studies have also associated mutations in RYR2 with catecholaminergic polymorphic ventricular tachycardia (CPVT) (Cerrone, Napolitano et al. 2009, Yano, Yamamoto et al. 2009). Both ARVC and CPVT exhibit similar cardiac arrhythmia features including exercise induced tachycardia suggesting that they may share similar underlying electrical defects driving disease (Comelli, Gonzi et al. 2014, Patel, Shah et al. 2015). RYR2 is a sarcoplasmic reticulum protein that controls Ca2+ release during cardiomyocyte contraction (Marx and Marks 2013). Exogenous expression of ARVC-associated RYR2 mutant proteins (G1885E and G1886S) in HEK293 cells revealed increased Ca2+ leakiness, which may alter calcium dynamics (Koop, Goldmann et al. 2008). It has been proposed that an unrecognized role for calcium sensitive signaling may exist in ARVC (van Opbergen, Delmar et al. 2017), however, these mechanisms remain to be dissected.

Mutations in the giant sarcomeric protein titin (TTN) have also been associated with a biventricular form of ARVC (Rampazzo, Nava et al. 1997, Taylor, Graw et al.

2011). However, TTN mutations have been more commonly associated with dilated cardiomyopathy (DCM) as well as hypertrophic cardiomyopathy (HCM) (Satoh, Takahashi et al. 1999, Itoh-Satoh, Hayashi et al. 2002, Herman, Lam et al. 2012). TTN is expressed longitudinally along the sarcomere and connects the Z-disc to the M-band to mediate passive and restorative/diastolic forces during contraction (LeWinter and Granzier 2010). *In vitro* studies performed on an ARVC-associated mutation in TTN (T2896I) suggested alterations in protein stability as a mechanism underlying the mutation as it lead to increased unfolding of the immunoglobulin-like domain 10 (Ig10) (Taylor, Graw et al. 2011). *In vivo* analysis of a different ARVC-associated TTN mutation (T2850I) expressed in mice through genetic knock-in revealed left ventricular diastolic dysfunction (Bogomolovas, Fleming et al. 2016). Although other key ARVC features were not reported, changes in TTN conformational dynamics were observed that may suggest potentially distinct disease mechanisms associated with non-native sarcomeric interactions and TTN instability leading to reduced I-band compliance (Bogomolovas, Fleming et al. 2016). Thus, the precise mechanisms of how the identified TTN mutations may lead to classic ARVC disease features remain unclear.

A locus containing transmembrane protein 43 (TMEM43), which codes for the protein LUMA, has also been associated with ARVC in a patient population in New Foundland, Canada (Ahmad, Li et al. 1998, Merner, Hodgkinson et al. 2008). TMEM43 mutations are also associated with Emery Dreifuss muscular dystrophy, which affects both skeletal muscle and the heart (Liang, Mitsuhashi et al. 2011). TMEM43 mutations have also been detected in patients with DCM, though a causal relationship is unproven (Milting, Klauke et al. 2015). TMEM43 is a member of the LINC (linker of nucleoskeleton and cytoskeleton) complex that forms the mechanical link between the nucleus and cytoskeleton (Meinke, Nguyen et al. 2011). Using patient fibroblasts from TMEM43

mutation positive (S358L) ARVC patients, it was observed that mutant nuclei had increased stiffness in culture (Milting, Klauke et al. 2015). *In vitro* studies expressing mutant TMEM43 in HL-1 cells showed (i) reduced zonula occludens 1 (ZO-1), an ICD protein, (ii) mislocalized JUP and α-catenin, which are also ICD proteins (iv) altered Cx43 phosphorylation and (v) reduced conduction velocity, suggesting a potential role for TMEM43 in molecular and disease hallmarks for ARVC (Siragam, Cui et al. 2014). However, the role of TMEM43 in the heart and ARVC remains to be assessed.

Desmin (DES) mutations have also been associated with ARVC (Melberg, Oldfors et al. 1999, Klauke, Kossmann et al. 2010). However, DES has also been associated with many other muscle diseases including DCM (Li, Tapscoft et al. 1999), HCM (Olive, Armstrong et al. 2007), restrictive cardiomyopathy (RCM) (Hager, Mahrholdt et al. 2006), myofibrillar myopathy (Goldfarb, Park et al. 1998), neurogenic scapuloperoneal syndrome (Walter, Reilich et al. 2007), and limb girdle muscular dystrophy (Cetin, Balci-Hayta et al. 2013). Interestingly, patients with DES associated ARVC mutations have been observed with and without skeletal muscle myopathy suggesting that mechanisms may be shared between cardiac and skeletal muscle (Melberg, Oldfors et al. 1999, Klauke, Kossmann et al. 2010). DES forms the intermediate filament network in cardiomyocytes and mechanically links the desmosome, sarcomere, nucleus and costamere (Azzimato, Genneback et al. 2016). Hearts from patients harboring DES associated ARVC mutations, exhibited cytoplasmic aggregates associated with reduced DSP and PKP2 protein levels, suggesting that mechanisms related to desmosomal protein loss may be at play (Klauke, Kossmann et al. 2010, Otten, Asimaki et al. 2010).

Through candidate gene sequencing, the R14del phospholamban (PLN) mutation was identified in a large ARVC patient population in the Netherlands (van der

Zwaag, van Rijsingen et al. 2012). This same ARVC associated mutation was also identified in DCM patients that exhibited prevalent cardiac arrhythmias, suggesting that PLN may be involved in shared mechanisms in ARVC and DCM (van der Zwaag, van Rijsingen et al. 2012). The recently identified existence of left dominant and biventricular ARVC (Michalodimitrakis, Papadomanolakis et al. 2002) suggest that these two diseases may be more similar than previously appreciated. PLN has established roles in calcium handling, and loss of PLN function in mice has been previously shown to lead to DCM (MacLennan and Kranias 2003). Human induced pluripotent stem cell (hiPSC) derived cardiomyocytes from patients with the R14del mutation were shown to exhibit defects in PLN localization and Ca^{2+} handling (Karakikes, Stillitano et al. 2015). Changes in calcium handling have been linked to pathogenic mechanisms in cardiac disease, however it remains unclear how this PLN mutation and calcium handling defects may drive classic ARVC disease features.

Mutations in lamin A (LMNA) have also been identified in patients with ARVC (Quarta, Syrris et al. 2012, Kato, Takahashi et al. 2016). However, similar to many of the non-desmosomal genes associated with ARVC, it has been associated with multiple systemic diseases including Hutchinson-Gilford progeria (De Sandre-Giovannoli, Bernard et al. 2003), Emery Dreifuss muscular dystrophy (Bonne, Di Barletta et al. 1999), and DCM with conduction disease (Fatkin, MacRae et al. 1999, MacLeod, Culley et al. 2003). LMNA is a structural protein of the nuclear membrane and contributes to stiffness of the nuclear envelope (Carmosino, Torretta et al. 2014). Genetic knockout of LMNA in mouse embryonic fibroblasts has demonstrated increased nuclear deformation, defective mechanotransduction, and impaired viability under mechanical strain (Lammerding, Schulze et al. 2004). Interestingly, altered response to mechanical stress has previously been proposed as a disease mechanism underlying ARVC (Protonotarios

and Tsatsopoulou 2004, Basso, Corrado et al. 2009); however, the precise mechanisms connecting LMNA function to ARVC associated mutations remain to be examined.

Mutations in the sodium voltage gated channel alpha subunit 5 (SCN5A) have recently been identified in patients with ARVC (Erkapic, Neumann et al. 2008). Mutations in SCN5A have also been previously associated with long QT syndrome type 3, Brugada syndrome, progressive cardiac conduction disease, and DCM (Remme 2013). SCN5A is a major channel responsible for Na+ release during cardiomyocyte excitation (Miller, Wang et al. 2014). Though it is not known how SCN5A mutations affect the heart *in vivo*, expression of ARCV-associated SCN5A mutations in hiPSC-derived cardiomyocytes revealed reduced sodium current (Te Riele, Agullo-Pascual et al. 2017) which has also been observed in a heterozygous PKP2 knockout mouse model that exhibits arrhythmogenic features found in ARVC (Cerrone, Noorman et al. 2012). Stimulated PKP2 deficient neonatal mouse cardiomyocyte cultures displayed arrhythmic behavior including vortex shedding, wavebreaks, and rotors that were dependent on sodium current kinetics (Deo, Sato et al. 2011). Altogether, these findings suggest that SCN5A may have link to the arrhythmic features of ARVC; however, its connection to the structural features of ARVC has not been examined.

Mutations in the fascia adherens junction (FAJ) protein, αT-catenin (CTNNA3) were also found in patients with ARVC (van Hengel, Calore et al. 2013). These mutations appear to disrupt the interaction between αT-catenin and β-catenin *in vitro* (van Hengel, Calore et al. 2013), though mouse models targeting desmosomal mutations/loss and leading to ARVC have otherwise exhibited no FAJ involvement (Saffitz, Asimaki et al. 2009, Sheikh, Ross et al. 2009). In addition, cardiac-specific αT-catenin knockout mice exhibited left ventricular dysfunction without major classic ARVC features (Li, Goossens et al. 2012). Thus, ARVC-associated αT-catenin mutations may

not function as loss-of-function mutations and the role of αT-catenin in ARVC remains unclear.

Although there remain gaps in knowledge of how the aforementioned non-desmosomal genes directly lead to ARVC, ultrastructural evaluation of cardiac biopsies from ARVC patient hearts with no known mutation and with classic desmosomal mutations reveal that desmosomal ultrastructural defects are a common feature regardless of the genetic mutation (Basso, Czarnowska et al. 2006). These results suggest that mechanisms associated with desmosomal protein loss may be a common underlying mechanism impacted by ARVC and warrant further study.

1.3 The Cardiac Desmosome

1.3.1 The cardiac intercalated disc

In cardiac muscle, desmosomes are located at cell-cell junctions between cardiac muscle cells known as the intercalated disc (ICD) (Sheikh, Ross et al. 2009). The ICD houses multiple protein complexes known to couple mechanical and electrical activity between neighboring cardiomyocytes including desmosomes, FAJ, and gap junctions.

Mechanical coupling is mediated by desmosomal junctions and FAJ. The cardiac desmosome is classically made up of three types of proteins: plakins (desmoplakin; DSP), armadillo proteins (plakophilin 2; PKP2 and plakoglobin; JUP), and desmosomal cadherins (desmocollin 2; DSC2 and desmoglein 2; DSG2). The desmosome interacts with the intermediate filament network, made of desmin in the heart, through the DSP C-terminal domain. The DSP N-terminus binds to the armadillo proteins and desmosomal cadherins through its N-terminus, and is therefore though to be a “hotspot” for desmosomal protein interactions (Smith and Fuchs 1998). Intercellular desmosomal

interactions are mediated by desmosomal cadherin binding in the intercellular space. In addition to the classical desmosomal proteins, new protein interactions have been identified at the desmosome. The scaffolding protein myozap and the p53 inhibitor, inhibitor of apoptosis-stimulating protein of p53 (iASPP), have separately been observed in a complex with DSP (Seeger, Frank et al. 2010). The cytoskeletal adaptor protein ankyrin G has also been identified at the ICD through interactions with both PKP2 and the gap junction protein connexin 43 (Sato, Coombs et al. 2011). Ion channels have also been found to complex with desmosomal proteins. For example, the voltage gated sodium channel NaV1.5 associated with PKP2 and DSG2 in cardiomyocytes (Sato, Musa et al. 2009, Rizzo, Lodder et al. 2012). The ventricular ATP-sensitive potassium channel subunits Kir6.2 and SUR2A have also been found in a complex with PKP2 and JUP (Hong, Bao et al. 2012).

The FAJ also consists of three major classic types of proteins: catenin-related proteins (vinculin and α-actinin), catenins (α-, β-catenin, γ-catenin/plakoglobin, and p120-catenin), and cadherins (N-cadherin; NCAD) (Montonen, Aho et al. 2001, Sheikh, Ross et al. 2009). The FAJ interacts with the actin cytoskeleton through the catenin-related proteins, which in turn bind to the catenins and the cadherins. Intercellular interactions are mediated by binding of cadherins in the intercellular space. Coxsackievirus and adenovirus receptor (CAR) has been identified at the ICD through interactions with β-catenin and is thought to influence gap junction function through interactions with connexin 45 (Lim, Xiong et al. 2008). More recently, Xinα and Xinβ have been identified to interact with the FAJ catenin proteins β-catenin and p120-catenin as well as with the actin binding protein cortactin (Wang, Lu et al. 2013).

Electrical coupling is mediated by gap junctions, which are composed of connexin proteins arranged in corresponding hexamers, or connexons, on adjacent

cardiomyocyte plasma membranes. The predominant connexin in the heart is connexin 43 (Cx43). However, subpopulations of cardiomyocytes in the cardiac conduction system express different connexins. The predominant connexins in the sinus node are Cx30, Cx30.2, CX45; those in the atrioventricular node are Cx30.2, Cx45; and those in the His-Purkinje network are Cx40, Cx45 (Mezzano, Pellman et al. 2014). Additional proteins have also been identified interacting at the gap junction. These include zonula occludens-1 (ZO-1), which is thought to interact with Cx43 and has been proposed as a positive regulator of gap junction formation (Giepmans and Moolenaar 1998, Toyofuku, Yabuki et al. 1998, Rhett, Jourdan et al. 2011).

The ICD has been revealed as an increasingly complex structure based on evidence of new protein interactions that bridge components from different complexes together. For example, a direct interaction between the FAJ protein αT-catenin and the desmosomal protein PKP2 was recently identified (Goossens, Janssens et al. 2007), suggesting that additional uncharacterized interactions between junctional components may exist. Recent studies using immunogold electron microscopy have also uncovered evidence of structures that encompass a mixture of junctional components (desmosomes and FAJs), which are referred to as the area composite (Borrmann, Grund et al. 2006, Franke, Borrmann et al. 2006). Furthermore, while the link between the desmosome and ARVC is established, the mechanisms that bridge desmosome function to the rest of the cardiomyocyte are unknown, suggesting that there may exist novel proteins and pathways at the ICD that mediate these processes. Furthermore, there are distinct clinical phenotypes associated with alterations in different complexes (e.g., NCAD loss is associated with DCM and desmosomal loss is associated with ARVC) (Sheikh, Ross et al. 2009). Mouse models have been used as a pivotal tool to

assess how complex-specific proteins and mechanisms may function in the ICD and heart.

1.3.2 Mouse models of ARVC: Insight into Mechanisms

Multiple genetic mouse models have been generated to recapitulate ARVC disease features (Table 1 and Table 2). The first mouse knockout model targeted DSP using the cardiac-specific promoter alpha myosin heavy chain (αMHC)-Cre (Garcia-Gras, Lombardi et al. 2006). Although homozygous DSP loss resulted in embryonic lethality, cardiac-specific heterozygous DSP deficient mice displayed a subset of ARVC features including left ventricular dysfunction, fibrofatty replacement, as well as spontaneous and pacing-induced arrhythmias. Using siRNA-mediated knockdown of DSP in HL-1 (atrial) cells, it was shown that DSP loss leads to JUP translocation to the nucleus to suppress Wnt/β-catenin signaling and drive adipogenic and fibrotic signaling pathways (Garcia-Gras, Lombardi et al. 2006). The role of Wnt signaling in ARVC was further assessed in recent studies that characterized a mouse model expressing a dominant negative form of Rho-kinase (DN-RhoK) under the control of the early embryonic heart promoter, smooth muscle protein 22 α (SM22α) (Ellawindy, Satoh et al. 2015). Rho-kinase, a downstream effector of the small GTPase Rho, is an intracellular regulator of Wnt signaling (Shimokawa and Takeshita 2005). Hearts from DN-RhoK mice exhibit features of ARVC including cardiac dysfunction, fibrofatty accumulation, ventricular arrhythmias and ultrastructural defects resulting in premature sudden death (Ellawindy, Satoh et al. 2015). Hearts from DN-RhoK mice exhibited a switch in Wnt signaling as evidenced by a reduction in Wnt/β-catenin signaling pathways and stimulation of pro-adipogenic Wnt5a signaling pathways (Ellawindy, Satoh et al. 2015). Furthermore, studies exploiting heterozygous DSP knockout mice driven by Nkx2.5-Cre

as well as a JUP transgenic model driven by the αMHC promoter also demonstrated that adipogenic genes were activated by Hippo signaling, and these pathways were elevated in cardiac biopsies from ARVC patients (Chen, Gurha et al. 2014). Inhibition of the Hippo mediators large tumor suppressor kinases 1 and 2 (LATS1 and LATS2) in diseased PKP2-deficient HL-1 cells was also able to decrease adipogenesis (Chen, Gurha et al. 2014); however, the effects of Hippo inhibition in the heart and in ARVC have not been determined.

To more closely determine the cell populations contributing to the fatty deposition in ARVC, three DSP knockout lines with an enhanced yellow fluorescent protein (EYFP) lineage tracing reporter were generated using the (i) Nkx2.5, an early and pan-cardiac promoter, (ii) Mef2C, a second heart field promoter, and (iii) αMHC, a late cardiogenesis promoter (Lombardi, Dong et al. 2009). Analysis of these lines revealed EYFP expression in a majority of adipocytes in Nkx2.5 and Mef2c lineage traced hearts and very few EYFP positive adipocytes in αMHC lineage traced hearts (Lombardi, Dong et al. 2009). These findings suggested that adipocytes in ARVC may arise from the secondary heart field (Lombardi, Dong et al. 2009). Independent studies from our lab that generated a novel genetic mouse model of ARVC by targeting DSP loss using the cardiomyocyte specific myosin light chain 2 ventricular isoform (MLC2v)-Cre (Lyon, Mezzano et al. 2014) was also used to lineage trace the cellular origin of fatty deposition in ARVC by crossing this mouse line to the R26RtdTomato reporter line. In this model, TomatoRed positive cells co-localizing with an adipocyte lipid droplet marker (double positive for perilipin and TomatoRed (representative of MLC2v)) were observed in the subepicardial layer of knockout mice, suggesting that the fatty accumulation is of cardiomyocyte origin (Lyon, Mezzano et al. 2014). In a separate study, an adipocyte progenitor population was also identified by sorting for c-Kit+:Sca1+ cardiac progenitor

cells (CPCs) in a mouse model of ARVC utilizing overexpression of wildtype JUP to mimic nuclear accumulation of JUP)under the αMHC promoter (Lombardi, Dong et al. 2009). This population exhibited enhanced adipogenic signaling, suggesting that adipocytes in ARVC may arise in part from CPCs. Interestingly, studies using biopsies from ARVC human hearts suggested that adipocyte progenitors originated from a non-cardiomyocyte cell population, the cardiac mesenchymal stromal cells (C-MSC) (Sommariva, Brambilla et al. 2016). It remains unclear whether this is a difference due to model system or if there may be multiple cardiac cell populations that can give rise to adipocytes in the heart in ARVC.

To assess the effects of homozygous recessive loss of DSP, which has been associated with a biventricular form of ARVC in patients (Uzumcu, Norgett et al. 2006), our lab targeted DSP loss using MLC2v-Cre (Lyon, Mezzano et al. 2014). This mouse recapitulated many of the postnatal features of a biventricular form of ARVC including fibrofatty replacement of the ventricles, biventricular dysfunction, ventricular arrhythmias and premature death. These ventricular arrhythmias could also be exacerbated with exercise and catecholamine stimulation (Lyon, Mezzano et al. 2014) similar to what is observed in athletes with ARVC where exercise induced catecholamine release is a trigger of ventricular arrhythmias and sudden death (Furlanello, Bertoldi et al. 1998, Heidbuchel, Hoogsteen et al. 2003). This model also uncovered right bundle branch block associated with loss of connexin 40 (Lyon, Mezzano et al. 2014) the former of which is a clinical feature observed in ARVC patients (Fontaine, Frank et al. 1984). In contrast to the heterozygous αMHC-Cre DSP knockout mouse model (Garcia-Gras, Lombardi et al. 2006), this model did not exhibit loss of JUP suggesting that this biventricular form of ARVC may target different underlying mechanisms (Lyon, Mezzano et al. 2014). *In vitro* studies exploiting DSP floxed cardiomyocytes demonstrated that

loss of DSP triggered primary and early loss of Cx43 and conduction defects in the absence of fibrofatty deposition and prior to complete loss of desmosomal proteins (Lyon, Mezzano et al. 2014), suggesting that there may exist crosstalk between desmosomes and gap junctions. These studies provided validation to independent studies in young heterozygous DSP deficient mice using αMHC-Cre and early stage ARVC patient tissues that suggested that Cx43 loss may be an early feature of ARVC (Gomes, Finlay et al. 2012).

Cardiac-specific transgenic models have also been generated to more closely evaluate the impact of desmosomal mutations in ARVC. Transgenic cardiac-specific overexpression of DSP mutations at the N-terminal region (V30M and Q90R) and C-terminus (R2834H) of DSP were generated (Yang, Bowles et al. 2006). Transgenic models overexpressing N-terminus DSP mutations resulted in embryonic lethality after E13.5 with cardiac defects (Yang, Bowles et al. 2006). However, transgenic overexpression of C-terminal DSP mutation, R2834H, which is thought to disrupt the interaction between DSP and desmin, survived postnatally and developed biventricular cardiac dysfunction, cardiac fibrosis, lipid accumulation, and ultrastructural defects (Yang, Bowles et al. 2006). Although the electrophysiology was not examined, these studies demonstrate disruption of desmosomal integrity as a key factor leading to structural features associated with ARVC.

The inhibitor of apoptosis-stimulating protein of p53 (iASSP) was recently identified as a novel desmosomal protein able to complex with DSP in the heart and implicated in ARVC disease pathogenesis (Notari, Hu et al. 2015). Global iASSP knockout mice exhibited biventricular dysfunction, fibrofatty accumulation, and ventricular arrhythmias (Notari, Hu et al. 2015). These defects were associated with loss of DSP and DES from the ICD (Notari, Hu et al. 2015). Examination of cardiac biopsies

from patients with ARVC also revealed loss of iASSP from the ICD (Notari, Hu et al. 2015), altogether suggesting that loss of iASSP and its interaction with DSP may contribute to development of ARVC.

Several mouse knockout models have also targeted PKP2. The first PKP2 deficient mouse model was a global PKP2 knockout (Cerrone, Noorman et al. 2012). Homozygous PKP2 knockout mice were embryonic lethal at E10.5-E11 (Grossmann, Grund et al. 2004); however, examination of heterozygous PKP2 knockout mice revealed ultrastructural defects at the ICD with no baseline disease features (Cerrone, Noorman et al. 2012). Further analysis of these hearts revealed sodium current insufficiency that could be exacerbated with the sodium channel blocker, flecainide, and lead to ventricular arrhythmias (Cerrone, Noorman et al. 2012). These arrhythmias occurred in the absence of structural disease suggesting that heterozygous loss of PKP2 levels can impair the function of the voltage-gated sodium channel complex and alter cardiac electrophysiology without negatively affecting heart function. To determine the impact of ARVC-associated PKP2 mutations, adeno-associated viral (AAV) gene delivery methods were used to express mutant PKP2 (R735X) in wildtype mice *in vivo* (Cruz, Sanz-Rosa et al. 2015). No overt phenotype could be observed in these mice at baseline; however, right ventricular dysfunction and Cx43 mislocalization could be observed after exercise in the absence of cardiac fibrofatty deposition and thus, these mice only developed a subset of features associated with ARVC. In addition, the electrical features were not determined in this model. Truncations of PKP2 have also been previously associated with ARVC (Rasmussen, Nissen et al. 2014). In a recent study, transgenic mice were generated that overexpressed a truncated PKP2 (amino acids 1-329) at increasing levels of expression (Moncayo-Arlandi, Guasch et al. 2016). Hearts from transgenic mice expressing the highest level of truncated PKP2 were shown

to exhibit features of ARVC including, ventricular dilation and dysfunction, inducible arrhythmias and ultrastructural defects (Moncayo-Arlandi, Guasch et al. 2016). Interestingly, the specific truncation in this model was not related to a known ARVC mutation; thus, future models expressing truncations related to known ARVC mutations may provide further relevance of these findings to humans.

Mouse models targeting JUP have also been developed. Global homozygous loss of JUP leads to embryonic lethality from E10.5-E16.5 (Bierkamp, McLaughlin et al. 1996, Ruiz, Brinkmann et al. 1996). Global heterozygous loss of JUP does not lead to an overt basal phenotype (Kirchhof, Fabritz et al. 2006). However, with age and exercise, heterozygous mice exhibit a subset of ARVC features including enlarged right ventricles, increased ventricular arrhythmias, and conduction slowing without histological or ultrastructural defects (Kirchhof, Fabritz et al. 2006). Interestingly, load reducing therapy (furosemide and nitrates) in exercised global heterozygous JUP knockout mice lead to a reduction in chamber dilation, arrhythmia inducibility, and Cx43 loss from the ICD, suggesting that the increased load on the heart associated with exercise contributes to disease progression (Fabritz, Hoogendijk et al. 2011). Cardiac-specific JUP knockout mouse have also been generated using the αMHC-Cre (Li, Liu et al. 2011). These mice displayed a subset of ARVC disease features including, ventricular dilation, fibrosis, arrhythmias, ultrastructural defects, and sudden death without evidence of fatty deposition. Interestingly, hearts from these mice exhibited increased TGFβ signaling, which along with human clinical studies identifying mutations in TGFβ3 in ARVC patients (Beffagna, Occhi et al. 2005) support a potential role for TGFβ3 in ARVC that remains to be tested. In contrast to this model, cardiac specific ablation of JUP in adult mice via a tamoxifen inducible αMHC-mER-Cre-mER lead to a smaller subset of ARVC disease features including ventricular dysfunction, fibrosis, and ultrastructural defects without

fatty deposition or arrhythmias (Li, Swope et al. 2011). The presence of cardiac arrhythmias in the cardiac specific JUP knockout mouse (Li, Liu et al. 2011) and their absence in the inducible cardiac specific JUP knockout mouse (Li, Swope et al. 2011) suggest that developmental mechanisms may underlie the distinct disease etiologies.

The JUP mutation associated with the human disease Naxos (2157del2) has also been modeled in mice. The mouse equivalent of the human Naxos disease JUP mutation (2157del2) was overexpressed in the heart using the αMHC promoter (Lombardi, da Graca Cabreira-Hansen et al. 2011). These mice exhibited left ventricular dysfunction, fibrofatty accumulation, and cardiac arrhythmias with underlying nuclear localization of mutant JUP (Lombardi, da Graca Cabreira-Hansen et al. 2011). Naxos-related JUP mutant knock in mice have also been generated to address the role of this mutation and its expression in disease (Zhang, Stroud et al. 2015). Genetic knockin of the equivalent human Naxos mutation into the endogenous locus of mouse lead to a significant downregulation of JUP mRNA associated with perinatal lethality and reduced levels of JUP and other desmosomal proteins (Zhang, Stroud et al. 2015). Cardiac morphology, fibrosis, and stress markers were not altered in knockin mice and cardiac function and electrophysiology were not reported, therefore this model may not exhibit features of ARVC at time of death (Zhang, Stroud et al. 2015). In contrast, stabilization of Naxos mutant JUP mRNA via fusion of the last 5 exons of the gene lead to restoration of mutant JUP protein to wildtype levels and no basal phenotype (Zhang, Stroud et al. 2015). These findings suggested that restoration of mutant JUP protein levels may have potentially therapeutic effects.

Several mouse models have been used to dissect the mechanisms by which JUP, and more specifically accumulation of nuclear JUP, and its downstream signaling plays a role in ARVC. Overexpression of wildtype JUP under the αMHC promoter

demonstrated that JUP transgenic mouse hearts displayed fibrofatty replacement without functional or ultrastructural defects (Lombardi, Dong et al. 2009). Molecular analyses revealed the appearance of nuclear JUP and concordant suppression of Wnt/β-catenin target genes, suggesting that nuclear JUP translocation may underlie the fibrofatty features of ARVC (Lombardi, Dong et al. 2009). A high throughput chemical screen identified the glycogen synthase kinase 3 beta (GSK3β) inhibitor, SB216763, as an agent capable of preventing heart failure and reducing mortality in an ARVC-like zebrafish model overexpressing the Naxos associated JUP mutation (Asimaki, Kapoor et al. 2014). Interestingly, GSK3β is itself an inhibitor of Wnt signaling, thus a reduction in GSK3β activity is thought to reverse the suppression of Wnt signaling thought to underlie ARVC. To test the effect of SB216763 in ARVC, transgenic JUP mutant (2157del2) mice, which were shown to exhibit cardiac arrhythmias and fibrosis, were treated with SB216763 (Chelko, Asimaki et al. 2016). SB216763 treated JUP mutant mice exhibited attenuated arrhythmias and fibrosis (Chelko, Asimaki et al. 2016), suggesting that activation of Wnt signaling though inhibition of GSK3β may be an effective therapeutic approach in ARVC.

DSG2 has also been targeted in genetic mouse models. Cardiac specific knockout of DSG2 leads to chamber dilation, interstitial and focal replacement fibrosis, conduction defects, and ultrastructural defects (Kant, Holthofer et al. 2015). Cardiac function and fat deposition were not examined in this model, however calcifying cardiomyocyte necrosis was consistently observed in DSG2 knockout hearts (Kant, Holthofer et al. 2015). DSG2 mediates direct interactions between each half of the desmosome through its extracellular domains (Garrod and Chidgey 2008). The role of DSG2 extracellular domains was more directly tested through two mouse models, which include DSG2 (EC1 and EC2) knockout mice harboring a DSG2 deletion that lacks the

extracellular EC1 and EC2 domains (Krusche, Holthofer et al. 2011, Kant, Krull et al. 2012) and transgenic mice overexpressing a DSG2 mutation (N271S) between the EC2 and EC3 domains (Pilichou, Remme et al. 2009). Both models could recapitulate the ARVC disease features exhibited by the cardiac-specific DSG2 knockout mice, suggesting that the adhesive domains of DSG2 adhesion are critical to desmosomal integrity and their loss contributes to disease features of ARVC. In a separate study using the same DSG2 mutation (N271S) mouse, electrical and ultrastructural defects were observed prior to development of structural features of disease including myocyte necrosis and fibrosis suggesting that these may be early features of disease (22764152). Similar to PKP2 heterozyogus knockout mice (Cerrone, Noorman et al. 2012), hearts of these DSG2 transgenic mice also exhibited reduced sodium current density (Rizzo, Lodder et al. 2012). These findings suggested that DSG2 loss may also contribute to early electrical defects in ARVC through disruption of the NaV1.5 sodium channel. Recent studies from an independent group, generated a DSG2 global knockout mouse model the exhibited ventricular dysfunction and biventricular fibrosis, though electrical or fatty accumulation features were not reported (Chelko, Asimaki et al. 2016). Treatment of these mice with the GSK3β inhibitor SB216763 lead to attenuation of ventricular dysfunction and fibrosis, suggesting that activation of Wnt signaling though inhibition of GSK3β may be an effective therapeutic approach in ARVC.

Human clinical studies have associated DSC2 mutations with ARVC (Heuser, Plovie et al. 2006); however, to date, their role in mice *in vivo* has not been tested. ARVC-associated DSC2 mutants (E102K and I345T) have been overexpressed in HL-1 cells (Beffagna, De Bortoli et al. 2007). These DSC2 mutations were shown to lead to mislocalization of mutant DSC2 to the cytoplasm, suggesting that DSC2 is effectively lost from the desmosome in this setting. Independent studies expressing distinct ARVC-

associated DSC2 mutations (R203C and T275M) in cultured neonatal rat cardiomyocytes demonstrated that these mutations prevented proper proteolytic cleavage and maturation of DSC2 leading to loss of functional protein (Gehmlich, Syrris et al. 2011). These findings altogether suggested that loss of mature DSC2 protein and desmosomal protein targeted mechanisms rather than dominant negative activity could be responsible for disease development in this setting.

Altogether these studies suggest that mutations and/or loss of molecular components of the classic desmosomal complex, result in loss of desmosomal protein levels, which are molecular triggers for ARVC. Despite this link, the mechanisms that control desmosomal protein levels (degradation) and function in health and disease remain largely undefined.

1.4 Protein Degradation Mechanisms at the ICD

1.4.1 Protein degradation pathways in the heart

The heart is a major target of protein quality control as it undergoes constant stress and thus, requires constant turnover of cardiac proteins (protein synthesis and protein degradation) to maintain cardiac function (Lyon, Lange et al. 2013). Recent advances in the field of protein turnover have linked defects in protein degradation to human cardiac diseases (Su and Wang 2010). Protein degradation in the heart is mediated by two major cellular mechanisms, the ubiquitin-proteasome system (UPS) and autophagy (Portbury, Willis et al. 2011). These mechanisms recycle damaged, misfolded, or otherwise unneeded proteins into free amino acids to be used again in future cellular processes (Portbury, Willis et al. 2011).

Protein degradation via the UPS begins with selection of a protein target via covalent attachment of a ubiquitin moiety in a process known as ubiquitination (Lyon,

Lange et al. 2013). This process occurs through a multi-step step enzymatic cascade consisting of (i) activation of ubiquitin monomers by the E1 ubiquitin-activating enzyme UBA1, (ii) transfer of the activated ubiquitin to an E2 ubiquitin-conjugating enzyme via trans-esterification, and (iii) ligation of the ubiquitin to the target protein by an E3-ubquitin ligase, ultimately generating a polyubiquitin-tagged protein (Lyon, Lange et al. 2013). This newly marked protein can now be recognized by the 26S proteasome for degradation (Lyon, Lange et al. 2013). Targeting of proteins for ubiquitination typically occurs through binding of a substrate adaptor that links the target protein to the E3-ubiquitin ligase complex (Lyon, Lange et al. 2013).

Protein degradation via autophagy begins through sequestration of protein or organelle targets into a specialized double membraned vesicle called the autophagosome (Portbury, Willis et al. 2011). The steps of autophagy are also dependent on an enzymatic cascade that generates the autophagy proteins (ATG) conjugate ATG5-ATG12 that converts microtubule associated protein 1 light chain 3 (LC3-I) to its lipidated form LC3-II, which allows for formation of the autophagosomal membrane (Johansen and Lamark 2011). After LC3-II activation the main steps of autophagy are (i) cargo sequestration, (ii) fusion with the lysosome, and (iii) degradation. Cargo can be non-selectively sequestered or selectively sequestered by cargo-specific adaptor proteins including p62 (sequestome-1) and NBR1 (neighbor to Brca1) and ALFY (autophagy linked FYVE protein) (Johansen and Lamark 2011). These adaptor proteins can also mediate crosstalk between the UPS and autophagy, as p62 and NBR1 can recognize polyubiquitinated substrates (Kirkin, McEwan et al. 2009). After degradation, the molecular components of the cargo are released and become available for reuse (Johansen and Lamark 2011).

1.4.2 Protein degradation plays an important role in cardiac disease

Defects in the UPS have been observed in in cardiac disease including heart failure, dilated cardiomyopathy, hypertrophic cardiomyopathy, cardiac hypertrophy, and atherosclerosis (Day 2013). In these settings, accumulation of polyubiquitinated proteins is the key feature of altered protein degradation (Day 2013). Though accumulation of the intermediate product of the UPS, i.e. polyubiquitinated proteins, might suggest reduced rates of degradation, further studies have revealed that both increased and decreased UPS activity have been observed in diseased settings. In cases of failing and hypertrophic cardiomyopathic hearts, reduced proteasomal activity has been observed (Predmore, Wang et al. 2010) whereas in cases of dilated cardiomyopathy, increased proteasomal activity has been observed (Birks, Latif et al. 2008).

Mouse models have been used to assess the role of UPS in cardiac disease. Upregulation of UPS activity through overexpression of a proteasome subunit has been used to determine the relationship between UPS degradation and cardiac injury (Li, Horak et al. 2011). In a mouse model of ischemia reperfusion injury, cardiac overexpression of the proteasome subunit, PA28α, leads to increased proteasome activity and improved recovery after injury (Li, Horak et al. 2011). Conversely, when ischemia reperfusion injury was performed in a transgenic mouse model overexpressing a catalytically inactive β5 proteasome subunit (β5T1A), mice exhibited a worse response to injury (Tian, Zheng et al. 2012). The role of cardiac proteasome activity was also assessed in a pressure overload model using abdominal aortic banding (Chen, Ma et al. 2010). Banded mice treated with the proteasomal inhibitor MG132, exhibited reduced cardiac hypertrophy and improved cardiac function compared to untreated mice, suggesting that inhibiting proteasome function in a pressure overload setting is beneficial (Chen, Ma et al. 2010). Similarly, in a study treating an OVE26 diabetic cardiomyopathy

mouse model with MG132 demonstrated that treated mice exhibited attenuated cardiomyopathy features (Wang, Sun et al. 2013). Altogether these studies suggest that alterations in protein degradation activity via the UPS can be beneficial though this effect appears to be highly dependent on disease etiology.

Autophagy is upregulated in various human heart disease settings (Nishida, Kyoi et al. 2009). The lysosomal protein, lysosome-associated membrane glycoprotein 2 (LAMP2), is disrupted by loss of function mutations in Danon's disease, where patients exhibit hypertrophic cardiomyopathy, skeletal myopathy and muscle wasting (Danon, Oh et al. 1981, Cheng and Fang 2012). A key molecular feature of Danon's disease is the accumulation of autophagosomes in cardiomyocytes due to impaired lysosomal degradation (Nishino, Fu et al. 2000, Tanaka, Guhde et al. 2000). Autophagosomes have also been observed in human dilated cardiomyopathy (Shimomura, Terasaki et al. 2001) and ischemic heart disease (Elsasser, Vogt et al. 2004, Yan, Vatner et al. 2005), though the disease driving mechanisms for the accumulation of autophagosomes remain unclear.

The role of autophagy in cardiac disease has been more directly investigated through mouse models. Inducible cardiac specific loss of the autophagy protein Atg5 in adult mice, leads to rapid left ventricular dilation and contractile dysfunction (Nakai, Yamaguchi et al. 2007). However, constitutive cardiac specific loss of Atg5 leads to a much later onset of cardiac disease with sudden death and left ventricular dysfunction, suggesting that Atg5 function may be more important for short-term stress responses (Nakai, Yamaguchi et al. 2007). Developmental compensation has also been proposed to account for these differential responses via a molecular switch from one autophagosome production pathway, Unc-51-like kinase dependent, to an alternative one, Rab9-dependent (Nishida, Arakawa et al. 2009, Honda, Arakawa et al. 2014). To

investigate the role of autophagy in cardiac hypertrophy regression, Atg5 cardiac specific knockout mice and wildtype controls were subjected to cardiac hypertrophy induction via angiotensin II infusion (Oyabu, Yamaguchi et al. 2013). Wildtype mice exhibited elevated autophagic markers upon removal of angiotensin II (Oyabu, Yamaguchi et al. 2013). Regression from cardiac hypertrophy was delayed in mice lacking Atg5 compared to wildtype controls (Oyabu, Yamaguchi et al. 2013), suggesting that autophagy is necessary for regression after unloading of the heart. It has also been shown that the FoxO family of proteins are important regulators of autophagy during this process (Cao, Jiang et al. 2013, Hariharan, Ikeda et al. 2013).

Studies in mouse models of cardiac disease have explored the potential for therapeutically targeting autophagy. In a mouse model of a desmin-related cardiomyopathy generated through transgenic overexpression of mutant chaperone protein, αB-crystallin (R120G), autophagy was blunted via heterozygous deletion of Beclin-1, a positive regulator of autophagy (Tannous, Zhu et al. 2008). This lead to accelerated disease progression (Tannous, Zhu et al. 2008). In a separate study using the same αB-crystallin (R120G) mouse, autophagy was upregulated via overexpression of Atg7, which lead to an attenuation of disease progression, suggesting that upregulation of autophagy can reverse the course of disease in this setting (Bhuiyan, Pattison et al. 2013). However, results from mouse models are conflicting in the setting of pressure overload. The response to pressure overload (via TAC) was worsened in cardiac specific Atg5 knockout mice (Nakai, Yamaguchi et al. 2007). In contrast, heterozygous loss of beclin-1, which also reduces autophagy activity leads to improved cardiac function after pressure overload via TAC (Zhu, Tannous et al. 2007). These findings suggest that impact of targeting autophagy may be dependent on disease state and differentially affected by specific autophagy proteins.

1.4.3 Compartmentalization of protein degradation in cardiac muscle

Protein degradation mechanisms can selectively act at specific subcellular localizations in the cardiomyocyte and may impact disease (Lyon, Lange et al. 2013). The cardiomyocyte sarcomere has been shown to be an important site of localized protein degradation. For example, muscle ring finger (MURF) proteins, a type of ubiquitin-E3 ligase, have been observed at the sarcomere at the M-line and Z-disc in cardiomyocytes (Spencer, Eliazer et al. 2000, Centner, Yano et al. 2001, Kedar, McDonough et al. 2004). Yeast-two-hybrid analyses have demonstrated interactions between the three MURF family members, MURF1, 2, and 3, and multiple sarcomeric proteins, suggesting that they may participate in their degradation (Spencer, Eliazer et al. 2000, Witt, Granzier et al. 2005). Overexpression and loss of function studies in cardiomyocytes revealed that MURF1 increases UPS-mediated degradation of the sarcomeric protein troponin-I (Kedar, McDonough et al. 2004). Global knockout of MURF1 and MURF2 simultaneously leads to cardiac hypertrophy leading to acute heart failure and early lethality with underlying defects in Z-disc ultrastructure and upregulation of the MURF1 and 2 target proteins, four and a half lim domain 2 (FHL2) and cardiac ankyrin repeat protein (CARP) (Witt, Witt et al. 2008). MURF3 global knockout mice do not exhibit a phenotype at baseline; however, these mice are predisposed to cardiac rupture after myocardial infraction with underlying upregulation of the MURF3 targets, FHL2 and γ-filamin (Fielitz, van Rooij et al. 2007). These findings emphasize the importance of sarcomere localized protein degradation components in maintenance of sarcomere and cardiac function.

The specialized cardiomyocyte cell membrane, the sarcolemma, is also a site of protein degradation. In neonatal rat cardiomyocytes, the E3 ligase, Casitas b-lineage

lymphoma (c-Cbl), has been observed at focal adhesion sites (Rafiq, Guo et al. 2012). Furthermore, by activating c-Cbl activity through stimulation with the neutrophil-derived serine protease, cathepsin G, the focal adhesion complex proteins, paxilin and focal adhesion kinase (FAK) were degraded (Rafiq, Guo et al. 2012). This effect could be restored with proteasomal inhibitors (Rafiq, Guo et al. 2012). Altogether these data suggested that the cardiomyocyte harbors molecular machinery that is directed to perform protein degradation functions at specific subcellular sites in order to mediate targeted protein degradation.

1.4.4 ICD as a site of protein degradation that may have importance in cardiac disease

There is evidence that the ICD is also an active site for protein degradation as ubiquitin conjugates, p62 and autophagosomes, were shown to accumulate at the ICD in cardiomyocytes in both healthy and diseased settings (Hilenski, Terracio et al. 1992, Nepomnyashchikh, Lushnikova et al. 2000, Lange, Xiang et al. 2005, Balasubramanian, Mani et al. 2006, Hirschy, Croquelois et al. 2010). In addition, members of the ICD complex can be targeted by UPS-related protein degradation mechanisms. In an *in vitro* study in PKP2-deficient rat cardiomyocytes, DSP loss can be restored by protein degradation inhibition using the proteasome inhibitor MG132 (Dubash, Kam et al. 2016), suggesting that desmosomal proteins are targeted by protein degradation mechanisms. Furthermore, β-catenin is an established target of the UPS, though this has only been shown for cytosolic β-catenin and not junctional β-catenin (Wu, Xu et al. 2003). Degradation of cytosolic β-catenin is thought to regulate its transcriptional activity as part of the Wnt/β-catenin signaling pathway, which has been implicated in cardiac differentiation and diseases such as heart failure and ARVC (17609106, 14613867). Cx43, the major component of gap junctions in the myocardium, can be regulated in

stressed cardiomyocytes by autophagy (Su and Lau 2012, Basheer, Harris et al. 2015). In cardiomyocytes, chemical and genetic inhibitors of autophagy are able to rescue ischemia-induced loss of Cx43, suggesting that Cx43 is degraded through autophagy under these conditions (Martins-Marques, Catarino et al. 2015, Martins-Marques, Catarino et al. 2015). WW domain containing E3 ubiquitin ligase 1 (WWP1) is the E3 ligase thought to target Cx43. Global transgenic overexpression of WWP1 in mice lead to left ventricular hypertrophy and ventricular arrhythmias with underlying Cx43 loss (Basheer, Harris et al. 2015), suggesting that protein degradation control is required for Cx43 homeostasis and function. Altogether these data suggest that the ICD complex and proteins are under protein degradation control; however, to date, there exists limited biological information on the molecular machinery that are important in driving their degradation.

ARVC is a disease associated with specific loss/dysregulation of desmosomal proteins (Basso, Czarnowska et al. 2006, Bhuiyan, Jongbloed et al. 2009, Bao, Wang et al. 2013). Although the impact of protein degradation mechanisms has not been investigated in the context of ARVC and the desmosome, several pieces of evidence warrant further studies in this area. First, ARVC is a cardiac disease of the desmosome, where desmosomal protein loss is a key molecular feature of the disease. Second, a recent study investigating mechanisms underlying ARVC-associated mutations in desmocollin 2 suggested that these mutations prevented proper proteolytic cleavage and maturation of DSC2 leading to reduced levels of functional DSC2 (Gehmlich, Syrris et al. 2011), highlighting a potential impact on faulty protein turnover. Third, in PKP2-deficient cardiomyocytes *in vitro,* which exhibit ARVC-associated electrical defects *in vivo*, exhibit DSP protein loss that could be restored by proteasomal inhibition (Dubash, Kam et al. 2016). These studies suggest that defects in protein turnover/processing mechanisms

may contribute to desmosomal protein loss. Altogether this highlights the need for research to better understand protein-protein interactions and protein regulatory mechanisms at the desmosome, which may provide unique insights on the compartmentalized disease features encompassed by diseases of the ICD, such as ARVC.

1.5 Rationale, Hypothesis, and Specific Aims

ARVC is a genetic-based heart disease characterized by ventricular dysfunction, fibrofatty replacement, and ventricular arrhythmias leading to sudden death. Human genetic studies have linked up to 30-60% ARVC cases to mutations in classic genes encoding components of the desmosome, a type of cell-cell junction, thus ARVC is termed a cardiac disease of the desmosome. The first desmosomal gene linked to autosomal dominant ARVC was DSP (Rampazzo, Nava et al. 2002). DSP is a central protein in the desmosomal complex that connects the intermediate filament network to the core of the desmosomal complex through interactions with its C-terminus. DSP binds to the armadillo proteins and desmosomal cadherins through its N-terminus. Thus, the N-terminal region is thought to be a “hotspot” for desmosomal protein interactions as well as common site for ARVC-associated mutations, which can be a potential region of DSP to uncover novel protein interactions to better understand ARVC disease pathogenesis.

To better understand the role of DSP in mechanisms driving ARVC, our laboratory developed a novel mouse model of a biventricular form of ARVC through cardiomyocyte specific ablation of DSP (Lyon, Mezzano et al. 2014) that recapitulates all major human ARVC electrical and structural disease features. Our studies along with others demonstrate that desmosomal protein loss is considered a molecular hallmark of ARVC. Recent evidence highlights the intercalated disc as a site of protein degradation. Moreover, *in vitro* studies in cardiomyocytes suggest that DSP can be targeted by protein degradation mechanisms, however the mechanisms controlling desmosomal protein degradation remain uncharacterized. By targeting DSP in an unbiased protein interaction screen, we will have the potential to identify proteins that interact with the

desmosome and that may affect protein turnover mechanisms and contribute to ARVC pathogenesis.

Hypothesis:

There exist novel proteins at the cardiac desmosome that regulate protein degradation, and dysregulation of these pathways may drive cardiac defects in desmosomal diseases, such as ARVC.

Specific Aims:

1.1 To screen for novel cardiac N-terminal DSP-interacting proteins using an unbiased yeast-2-hybrid screen with an adult human heart cDNA library, identify a candidate protein that may impact protein degradation, and validate its expression in DSP-deficient models.

1.2 To determine the role of this novel DSP- interacting protein in cardiomyocytes and protein degradation through generation of cardiomyocyte-specific mouse model and cells.

1.3 To determine whether the cardiac protein degradation mechanisms associated with this novel DSP-interacting protein are similarly impacted in a mouse model of ARVC and other models of human disease.

The results of these studies are presented in chapters 3-6 and are discussed in terms of their implications on cardiac desmosomal biology and mechanisms impacting ARVC.

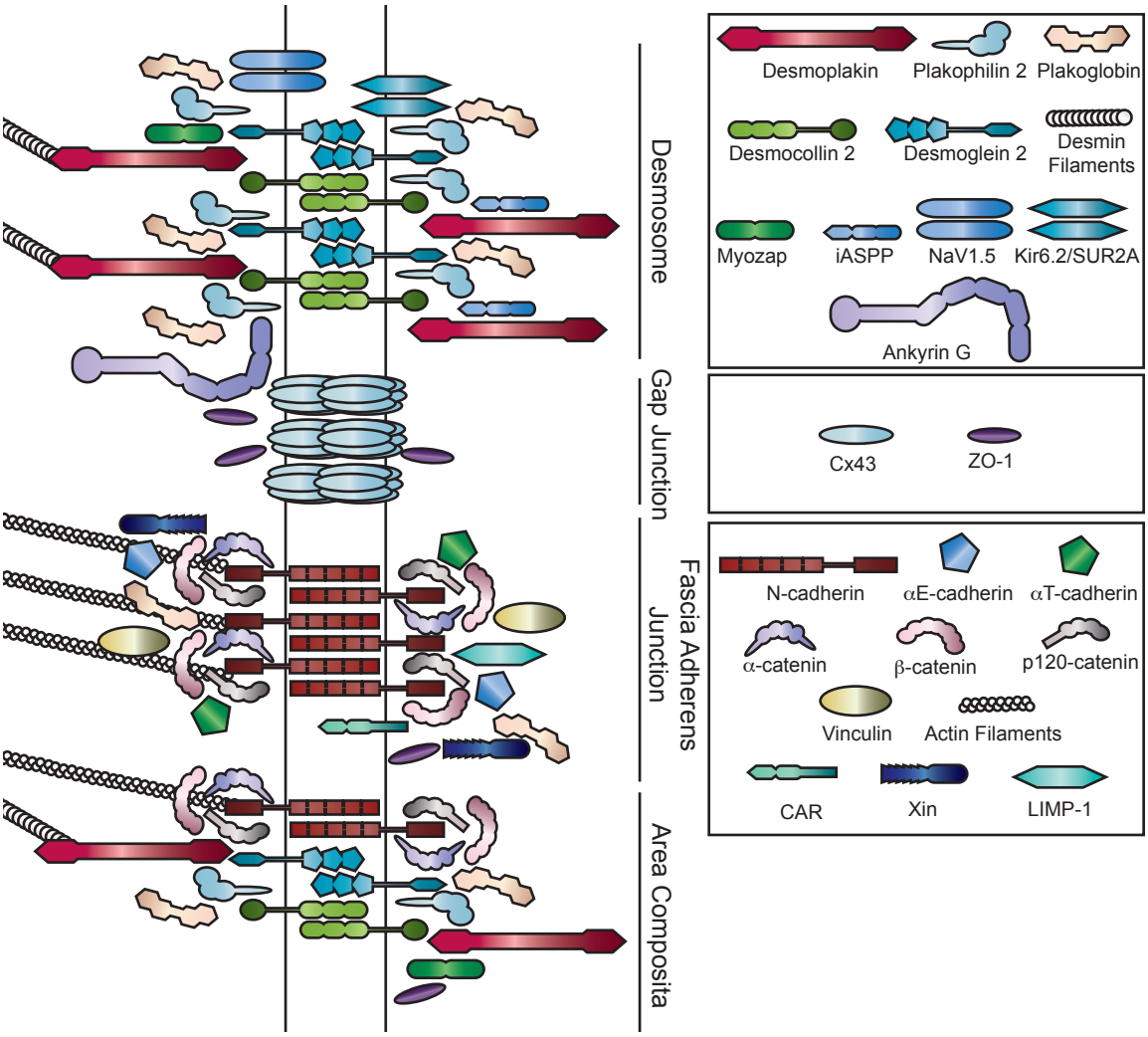


Figure 1. Diagram of cardiac intercalated disc proteins and complexes.

Table 1. Knockout Mouse Models of ARVC.

Protein	Model Type/ Zygosity	Cre Promoter	Cardiac Features	Ultrastructural Features	Reference
DSP	Cardiac Specific/ Heterozygous	aMHC-Cre	Left ventricular dysfunction, fibrofatty accumulation and both spontaneous and induced arrhythmias	Desmosomal defects	Garcia-Gras et al., 2006
	Cardiac Specific/ Homozygous	Mlc2v-Cre	Biventricular dysfunction, fibrofatty accumulation, both spontaneous and induced ventricular arrhythmias and premature death	ICD defects	Lyon et al., 2014
	Cardiac Specific/ Heterozygous	Nkx2.5-Cre	Left ventricular dysfunction and fibrofatty accumulation	Not examined	Lombardi et al., 2009
	Cardiac Specific/ Heterozygous	Mef2c-Cre	Fibrofatty accumulation	Not examined	Lombardi et al., 2009
PKP2	Global/ Heterozygous	-	Drug induced ventricular arrhythmias	Lower desmosome abundance; ICD membrane defects	Cerrone et al., 2012
JUP	Global/ Heterozygous	-	Right ventricular dysfunction and both spontaneous and induced ventricular arrhythmias	None	Kirchhof et al., 2006
	Cardiac Specific/ Homozygous	aMHC-Cre	Ventricular dysfunction, fibrosis and ventricular arrhythmias	ICD defects	Li et al., 2011
	Cardiac Specific/ Homozygous	aMHC-mER-Cre-mER	Ventricular dysfunction, fibrosis	ICD defects	Li et al., 2011
DSG2	Cardiac Specific/ Homozygous	aMHC-Cre	Chamber dilation, calcifying cardiomyocyte necrosis, aseptic inflammation,fibrosis, and conduction defects	ICD defects	Kant et al., 2015
	Global/ Homozygous	-	Left ventricular dysfunction and biventricular fibrosis; electrophysiology and fatty accumulation not examined	Not examined	Chelko et al., 2016
iASSP	Global/ Homozygous	-	Embryonic right ventricular wall thinning and dilatation; Adult biventricular dysfunction, fibrofatty accumulation, ventricular arrhythmias and sudden death	Desmosomal defects	Notari et al., 2015

Table 2. Knockin and Transgenic Mouse Models of ARVC.

Protein	Model Type	Mutation	Cardiac Features	Ultrastructural Features	Reference
DSP	Cardiac-Specific Transgenic	Human DSP R2834H	Biventricular dysfunction and fibrofatty accumulation	ICD defects	Yang et al., 2006
	Cardiac-Specific Transgenic	Human DSP V30M	Embryonic lethal at E13.5	Not examined	Yang et al., 2006
	Cardiac-Specific Transgenic	Human DSP Q90R	Embryonic lethal at E13.5	Not examined	Yang et al., 2006
PKP2	Viral Transmission	Human PKP2 R735X	Exercise induced right ventricular dysfunction	No ultrastructural defects	Cruz et al., 2015
	Cardiac-Specific Transgenic	Mouse PKP2 aa 1-329	Left ventricular dysfunction, inducible arrhythmias	ICD defects	Moncayo-Arlandi et al., 2016
JUP	Global Knock In	Mouse Naxos JUP	Perinatal lethality without cardiac defects	Not examined	Zhang et al., 2015
	Global Knock In	Stabilized Mouse Naxos JUP	No phenotype	Not examined	Zhang et al., 2015
	Cardiac-Specific Transgenic	Flag-WT	Fibrofatty accumulation without functional defects; electrophysiology not examined	None	Lombardi et al., 2009
	Cardiac-Specific Transgenic	Mouse 3xFlag-WT	Fibrofatty accumulation, cardiac arrhythmias and sudden death with no functional defects	Not examined	Lombardi et al., 2011
	Cardiac-Specific Transgenic	Mouse Naxos JUP	Left ventricular dysfunction, fibrofatty accumulation, and cardiac arrhythmias	Not examined	Lombardi et al., 2011
DSG2	Global Knock In	EC1/EC2 Deletion	Left and right ventricular dilatation, fibrosis, calcification, and spontaneous death	ICD defects	Krusche et al., 2011; Kant et al., 2012
	Cardiac-Specific Transgenic	Mouse DSG2 N271S	Spontaneous ventricular arrhythmias, conduction slowing, ventricular dilatation and aneurysms, and replacement fibrosis leading to sudden cardiac death	None	Pilichou et al., 2009
TTN	Global Knock In	T2850I	Left ventricular diastolic dysfunction	Not examined	Bogomolovas et al., 2016
Rho-Kinase	Smooth Muscle-Specific Transgenic	Dominant Negative RB/PH (TT)	Cardiac dysfunction, fibrofatty accumulation, ventricular arrhythmias, and sudden death	ICD defects	Ellawindy et al., 2015
	Cardiac-Specific Transgenic	Dominant Negative RB/PH (TT)	No phenotype	Not examined	Ellawindy et al., 2015

Chapter 2

Materials and Methods

2.1 Yeast-2-hybrid

All DNA fragments used for yeast-2-hybrid and forced yeast-2-hybrid analysis were amplified using PCR and cloned into pGBKT7 (bait plasmid) or pGADT7 (prey plasmid) and used in the mating yeast strains Y2HGold (bait strain, Clontech) or Y187 (prey strain). For yeast-2-hybrid screen, DSP bait containing yeast were mated with an adult human heart cDNA library (Mate n Plate Library, Clontech). Mated yeast were assayed for growth and β-galactosidase activity on selection plates. Library plasmid sequences from positive clones were PCR amplified and sequenced. To confirm interactions and search for minimal binding sites in a forced yeast-2-hybrid assay, bait and prey yeast were mated and assayed for beta-galactosidase activity according to manufacturer's instructions (Thermo Fisher). For detailed information on yeast methods and protocols refer to the yeast protocols handbook available on the Clontech homepage (www.clontech.com).

2.2 Protein expression analysis

2.2.1 Western blot

Neonatal and embryonic whole heart or adult ventricles were dissected, snap frozen in liquid nitrogen. Samples were then homogenized by polytron blade in 1% Triton-X buffer (Yang, Bowles et al. 2006). Intercalated disc enriched fractions were generated by centrifugation at 20,000g for 30 minutes followed by solubilization of Triton-X insoluble fraction in high detergent lysis buffer (NuPage LDS Buffer, Life Technologies). Equivalent amounts of protein were run on 4-12%-gradient BisTris polyacrylamide minigels using the NuPAGE buffer system (Life Technologies). The proteins were blotted overnight onto nitrocellulose. After correct transfer had been established by Ponceau red staining (Sigma-Aldrich), membranes were blocked by

incubation in 10% nonfat dry milk in washing buffer (0.9% NaCl, 9 mM Tris, pH 7.4, 0.1% Tween-20) for 1 h at RT. Blocked membranes were incubated with primary antibody overnight, washed three times in washing buffer, incubated with secondary HRP conjugated antibody for two hours, washed three times, and visualized with ECL substrate (Thermo-Fisher). Primary antibody dilution were a follows: SNAP29 (rabbit, 1:1000, Synaptic Systems), DSP (mouse, 1:1000, AbD Serotec), PKP2 (rabbit, 1:1000, Fitzgerald), JUP (goat, 1:1000, Sigma-Aldrich), DSC2 (rabbit, 1:1000, Fitzgerald), DSG 1/2 (mouse, 1:1000, Fitzgerald), Cx43 (rabbit, 1:5000, Sigma-Aldrich), NCAD (rabbit, 1:1000, Abcam), LC3A/B (rabbit, 1:1000, Cell Signaling), p62 (guinea pig, 1:1000, Progen), GAPDH (mouse, 1:5000, Santa Cruz Biotechnology), b-Actin (mouse, 1:5000, Sigma-Aldrich). Results from the chemiluminescence reaction were visualized on x-ray films. The figures show representative blots performed with extracts from one individual animal; the experiments were repeated at least two times with extracts from at least three different animals.

2.2.2 Immunostaining

Mouse heart cryosections were fixed in 100% acetone at −20°C and stained with primary antibodies against SNAP29 (rabbit, 1:100, Synaptic Systems), DSP (mouse, 1:100, AbD Serotec), NCAD (rabbit, 1:100, Abcam), perilipin (rabbit, 1:100, Cell Signaling), JUP (mouse, 1:100, Sigma-Aldrich; goat, 1:100, Santa Cruz Biotechnology), Cx43 (rabbit, 1:100, Invitrogen) sarcomeric α-actinin (mouse, 1:200, Sigma-Aldrich), LC3B (rabbit, 1:100, Cell Signaling). Sections and cells were subsequently stained with fluorescently labeled secondary antibodies (1:100, Jackson ImmunoResearch Inc.) and Hoescht nuclear stain in cases where indicated, followed by imaging using confocal microscopy (Olympus FV1000).

2.3 Mouse Models

DSP cardiac specific knockout (DSP-cKO) mice were previously generated and characterized (24108106). SNAP29 “knock-in first with conditional potential” (SNAP29-gKO) mice wer(Klionsky, Abdelmohsen et al. 2016)e obtained from the European Mutant Mouse Archive (EMMA). To generate the cardiac specific SNAP29 knockout mouse line, SNAP29-gKO mice were first bred with the flippase mouse line to remove the knockout cassette, then bred with the cardiac specific Xenopus myosin light chain 2- (XMLC2) Cre mouse line (Breckenridge, Kotecha et al. 2007). Controls for mouse studies were age matched and litter matched wildtype mice for SNAP29-gKO studies or SNAP29flox/flox Cre negative mice for SNAP29-cKO studies. All physiological studies were performed on male mice only. Mice were fed food and water ad libitum. A 24-hour diurnal light cycle was maintained, with standard 12-hour-on and off cycles. For experimental studies, adult mice were sacrificed by cervical dislocation following anesthesia by intraperitoneal injection of a mixture of ketamine (100 mg/kg) and xylazine (5 mg/kg), while the depth of anesthesia was monitored by toe pinch. Neonatal mice were sacrificed by decapitation. All animal procedures were in full compliance with the guidelines approved by the University of California-San Diego Animal Care and Use Committee and carried out in accordance with the Guide for the Care and Use of Laboratory Animals of the National Institutes of Health.

2.4 Generation of hiPSC-derived cardiomyocytes

hiPSCs were differentiated under a previously reported fully defined small molecule-based protocol (Lian, Zhang et al. 2013, Zanella and Sheikh 2016). Briefly, hiPSCs were washed once with RPMI medium before initial 48h treatment with 6μM

CHIR90021-HCl (Selleck Chemicals) in RPMI medium supplemented with B27 containing insulin (Life Technologies). Subsequently cells were washed once with RPMI medium and switched to RPMI medium supplemented with B27 without insulin (Life Technologies) and were maintained in that media for 48h. 96h after initiation conditioned medium generated by differentiating cells was combined at a 1:1 ratio with RPMI medium and B27 without insulin, supplemented with 5μM IWP-2 (Cayman Chemicals) and used to treat cells for 48h. Media were changed thereafter according to the time points established in the published protocol. On day 30 cells were switched to 75% DMEM and 25%M199 supplemented with B27 supplement containing insulin and were maintained in this medium composition until day 60.

2.5 *In vitro* knockout of SNAP29

Cardiomyocytes were prepared from 1-2 day old mice as previously described (Lyon, Mezzano et al. 2014). Adenovirus vectors containing the lacZ (AdLac-Z) and Cre recombinase (AdCre) cDNAs were prepared (UCSD Viral Vector Core) and used at multiplicity of infection 100 pfu/cell. Neonatal ventricular cardiac myocytes isolated from SNAP29-floxed mice were plated on laminin and infected with AdLacZ and AdCre, 2 days following isolation. Viral particle carrying medium was changed from cells after 24 h, and cells were subsequently maintained in a media consisting of DMEM, M199, 5% fetal bovine serum, 10% horse serum and 1% penicillin/streptomycin/glutamine for the duration of the study. To control for effects of variable baseline autophagy, cells cardiomyocytes were serum and glucose starved for 2 hours and returned to complete media for two hours prior to analysis. Cardiomyocytes were analyzed 48 hours post-infection.

2.6 *In vitro* contractility and electrophysiology measurement

Neonatal mouse cardiomyocytes were isolated as above and seeded on laminin coated E-Plate CardioECR 48 and infected with adenovirus as above. Media were refreshed with 90 µl of pre-warmed hiPSC-CMs maintenance medium at least 4 h prior to compound addition. 10 µl of compound solutions were added to the wells in a single dose per well mode. xCELLigence® RTCA CardioECR system (ACEA Biosciences, Inc.) was used to monitor cardiomyocyte attachment, viability, contraction and field potential (FP) from spontaneously beating hiPSC-CMs. Impedance (IMP) data were sampled at 2 ms (500 Hz), while FP data were collected at 0.1 ms (10 K Hz) with a bandwidth of 1 Hz to 3 KHz. Data acquisition is controlled by xCELLigence® RTCA CardioECR Data Acquisition software. In a typical experiment, a 30-min baseline of IMP and FP signals was taken by sampling hiPSC-CMs every 5 min for 20 or 60 s. Cells were then treated with vehicle control and studied compounds. The cell responses to compound were captured by measuring both IMP and FP signals every 2 min for 20 or 60 s during the first 1 h to evaluate short-term effects of compounds.

Raw data collected from IMP electrodes and ECR electrodes were analyzed offline using xCELLigence® RTCA CardioECR Data Analysis software. In order to analyze the complex wave forms derived from hiPSC-CMs contractility and FP responses, which is a measure of integrated ion channel activity, a number of parameters were derived. Contractility signal was evaluated by the beating rate (BR), beating period (BP) and beating amplitude (BAmp) parameters. Beating rate is defined as the number of beats per unit of time and is expressed as beats/min. Beating period defines the time period between two successive major peaks. BAmp is defined as the absolute (delta) Cell Index (CI) value between lowest and highest points within a beating waveform. For analysis of FP signal, the FP spike amplitude (FPAmp) is derived, which

is the absolute (delta) value in mV from lowest point of the initial spike to the highest point of the spike. The FP Duration (FPD) is defined as the time period between the negative peak of the FP spike to the maximum or minimum point of the reference wave. The reference wave can be negative or positive depending on how the cardiomyocytes are situated with respect to the FP electrodes.

2.7 *In vitro* autophagic flux measurement

Cells were transduced for overnight with BacMam GFP-LC3B (Life technologies). Cell were incubated with Lysotracker Far Red (Life Technologies) 30 minutes prior to analysis according to manufacturer details. Cells were imaged live by confocal microscopy (Olympus FV1000) 48 hours after Adeno-Cre or Adeno-LacZ infection.

2.8 Cardiac physiology measurement

2.8.1 Echocardiography

Animals are anesthetized with 5% isoflurane for 30 seconds and then maintained at 0.5% throughout the examination. The anterior chest wall is shaved and then Nair is applied to remove any remaining hair. Small needle electrodes for simultaneous electrocardiogram are inserted into one upper and one lower limb. Transthoracic echocardiography (M-mode and 2-dimensional echocardiography) is performed using the FUJIFILM VisualSonics Inc., Vevo 2100 high-resolution ultrasound system with a linear transducer of 32-55MHz. Measurements of chamber dimensions and wall thicknesses are performed. Percentage fractional shortening (%FS) is used as an indicator of systolic cardiac function.

2.8.2 Surface electrocardiography

Adult (3 months old) mice were anesthetized with 1% isoflurane. Needle electrodes (30 gauge) were inserted subcutaneously into right forearm and left leg. ECG signals were amplified using Warner Instruments DP-304 Differential Amplifier bandpass filtered between 0.1 and 100 Hz. Signal was further filtered through a Quest Scientific HumBug 50/60 Hz Noise Eliminator and digitized at 3000 Hz.

2.8.3 Telemetry ECG

Conscious ECG telemetry using an implantable wireless transmitter/receiver system (Data Sciences International/Ponemah) was performed on mice as previously described (Lyon, Mezzano et al. 2014). For implantation procedures mice were anesthetized with isoflurane (5%for induction, 1.5-2.5% for maintenance in 100% oxygen) and monitored continuously. Under the stereomicroscope, a radio transmitter (TA10ETA-F20; Datasciences) was inserted subcutaneously at the subscapular thoracic region and secured via sutures to the muscular fascia and skin. Two leads were tunneled through the subcutaneous space cranially and caudally. Transmitters were detected by receiver platforms, placed directly underneath the animal's cage, which were linked to an immediately adjacent computer. DataquestART2.0 data acquisition software (Data Sciences International) was used for digitization of the signal (at a sampling rate of 1000 Hz). Studies were recorded continuously for 72 h following 1 week recovery from the implantation. Premature beat analysis was performed on LabChart® (ADInstruments) by manual inspection of ECG telemetry traces. Premature beats were defined as a QRS originating early and without a P-wave. Interbeat interval variability analyses were performed on LabChart® (ADInstruments). Twenty minutes of recorded telemetry ECGs were analyzed using the heart rate variability module. Traces were

manually inspected to check for R wave detection accuracy and artifacts (R-R intervals shorter than 20 msec and longer than 600 msec) were excluded.

2.8.4 Ventricular tachycardia induction

Invasive intracardiac electrophysiology was studied in adult mice (3 months old) following a previously established protocol with some modifications (Hong, Yang et al. 2014). Mice were anesthetized with 1.5% isoflurane in 100% oxygen; body temperature was maintained at 37 °C with a heating pad; and respiration was maintained using a respirator connected to an endotracheal tube placed into the mouse trachea. ECGs were recorded using PowerLab (ADInstruments) during the whole experimental procedure. After lateral thoracotomy, the heart was visualized, and an 8-electrode catheter was inserted into the heart through the superior vena cava for pacing. A constant current stimulus isolator (FE180, ADInstruments, Colorado Springs, CO) was used to deliver pacing currents, which was interfaced with a software-driven programmed electrical stimulator (LabChart Pro, ADInstruments, Colorado Springs, CO). Pacing thresholds were then determined, and stimulation was delivered at a 0.3- to 0.4-ms pulse width at twice the capture threshold. Standard single, double, and triple extrastimulations were performed. A drive cycle length of 100 ms (S1) was followed by S2 decremented by 2 ms until the ventricular effective refractory period was reached. After this, a train of programmed stimulation with one, two, or three extra stimuli after S1 (S1–S4) was performed and repeated every 1 s for 30 min to determine the incidence and frequency of induced VT. After baseline experiments, isoproterenol (2.5 mg kg^{-1} body weight) was injected i.p., and 1 min was allowed to elapse for stabilization of heart rate before the same S1–S4 pacing protocol was repeated. Nonsustained VT was defined as four to

nine consecutive beats, and sustained VT was defined as >9 QRS complexes not preceded by supraventricular activity. LabChart was used for data analysis.

2.9 Cardiac histological analysis

Whole hearts were paraffin embedded and 10μM transverse sections were obtained sequentially. Sections were stained with hematoxylin and eosin or Masson's trichrome (Sigma–Aldrich, St. Louis, MO, USA) according to manufacturer's instructions. For oil red O staining, hearts were embedded in OCT and 10mm sectioned were obtained sequentially. Sections were stained for oil red O and mounted in fluorescent mounting medium. Sections were imaged using the NanoZoomer 2.OHT Slide Scanning system (Hamamatsu, Hamamatsu City, Japan).

2.10 Ultrastructural Analysis

Deeply anesthetized adult mice were cervically dislocated and perfused with a fixation buffer containing 2% paraformaldehyde and 2.5% glutaraldehyde in 0.15 M sodium cacodylate buffered to pH 7.4. Fixed hearts were excised and only right and left ventricular free walls were processed for electron microscopy as previously described. Ultrathin sections were subsequently stained with 2% uranyl acetate and Sato lead as previously described. Electron micrograph images were obtained with a FEI Tecnai Spirit G2 BioTWIN transmission electron microscope.

2.11 Statistical analysis

Data presented in the text and figures are expressed as mean values ± SEM. Significance was evaluated by two-tailed Student's t-test or repeated-measures ANOVA. Significance of categorical data was evaluated for significance by Pearson's chi-squared

test. For Kaplan–Meier survival analysis, significance was evaluated by the log-rank test. $P < 0.05$ was considered statistically significant.

Chapter 3

Discovery of SNAP29 as a Novel Desmosomal Protein in the Heart

3.1 SNAP29 is a novel DSP interacting protein

To identify novel DSP-interacting protein in the heart, a yeast-2-hybrid screen was performed using DSP as bait. The N-terminal region of DSP has been previously shown to interact with other desmosomal proteins and was therefore selected to perform the interaction screen. Human DSP cDNA coding for amino acids 500-1030 was cloned into the yeast bait expression vector, pGBKT7 (Fig. 2A) and transformed into the Y2HGold mating strain. The DSP bait was screened against an adult human heart cDNA library in a yeast-2-hybrid mating system. Four selection markers were used to identify positive clones: (i) histidine production, (ii) adenine production, (iii) β-galactosidase activity, and (iv) aureobasidin A resistance. 44 colonies grew and turned blue on quadruple drop out media; all colonies were sequenced. Full length Synaptosomal associated protein 29 (SNAP29) (Fig. 2B) was identified during screening of positive clones. Previous studies have identified a link between SNAP29 and protein degradation mechanisms, specifically autophagy (Itakura, Kishi-Itakura et al. 2012) suggesting that it could have an effect on desmosomal protein degradation mechanisms.

To confirm the direct interaction between DSP and SNAP29, forced yeast 2-hybrid was performed with the original DSP N-terminus bait and full length SNAP29 as prey. β-galactosidase activity quantification revealed significantly higher activity and therefore interaction between DSP and SNAP29 compared to negative controls (Fig. 2C). To determine if SNAP29 colocalizes endogenously with DSP in the heart, immunofluorescence microscopy was performed on ventricular tissue sections from adult mouse and human hearts and revealed SNAP29 present with DSP at the ICD (Fig. 3).

3.2 SNAP29 expression is reduced in DSP deficient models

3.2.1 SNAP29 expression is reduced in a desmoplakin-deficient mouse model

To determine whether the localization of SNAP29 at the ICD *in vivo* requires DSP, ventricular heart tissue from our biventricular mouse model of ARVC caused by cardiac specific loss of DSP (DSP-cKO) (Lyon, Mezzano et al. 2014) was analyzed for SNAP29 expression. Immunofluorescence microscopy performed on DSP-cKO heart cryosections revealed the striking loss of SNAP29 from ICDs lacking DSP, which were identified by JUP staining, compared to littermate controls (Fig. 4A). Western blot analysis of the triton-X100 insoluble fraction which is ICD-enriched in adult DSP-cKO mouse hearts revealed that SNAP29 is significantly reduced (%, n=3) (Fig. 4B). These results suggest a molecular link between SNAP29 and DSP at the cardiac ICD.

3.2.2 SNAP29 expression is reduced in ARVC hiPSC derived cardiomyocytes

To interrogate SNAP29 expression in a human setting, human induced pluripotent stem cell derived cardiomyocytes (hiPSC-CMs) were generated from patients with ARVC harboring desmosomal protein mutations as well as from non-diseased human samples. The three hiPSC-CM lines analyzed were ARVC-PKP2 (c.1171-2A>G), ARVC-DSG2 (c.1498C>A), and Control. Western blot analysis of these cell lines revealed striking loss of SNAP29 specifically in PKP2-mutant hiPSC-CMs which also were deficient in desmosomal protein expression (Fig. 4C). Interestingly, SNAP29 expression was not reduced in DSG2-mutant hiPSC-CMs (Fig. 4C). These findings suggest that SNAP29 expression may be dependent on desmosomal protein expression in human cardiomyocytes.

Chapters 3-6, in part are currently being prepared for submission for publication of the material. Pellman, Jason; Lyon, Robert; Liang, Yan; Mezzano, Valeria; Zanella,

Fabian; Zhang, Jing; Nigam, Vishal; Gu, Yusu; Dalton, Nancy; Peterson, Kirk L.; Sheikh, Farah. The dissertation author was the primary investigator and author of this material.

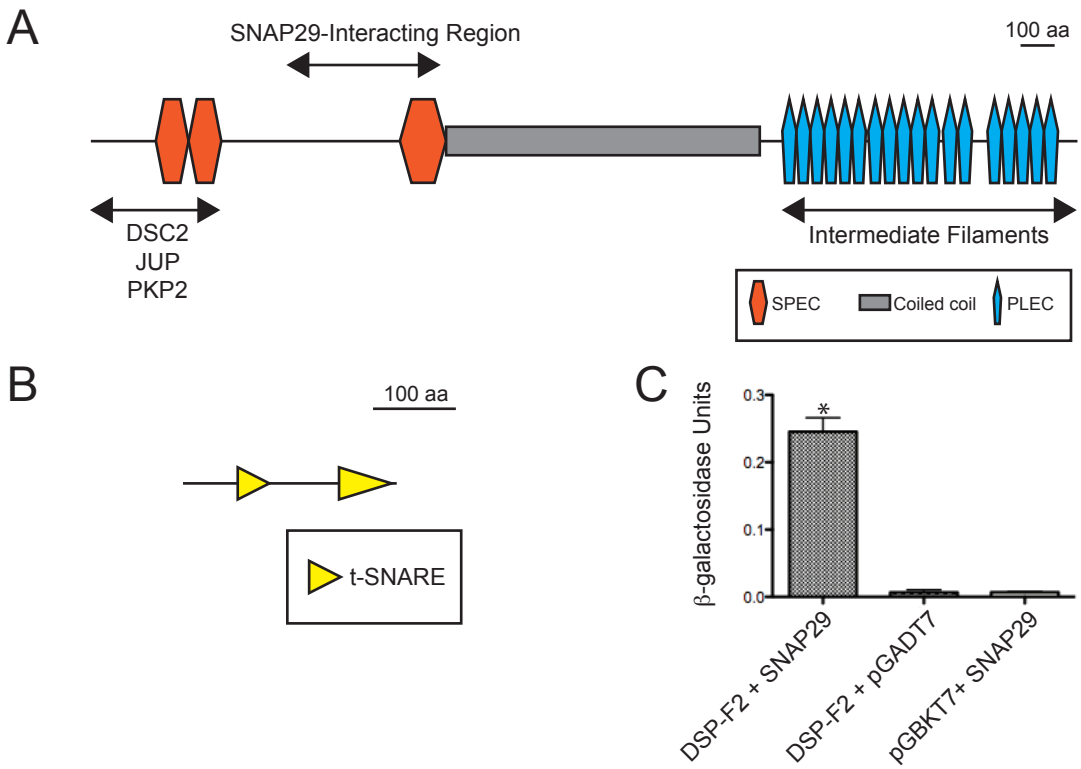


Figure 2. Identification of the novel cardiac desmosomal interacting protein SNAP29 in a yeast-2-hybrid screen using DSP as bait. (A) Diagram of DSP with region of N-terminus (amino acids 500-1030) used for construction of bait plasmid DSP-F2 in pGBKT7. (B) Diagram of full length SNAP29 region identified in yeast-2-hybrid screen using DSP-F2 as bait. (C) Assay of β-galactosidase reporter activity in mated yeast expressing DSP-F2 and SNAP29 yeast-2-hybrid constructs. DSP-F2 mated with empty prey vector (pGADT7) and SNAP29 mated with empty bait vector (pGBKT7) are negative controls. * = $p<0.05$

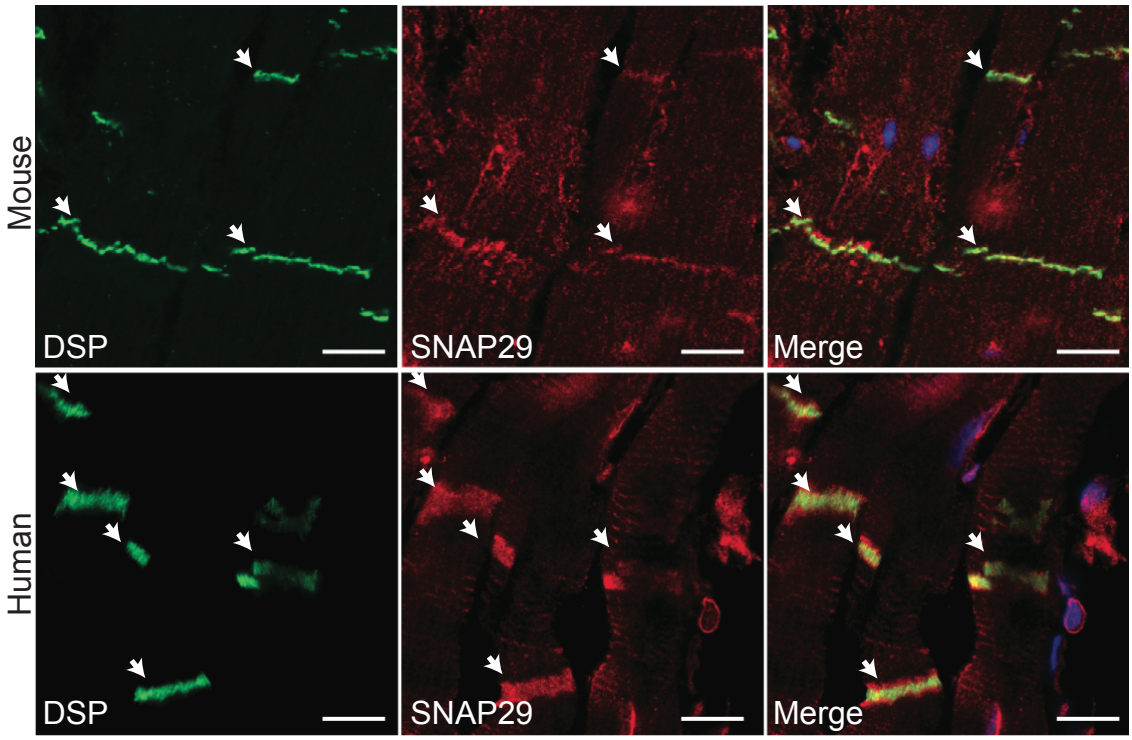


Figure 3. SNAP29 colocalizes with DSP at the ICD in adult mouse and human hearts. Immunofluorescence staining of SNAP29 and DSP in 2-month-old wildtype mouse heart ventricular or adult human heart ventricular cryosections were stained with antibodies against SNAP29 (red) and DSP (green) and counterstained with DAPI (blue). White arrowheads mark colocalization at ICDs. Scale bar = 10 μm

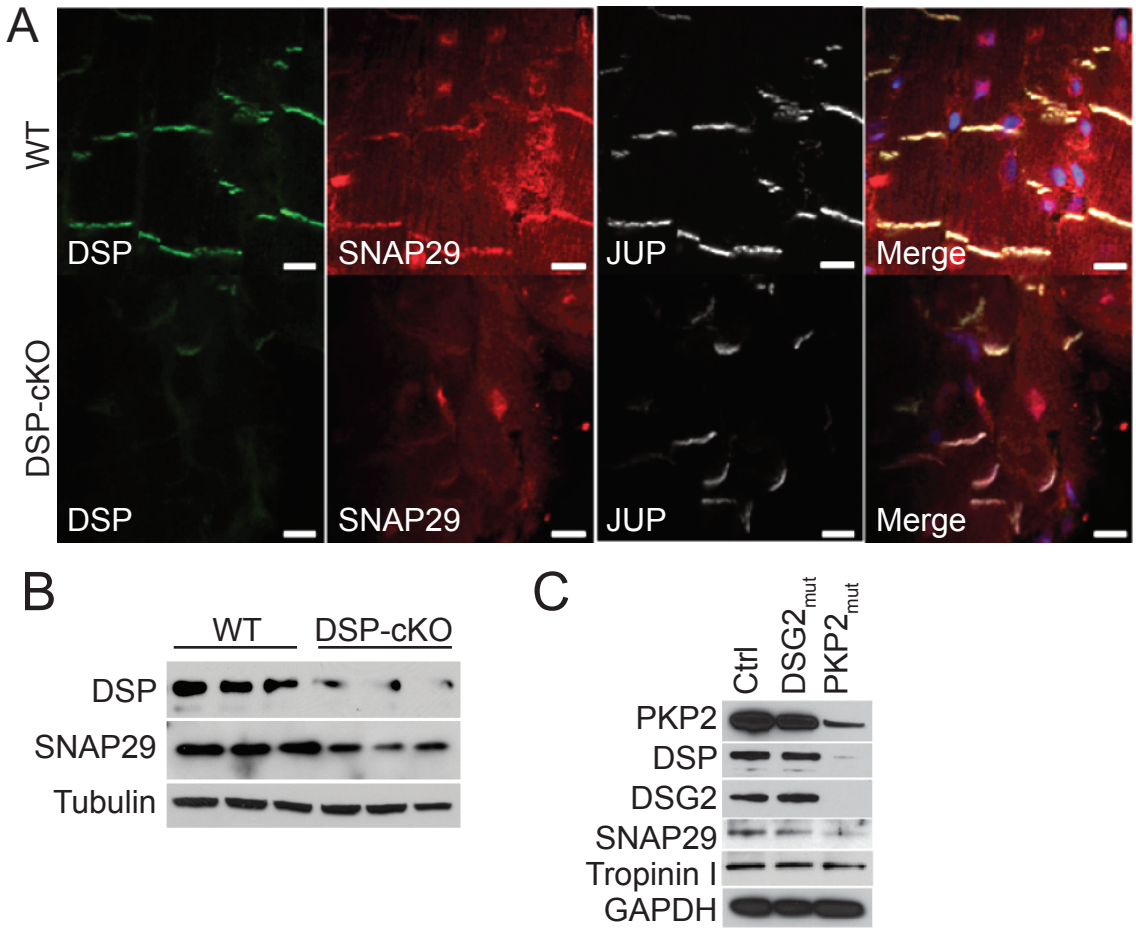


Figure 4. SNAP29 expression is reduced in a DSP-deficient mouse model and a hiPSC-derived cardiomyocyte model. (A) Immunofluorescence staining of 6-week-old hearts from DSP-cKO mice for SNAP29 (red), DSP (green), and JUP (white) and counterstained with DAPI (blue). (B) Western blot analysis of insoluble fraction of 6-week-old hearts from DSP-cKO mice for SNAP29 and DSP. Tubulin was used as a loading control. (C) Western blot analysis of cell lysates from hiPSC-derived cardiomyocytes from control and ARVC patient (ARVC-DSG2 and ARVC-PKP2) donors.

Chapter 4

The Effects of Cardiomyocyte-Specific Loss of SNAP29 in Mouse *in vivo*

4.1 Cardiac Characterization of a Cardiac-Specific SNAP29 Knockout (SNAP29-cKO) Mouse

4.1.1 SNAP29 expression is reduced in adult SNAP29-cKO mouse hearts

To determine the effects of cardiac specific loss of SNAP29, SNAP29-floxed mice (Fig. 5A) were crossed with the early and cardiac specific Xenopus myosin light chain 2-Cre recombinase (XMLC2-Cre) mouse line (Breckenridge, Kotecha et al. 2007). A breeding strategy was utilized to generate homozygous SNAP29-cKO (SNAP29flox/flox;XMLC2-Cre+), heterozygous SNAP29-cKO (SNAP29wt/flox;XMLC2-Cre+) and littermate controls (SNAP29flox/flox;XMLC2-Cre-) (Fig. 5B). Homozygous SNAP29-cKO and littermate control mice are used for all studies. SNAP29-cKO mice are born at Mendelian ratios (data not shown) and survive to adulthood but exhibit preliminary evidence of premature death at 9 months of age (Fig. 5C). To determine the efficiency of knock out in SNAP29-cKO hearts, western blot analysis was performed on hearts from 1 month old mice. A significant reduction (64±6%, $p < 0.05$) in SNAP29 levels was observed in whole ventricle samples (Fig. 5D).

4.1.2 SNAP29-cKO mice exhibit baseline and inducible ventricular arrhythmias

To determine whether SNAP29-cKO mice exhibit the characteristic ventricular arrhythmias of ARVC (Haugaa, Haland et al. 2016), telemetry electrocardiography (ECG) was performed on conscious and freely moving 3-month-old mice. Analysis of ECG recordings revealed significantly higher rates of spontaneous premature ventricular contractions (PVCs) in SNAP29-cKO mice compared to littermate controls (Fig. 6A). This parallels the high rates of PVCs observed in patients with ARVC (Sen-Chowdhry, Syrris et al. 2007, Thiene, Corrado et al. 2007).

To determine whether SNAP29-cKO mice exhibit the inducible ventricular arrhythmias characteristic of ARVC, 3 month old SNAP29-cKO were subjected to intracardiac ventricular burst pacing. As is evident from representative ECG recording, sinus rhythm resumed immediately after ectopic pacing in WT mice (Fig. 6B). However, sustained monomorphic ventricular tachycardia (VT) ensued after pacing in SNAP29-cKO hearts (Fig. 6B). VT was significantly more inducible in SNAP29-cKO mice compared to littermate controls (Fig. 6B). In patients with ARVC, VT inducibility is associated with increased risk of future adverse cardiac events (Saguner, Medeiros-Domingo et al. 2013), suggesting that the hearts of SNAP29-cKO mice may be more disease prone

4.1.3 SNAP29-cKO mice exhibit lipid accumulation in right ventricle

To determine whether SNAP29-cKO mouse hearts display the fatty accumulation observed in human ARVC (Fujita, Terasaki et al. 2008), oil red O staining was performed. Punctate oil red O staining was observed in cardiomyocytes throughout the right ventricle of SNAP29-cKO hearts and not in littermate controls (Fig. 7). Oil red O staining was not observed in the left ventricle or either atrium (Fig. 7).

4.1.4 Cardiac morphology, fibrosis, and function are not affected by cardiomyocyte loss of SNAP29

To determine whether SNAP29-cKO mice displayed other hallmarks of ARVC, SNAP29-cKO mice were assessed for morphological, histological, and functional features of ARVC. At 3 months of age, morphological analysis of SNAP29-cKO hearts revealed no significant differences from littermate controls in terms of gross morphology (Fig. 8A), heart weight to body weight ratio or heart weight to tibia length ratio (Fig. 8B).

Histological analysis by Masson's trichrome stain revealed no signs cardiac fibrosis (Fig. 8C). Transthoracic echocardiography revealed no differences in cardiac parameters or function in SNAP29-cKO hearts compared to littermate controls (Fig. 8D). Follow up analysis of older mice at 8 months of age also revealed no differences in cardiac parameters or morphology compared to littermate controls (Fig. 8D). These findings suggest that loss of cardiomyocyte SNAP29 does not contribute to changes in cardiac morphology, fibrosis or function.

4.1.5 SNAP29-cKO mice have selectively reduced desmosomal and gap junction protein levels

To determine how loss of SNAP29 in the heart affect ICD protein levels, western blot was performed for desmosomal, gap junction, an FAJ proteins in ventricular tissue from adult SNAP29-cKO mice. At 3 months of age, a significant reduction in DSP and PKP2 was observed, though the remaining desmosomal proteins were not affected (Fig. 9). Interestingly, the gap junction protein Cx43 was also reduced (Fig. 9). No changes were observed in FAJ protein levels (Fig. 9), suggesting loss of SNAP29 leads to specific effects on select desmosomal and gap junction proteins.

4.2 Protein Degradation Defects in SNAP29-cKO Heart

4.2.1 Markers of autophagy accumulate in SNAP29-cKO hearts

Previous studies in cell lines and fruit fly models have identified a potential role for SNAP29 in protein degradation, specifically as a mediator of autophagy (Itakura, Kishi-Itakura et al. 2012, Takats, Nagy et al. 2013). To determine how loss of SNAP29 in the heart affects autophagy, western blot, immunofluorescence microscopy, and transmission electron microscopy analysis were performed. Levels of the UPS-

autophagy crosstalk protein p62 were increased at 3 months of age (Fig. 10A), suggesting an elevated amount of proteins entering the autophagy protein degradation pathway. Immunofluorescence analysis further revealed that LC3B was localized at the ICD in SNAP29-cKO mouse heart while no LC3B signal was observed in littermate controls (Fig. 10B). TEM analysis of these hearts revealed ultrastructural defects at the ICD, specifically accumulation of multi-membrane vesicles similar to autophagosomes and autolysosomes (Fig. 10B), suggesting that the elevated LC3B is due to ICD-specific autophagosome accumulation.

4.2.2 Characterization of protein degradation in a model of ARVC

To determine whether autophagy is altered in ARVC, hearts from our DSP-cKO mouse model of ARVC (Lyon, Mezzano et al. 2014) were analyzed. Western blot analysis of DSP-cKO hearts revealed accumulation of LC3B and p62 (Fig. 11A). Immunofluorescence microscopy of DSP-cKO ventricular cryosections revealed the striking appearance of LC3B specifically at ICDs lacking DSP, which are marked by JUP (Fig. 11B). TEM analysis revealed the presence of multi-membrane vesicles similar to autophagosomes and autolyososomes specifically at the ICD in DSP-cKO mouse hearts and not in controls (Fig. 11B). These findings mirror the effects on autophagy observed in SNAP29-cKO hearts (Fig. 10). These findings in addition to the loss of SNAP29 at the ICD (Fig. 4A/B) suggest that loss of SNAP29 leads to accumulation of autophagosomes specifically at the ICD in DSP-cKO mouse hearts.

4.2.3 Characterization of heart and skin disease-associated DSP mutations

The region of DSP that SNAP29 binds is known to be a “hotspot” for desmosomal interactions and also contains heart and skin disease associated mutations

(Smith and Fuchs 1998, Boyden, Kam et al. 2016). The DSP mutations, Q616P and H618P, associated with the heart and skin disease erythrokeratodermia-cardiomyopathy syndrome (Boyden, Kam et al. 2016) were replicated in the DSP N-terminal yeast expression construct used for the initial yeast-2-hybrid screen (Fig. 12A). These constructs were tested against wildtype full length SNAP29 (Fig. 12B). β-galactosidase activity quantification revealed significantly lower activity between mutant DSP and wildtype SNAP29 (Fig. 12C), suggesting that these desmosomal mutations may lead to reduced interaction with SNAP29.

Chapters 3-6, in part are currently being prepared for submission for publication of the material. Pellman, Jason; Lyon, Robert; Liang, Yan; Mezzano, Valeria; Zanella, Fabian; Zhang, Jing; Nigam, Vishal; Gu, Yusu; Dalton, Nancy; Peterson, Kirk L.; Sheikh, Farah. The dissertation author was the primary investigator and author of this material.

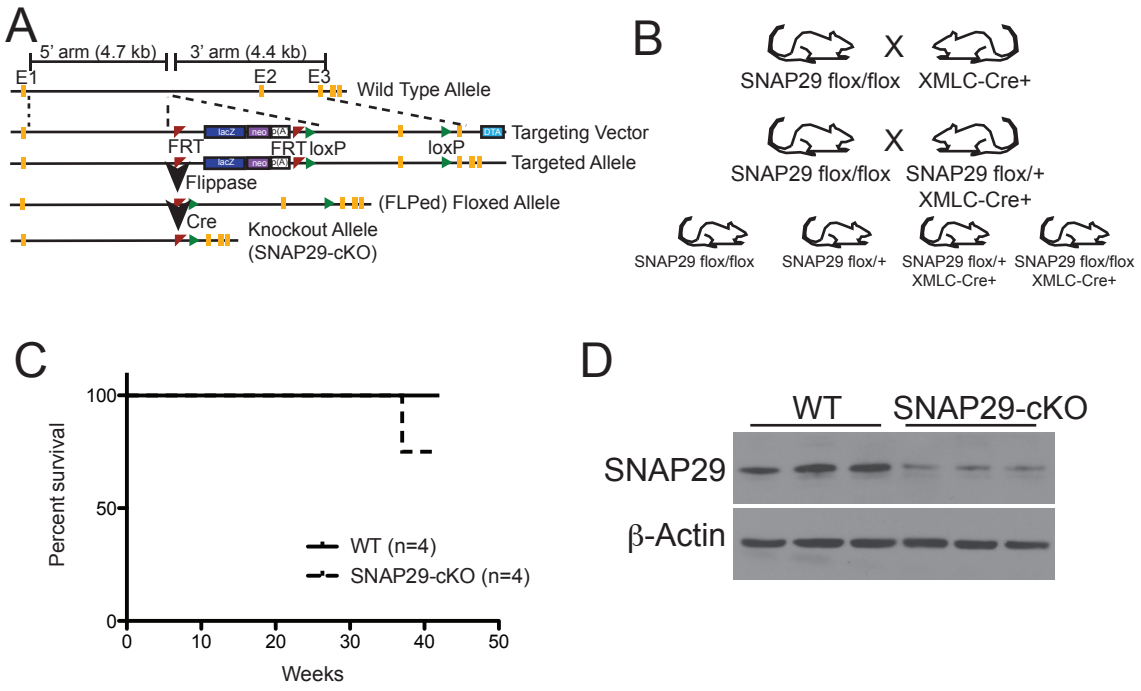


Figure 5. Generation, expression, and survival of a novel cardiac specific SNAP29 knockout (SNAP29-cKO) mouse line. (A) Genetic construct used to generate SNAP29-floxed and knockout alleles. (B) Breeding strategy to generate SNAP29-cKO (SNAP29flox/flox;XMLC2-Cre+) and littermate control (SNAP29flox/flox;XMLC2-Cre-) mice. (C) Kaplan-Meier survival curve for SNAP29-cKO mice and littermate controls. (D) Western blot analysis of 1-month-old hearts from SNAP29-cKO mice for SNAP29. β-actin was used as a loading control.

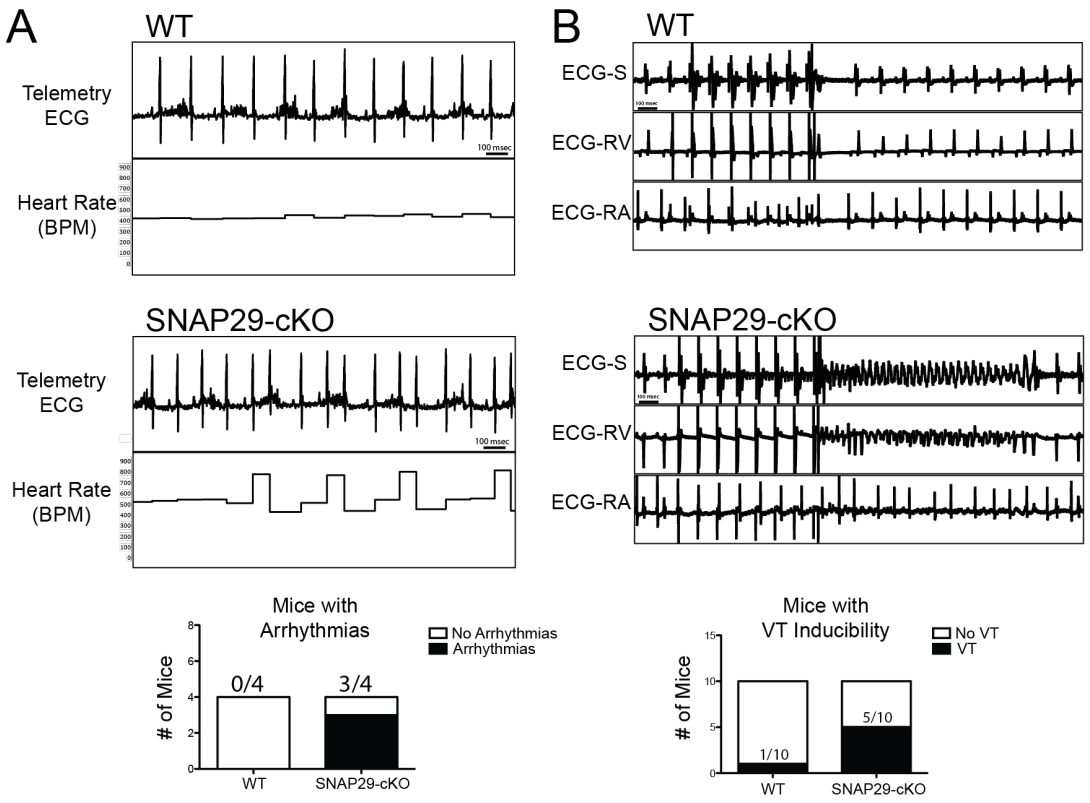


Figure 6. Telemetry electrocardiography analysis of adult SNAP29-cKO mice. (A) Representative telemetry ECG tracing from conscious 3-month-old SNAP29-cKO mice and littermate controls. Premature ventricular contractions (PVC) are marked by red arrows. (B) Representative surface and intracardiac ECG tracings from anesthetized 3-month-old SNAP29-cKO mice and littermate controls undergoing ventricular ectopic stimulation. Prevalence of VT in stimulated 3-month-old SNAP29-cKO mice and littermate controls below.

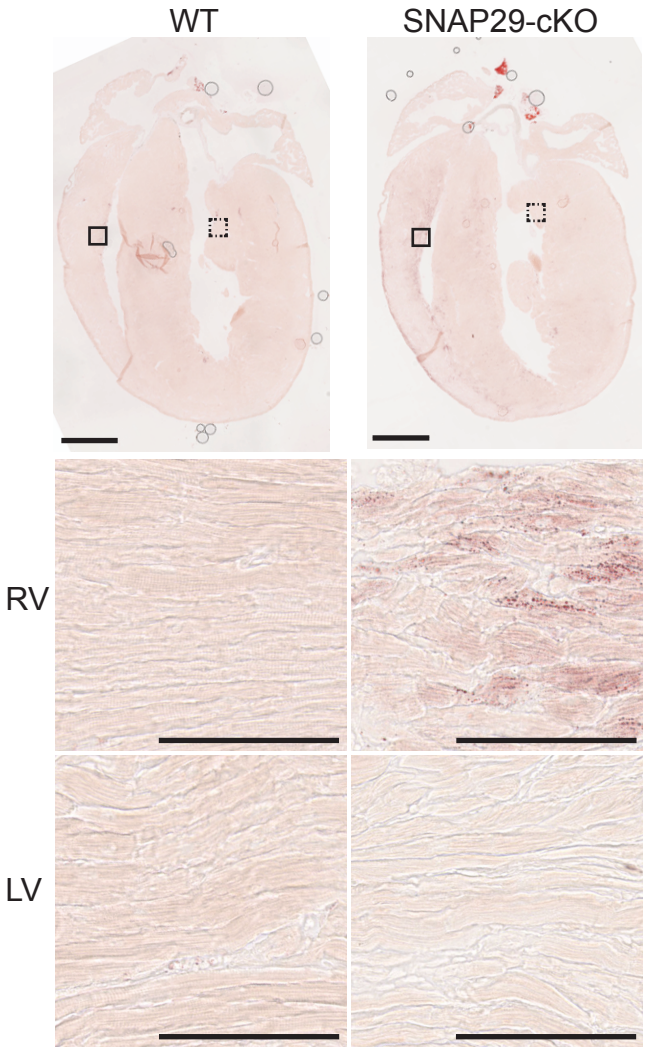
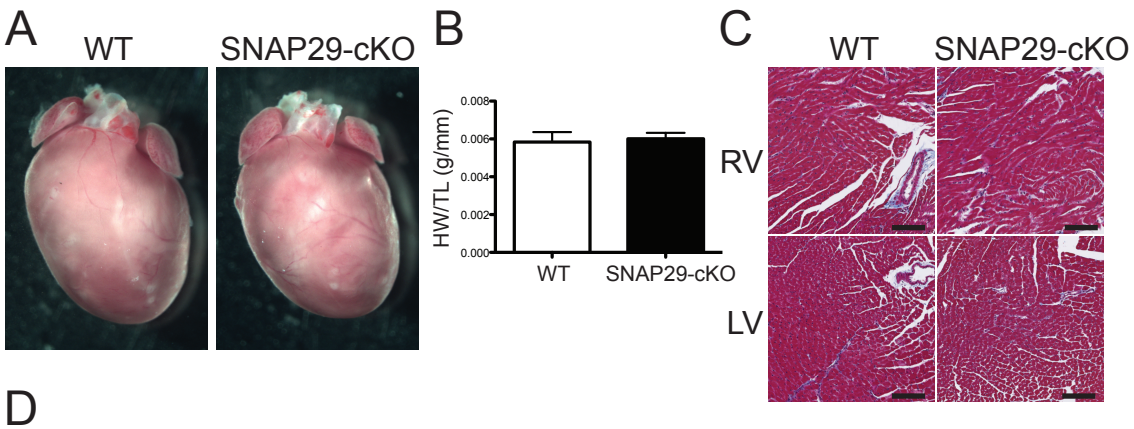


Figure 7. Lipid droplet accumulation in SNAP29-cKO hearts. Oil red O staining of cryosections from 3-month-old SNAP29-cKO hearts. RV = right ventricle from solid boxed area; LV = left ventricle from dashed boxed area; upper scale bar = 1 mm; lower scale bar = 100 μm



D

	3 months			8 months		
	WT	SNAP29-cKO	p-value	WT	SNAP29-cKO	p-value
BW (g)	39.8±6.7	38.8±2.4	0.79	38±4.1	45.5±12.5	0.32
HR (bpm)	612±70	629±62	0.73	591±103	636±36	0.46
LVIDd (mm)	3.33±0.29	3.28±0.29	0.81	3.04±0.5	3.41±0.42	0.31
LVIDs (mm)	2.2±0.21	2.12±0.36	0.74	2±0.34	2.2±0.23	0.38
FS (%)	34.1±3.4	35.7±5.6	0.66	33.9±7	35.3±4.4	0.75
IVSd (mm)	0.85±0.07	0.85±0.06	0.96	1.01±0.18	0.87±0.05	0.20
LVPWd (mm)	0.89±0.13	0.82±0.04	0.39	0.96±0.18	0.79±0.06	0.15
LVM/BW (mg/g)	2.53±0.33	2.38±0.38	0.57	2.78±0.76	2.19±0.52	0.25

Figure 8. Cardiac morphology, fibrosis, and function of SNAP29-cKO mice. (A) Wholemount images of representative 3-month-old SNAP29-cKO mouse heart with littermate control. (B) Heart weight to tibia length rations of SNAP29-cKO mouse hearts and littermate controls. (C) Masson's trichrome stain of right (RV) and left (LV) ventricles of 3-month-old SNAP29-cKO mouse heart with littermate control. (D) Echocardiography analysis of 3-month-old and 8 month-old of SNAP29-cKO mouse hearts with littermate controls.

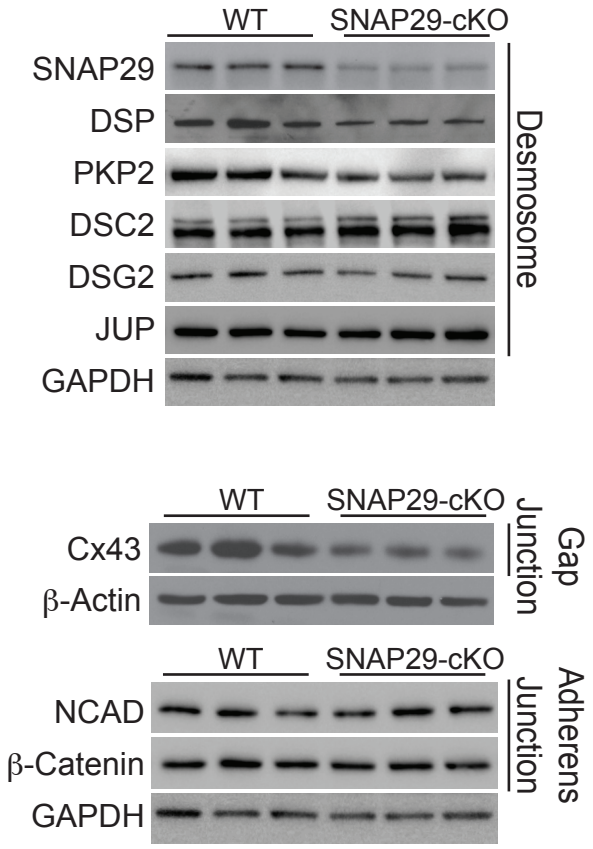


Figure 9. Expression levels of ICD proteins in SNAP29-cKO mouse hearts. Western blot analysis of desmosomal, gap junction, and FAJ proteins in 3-month-old SNAP29-cKO hearts. GAPDH was used as a loading control.

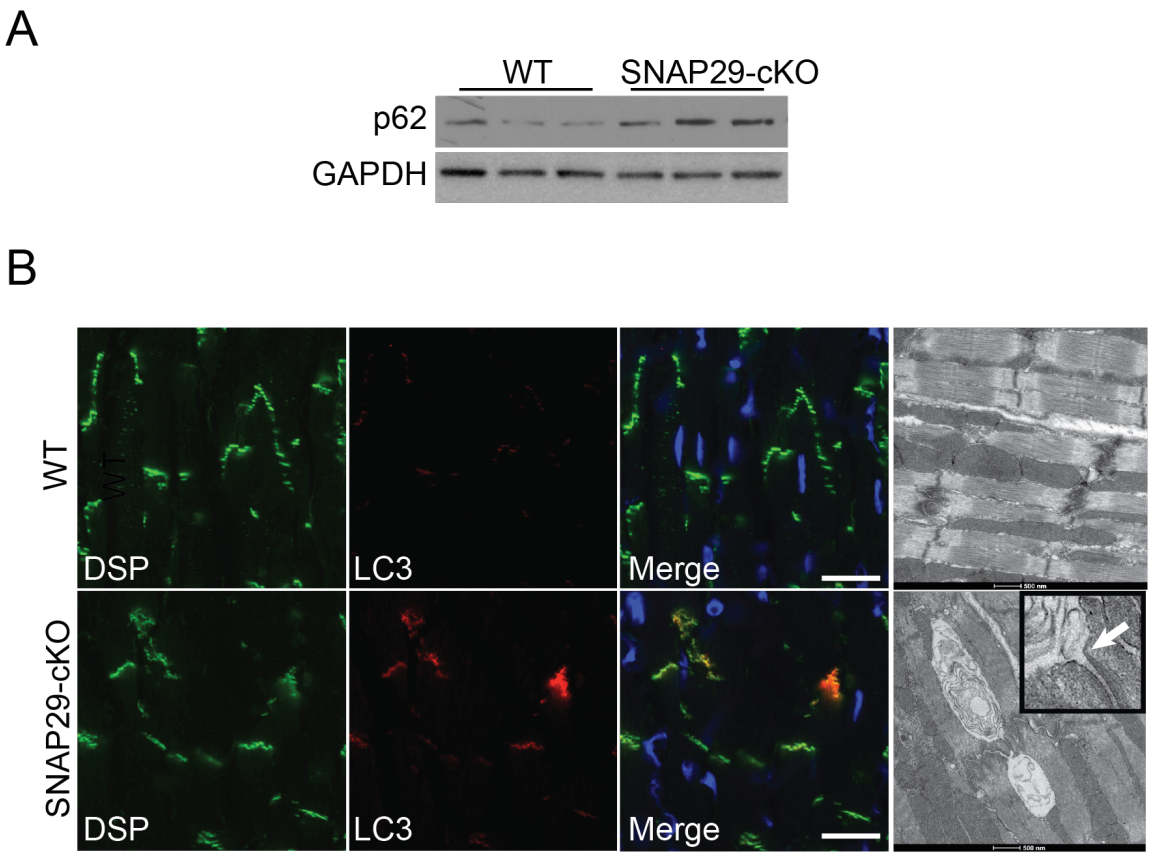


Figure 10. Autophagy defects in SNAP29-cKO mouse hearts. (A) Western blot analysis of 3-month-old SNAP29-cKO mouse hearts for LC3B and p62. GAPDH was used as a loading control. (B) Immunofluorescence staining of 3-month-old hearts from SNAP29-cKO mice for LC3B (red), DSP (green), and JUP (white) and counterstained with DAPI (blue). Scale bar = 10 μm. At right, transmission electron micrographs of intercalated discs of 3-month-old SNAP29-cKO hearts. Multi-membrane structures in proximity to the ICD are marked by white arrow. Scale bar = 500 nm.

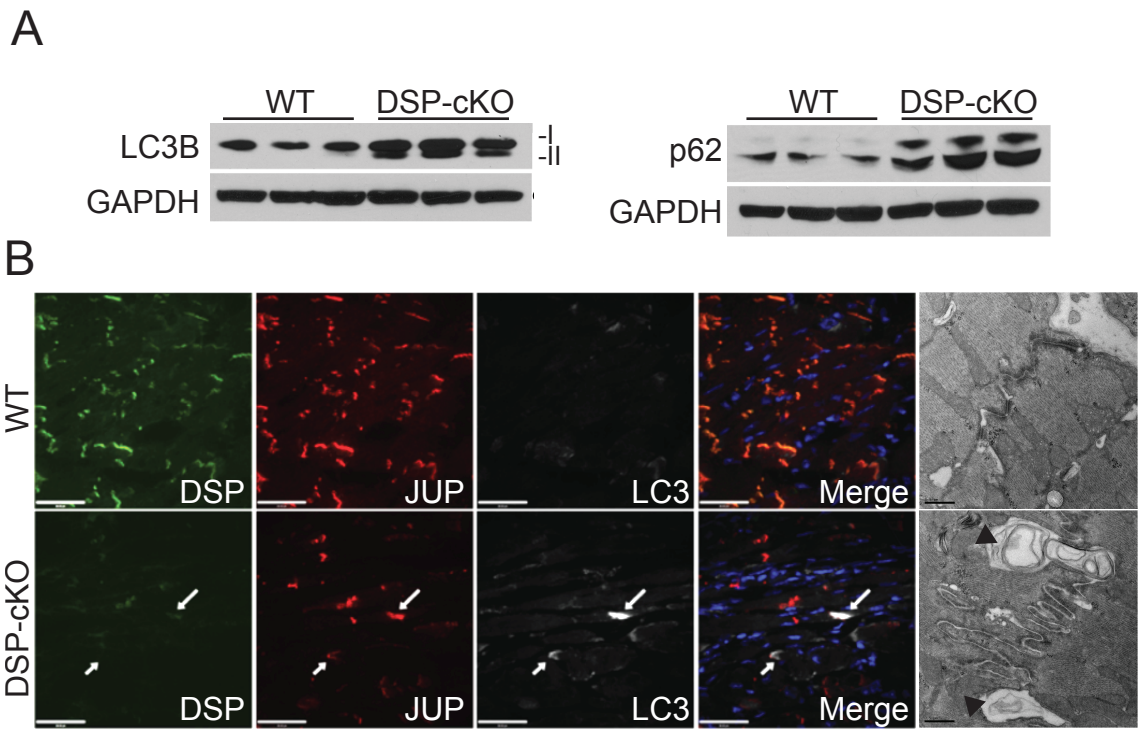


Figure 11. Autophagy markers are elevated in DSP-cKO mouse hearts. (A) Western blot analysis of 6-week-old hearts from DSP-cKO mice for LC3B and p62. GAPDH was used as a loading control. (B) Immunofluorescence staining of 6-week-old hearts from DSP-cKO mice for LC3B (red), DSP (green), and JUP (white) and counterstained with DAPI (blue). ICD localized LC3B marked by white arrows. Scale bar = 10 μm. Transmission electron micrographs at right of intercalated discs of 6-week-old DSP-cKO hearts. Multi-membrane structures are marked by black arrowheads. Scale bar = 500 nm.

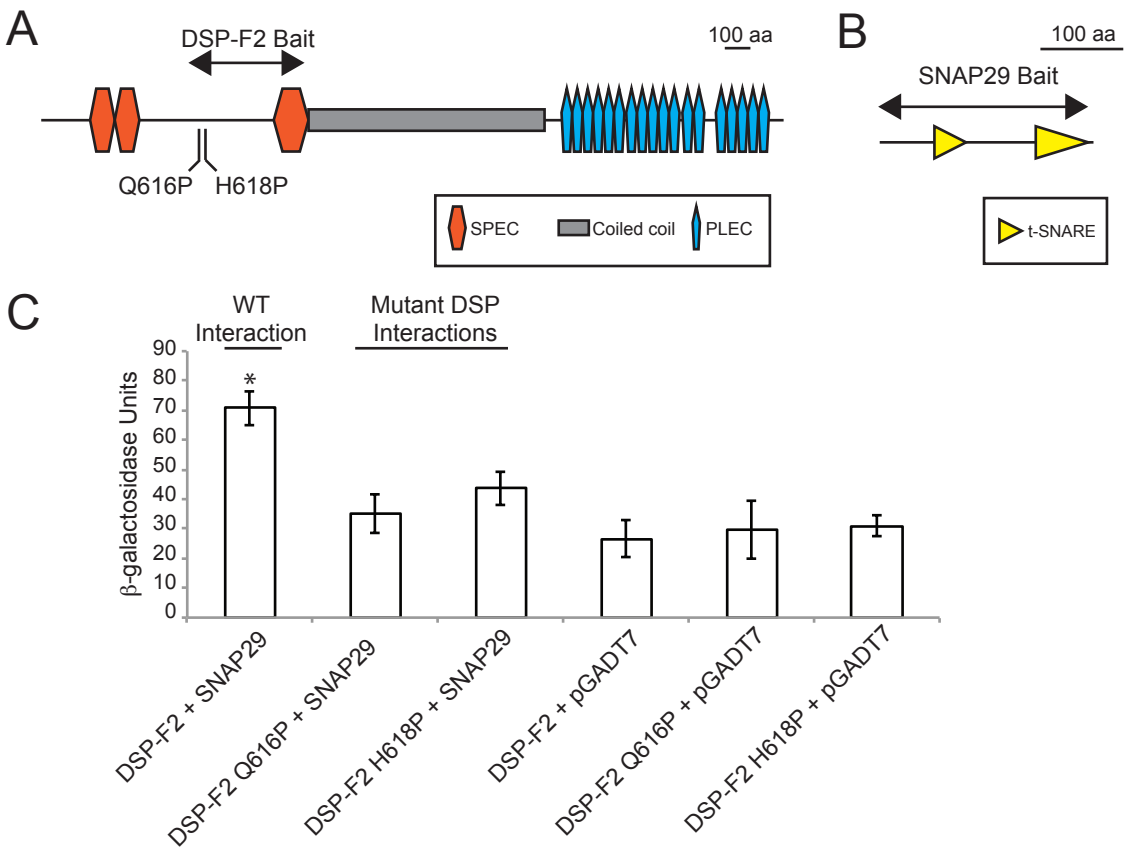


Figure 12. Disease-associated DSP mutations disrupt their interaction with SNAP29. (A) Diagram of DSP region (amino acids 500-1030) and mutations tested. (B) Diagram of SNAP29 region tested (full length). (C) Assay of β-galactosidase reporter activity in mated yeast expressing wildtype or mutant DSP-F2 and SNAP29 yeast-2-hybrid constructs. Wildtype or mutant DSP-F2 mated with empty prey vector (pGADT7) are negative controls. * = $p<0.05$

Chapter 5

Loss of SNAP29 in Neonatal Mouse Cardiomyocytes *in vitro*

5.1 Characterization of Cardiomyocyte Function following loss of SNAP29

5.1.1 Desmosomal and gap junction proteins are specifically reduced in SNAP29 KO CMs

To determine the primary effects of knockout of SNAP29 in cardiomyocytes, desmosomal, gap junction, and FAJ protein levels were assessed in SNAP29flox/flox neonatal cardiomyocytes infected by Ad-Cre or Ad-LacZ as control. To control for starvation induced autophagy in culture, cardiomyocytes were serum- and glucose-starved then returned to complete medium for 2 hours prior to collection. Western blot analysis revealed efficient loss of SNAP29 at 48 hours post infection (Fig. 13). All measured desmosomal and gap junction proteins were strikingly reduced with only minor effects on FAJ proteins in Ad-Cre infected neonatal cardiomyocytes compared to controls (Fig. 13), suggesting that SNAP29 has specific effects on the desmosome and gap junction *in vitro*. To determine the primary effects of knockout of SNAP29 on protein degradation in cardiomyocytes, western blot was performed in these cells for markers of autophagy. Western blot analysis revealed accumulation of the autophagosome marker LC3B and the UPS-autophagy crosstalk protein p62 (Fig. 13). These findings reveal that loss of SNAP29 in cardiomyocytes in vitro leads to molecular defects consistent with the SNAP29-cKO mouse, suggesting that these are primary consequences of loss of SNAP29.

5.1.2 SNAP29 knockout CMs exhibit baseline arrhythmias

To determine the functional effects of loss of SNAP29 *in vitro*, neonatal cardiomyocytes were grown in the xCELLigence® RTCA CardioECR system and monitored for electrical activity and contractility by measuring electrical field potentials and cell-induced impedence, respectively. Analysis of baseline electrical firing and

contractility rates revealed significantly increased variability as measured by coefficient of variance in SNAP29 deficient CMs (Fig. 14A/B). These effects were observed independent of any changes in average firing rate (Fig. 14C), suggesting that loss of SNAP29 has detrimental effects on cardiomyocyte electrophysiology independent of any histological changes in the heart.

5.1.3 Autophagic flux is maintained in SNAP29 KO CMs

Loss of cardiomyocyte SNAP29 appears to lead to accumulation of LC3 positive vesicles (Fig. 10B). This can be caused by either an increase in activation of autophagy (faster rate or autophagosome formation) or a reduction in autophagic flux (reduced rate of autophagosome clearance) (Klionsky, Abdelmohsen et al. 2016). To determine if loss of SNAP29 leads to reduced autophagic flux, SNAP29-deficient cardiomyocytes were infected with BacMam virus containing the autophagosome reporter LC3-GFP (green) and incubated with lysotracker (red) to stain lysosomes. In this system, autophagosomes are marked by LC3-GFP only and appear green while autophagosome that have fused with the lysosome, called autolysosomes, are both LC3-GFP and lysotracker positive and appear yellow. Analysis of SNAP29-deficient cardiomyocytes in this system reveal increased total levels of autophagic vacuoles (Fig. 15A/B). This occurred without effects on autophagic flux, as measured by the ratio between autophagosomes and lysosomes (Fig.15D). Altogether this suggests that autophagy is upregulated in SNAP29-deficient cardiomyocytes and that autophagic flux is not blocked.

5.1.4 Autophagy inhibition is sufficient to reverse desmosomal protein loss in SNAP29 KO CMs

To assess the requirement for autophagy for the desmosomal and gap junction protein loss in SNAP29 deficient CMs, infected CMs were treated for with the lysosomal inhibitor, chloroquine (CQ), which effectively blocks degradation of proteins through autophagy (Klionsky, Abdelmohsen et al. 2016). Analysis of cardiomyocytes revealed restoration of DSP levels in SNAP29 deficient CMs after treatment with CQ (Fig. 16), suggesting that DSP loss in this model is autophagy dependent.

Chapters 3-6, in part are currently being prepared for submission for publication of the material. Pellman, Jason; Lyon, Robert; Liang, Yan; Mezzano, Valeria; Zanella, Fabian; Zhang, Jing; Nigam, Vishal; Gu, Yusu; Dalton, Nancy; Peterson, Kirk L.; Sheikh, Farah. The dissertation author was the primary investigator and author of this material.

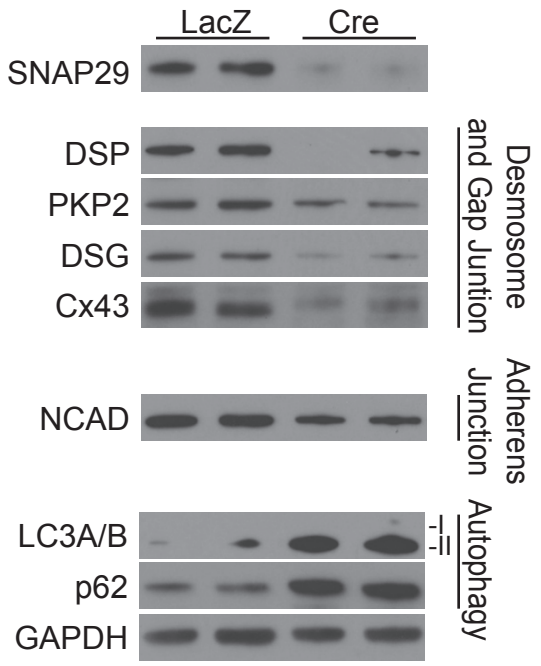


Figure 13. Altered expression of ICD and autophagy proteins in SNAP29-deficient neonatal mouse cardiomyocytes. Western blot analysis of Ad-Cre or Ad-LacZ control infected SNAP29-floxed neonatal mouse cardiomyocytes. Cells were infected 24 hours after plating and collected 48 hours after infection. GAPDH was used as a loading control.

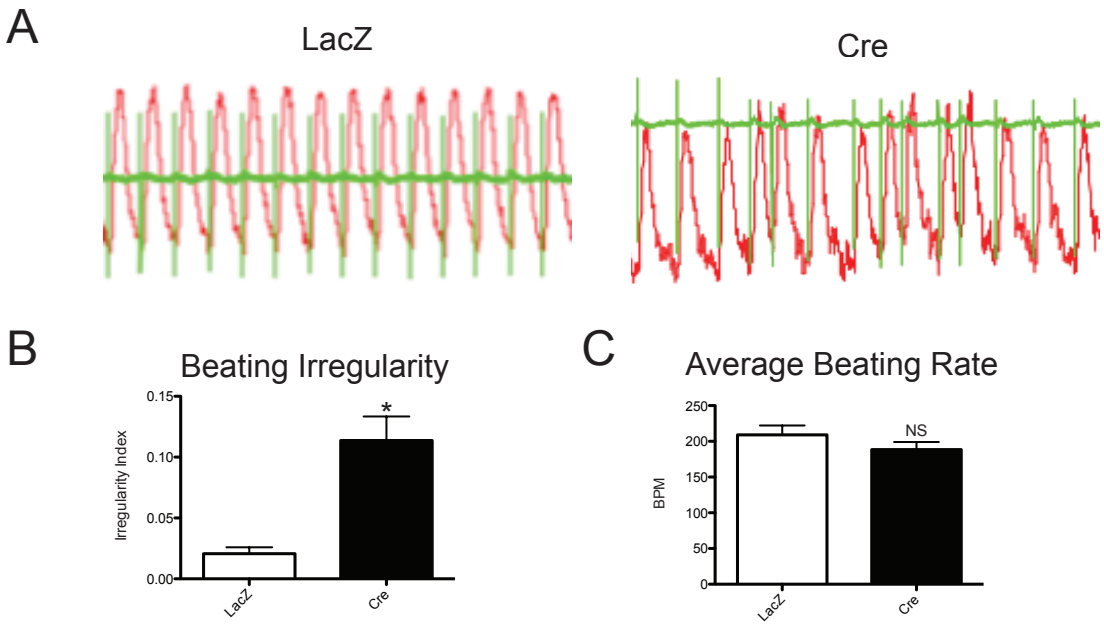


Figure 14. Electrophysiological function in SNAP29-deficient neonatal mouse cardiomyocytes. (A) Representative contraction and electrical potential tracings from Ad-Cre or Ad-LacZ control infected SNAP29-floxed neonatal mouse cardiomyocytes. (B) Analysis of beating rate variability via coefficient of variability in SNAP29-deficient neonatal mouse cardiomyocytes and controls. * = $p < 0.05$ (C) Average beating rates in Ad-Cre or Ad-LacZ control infected SNAP29-floxed neonatal mouse cardiomyocytes (mean ± SEM). NS = not significant.

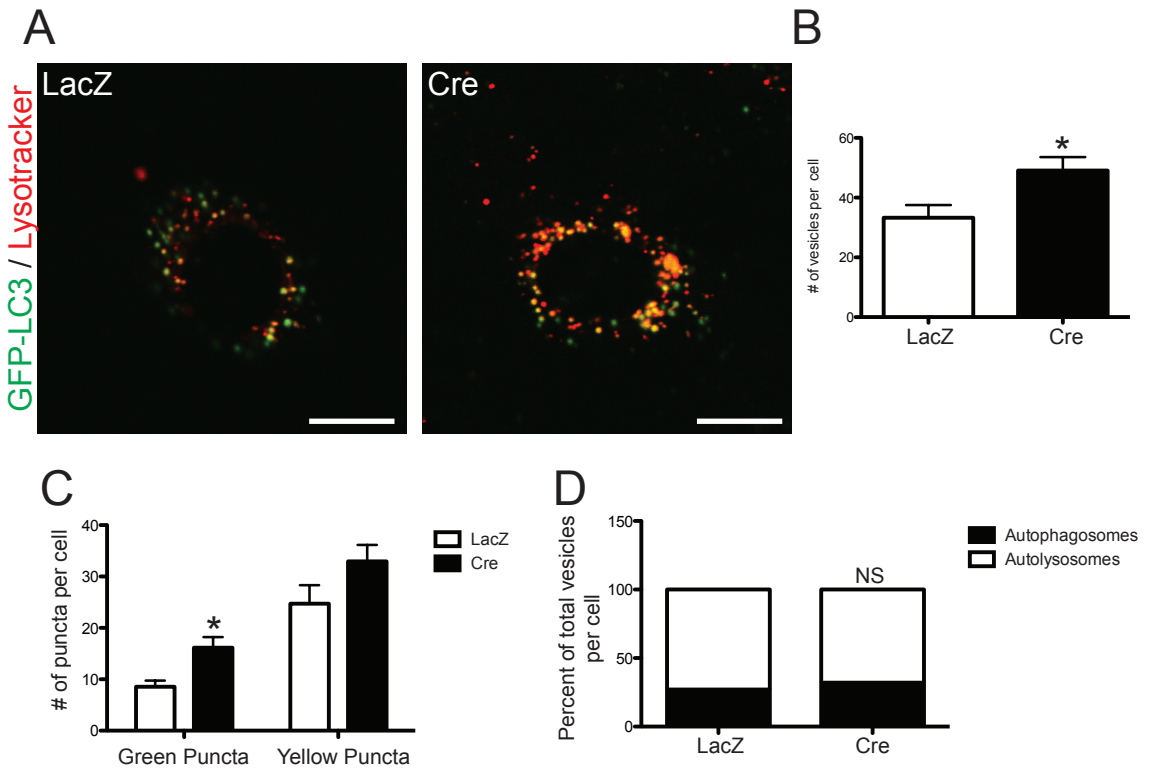


Figure 15. Elevated autophagy in SNAP29-deficient neonatal mouse cardiomyocytes. (A) Representative merged fluorescence microscopy images of Ad-Cre or Ad-LacZ control infected SNAP29-floxed neonatal mouse cardiomyocytes expressing GFP-LC3 (green) and stained with Lysotracker (red). Scale bar = 10 μm. (B) Analysis of total number of green (GFP-LC3 positive autophagosomes) and yellow (GFP-LC3 and Lysotracker positive autolysosomes) puncta per cell. (C) Average number of autophagosomes and lysosomes per cell. (D) Ratio of autophagosomes and lysosomes per cell. N = 22 cells. * = $p<0.05$. NS = not significant.

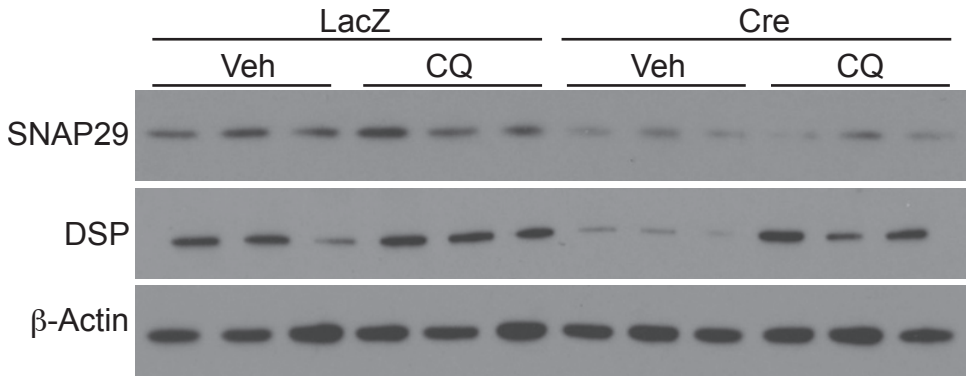


Figure 16. Effects of autophagy inhibition on ICD protein expression in SNAP29-deficient neonatal mouse cardiomyocytes. Western blot analysis of Ad-Cre or Ad-LacZ control infected SNAP29-floxed neonatal mouse cardiomyocytes treated with chloroquine (CQ) or vehicle control. GAPDH is used as loading control.

Chapter 6

The Cardiac Features of a SNAP29-Null Mouse Model of CEDNIK Syndrome

6.1 Cardiac Characterization of Global Loss of SNAP29 *in vivo*

6.1.1 SNAP29 expression is lost in SNAP29 global knockout (SNAP29-gKO) hearts

Global loss of SNAP29 has recently been shown to model features of the human neurocutaneous disease CEDNIK which stands for CErebral Dysgenesis, Neuropathy, Ichthyosis, and Keratoderma (Schiller, Seebode et al. 2016). This syndrome shares skin defects with the DSP mutation-based disease, Carvajal disease (Carvajal-Huerta 1998). Patients with CEDNIK are prone to sudden death during childhood, though the cause is poorly understood (Sprecher, Ishida-Yamamoto et al. 2005, Fuchs-Telem, Stewart et al. 2011). Sudden cardiac death is also a common feature of ARVC (Thiene, Corrado et al. 2007, Sen-Chowdhry, Morgan et al. 2010), therefore the global SNAP29 knockout mouse model was used to investigate the role of the heart in CEDNIK. The construct used for global knockout of SNAP29 (SNAP29-gKO) (Fig. 17A) ablates SNAP29 as evidenced by analysis of multiple organs for SNAP29 protein expression (Fig. 17B). This model was utilized to determine if CEDNIK syndrome exhibits underlying cardiac defects.

6.1.2 SNAP29-gKO mice exhibit perinatal lethality, growth retardation, and skin peeling

SNAP29-gKO mice are born but die after birth between postnatal day 0 (P0) and P5 (Fig. 18A). SNAP29-gKO mouse pups are born at similar weight to littermate controls but surviving pups are significantly smaller by P3 (P3) (Fig. 18B). Gross analysis of pups reveals skin peeling defects in SNAP29-gKO mice and not in littermate controls (Fig. 18B). These findings suggest that SNAP29 is essential for postnatal survival in the mouse.

6.1.3 SNAP29-gKO mouse hearts have normal morphology

To determine whether loss of SNAP29 affects heart morphology, embryonic and neonatal SNAP29-gKO hearts were collected at E18.5, P0 and P3. Analysis of gross morphology and normalized heart weight revealed no differences between SNAP28-gKO hearts and wildtype controls (Fig. 18C), suggesting that SNAP29 does not have a role in cardiac morphology development.

6.1.4 Cardiomyocytes from SNAP29-gKO mouse hearts exhibit arrhythmias in vitro

To determine the functional effects of global loss of SNAP29, neonatal SNAP29-gKO and littermate control cardiomyocytes were grown in the xCELLigence® RTCA CardioECR system and monitored for electrical activity and contractility by measuring electrical field potentials and cell-induced impedence, respectively. Analysis of baseline electrical firing and contractility rates revealed significantly increased variability as measured by coefficient of variance in SNAP29-gKO CMs (Fig. 19A/B). These effects were observed independent of any changes in average firing rate (Fig. 19C). These findings suggest that global loss of SNAP29 has early detrimental effects on cardiomyocyte electrophysiology.

6.1.5 Desmosomal proteins are specifically reduced in SNAP29-gKO hearts

To assess the effects of global loss of SNAP29 on ICD protein levels, embryonic SNAP29-gKO hearts were analyzed for desmosomal, gap junction, and FAJ protein levels. Western blot analysis revealed specific loss of desmosomal and gap junction protein levels with no effect on FAJ proteins (Fig. 20) suggesting that SNAP29 loss leads to specific effects on the desmosome and gap junction in the heart. These findings mirror the effects of cardiac specific knockout of SNAP29 (Fig. 9) in the adult heart.

6.1.6 Markers of autophagy accumulate in SNAP29-gKO hearts

To assess the effects of global loss of SNAP29 on autophagy, neonatal SNAP29-gKO hearts were analyzed. Western blot analysis revealed a significant increase in LC3B levels (Fig. 21A), suggesting that autophagosomes were accumulating. Immunofluorescence analysis further revealed that LC3B was localized to the ICD (Fig. 21B). TEM analysis revealed multi-membrane ultrastructural defects similar to autophagosomes and autolysosomes at the ICD (Fig. 21B), suggesting that the elevated LC3B is due to ICD-specific autophagosome accumulation. These findings mirror the results from SNAP29-cKO (Fig. 10) and DSP-cKO (Fig. 11) adult hearts, suggesting that autophagosomes and autolysosomes are consistently accumulated after loss of SNAP29.

Chapters 3-6, in part are currently being prepared for submission for publication of the material. Pellman, Jason; Lyon, Robert; Liang, Yan; Mezzano, Valeria; Zanella, Fabian; Zhang, Jing; Nigam, Vishal; Gu, Yusu; Dalton, Nancy; Peterson, Kirk L.; Sheikh, Farah. The dissertation author was the primary investigator and author of this material.

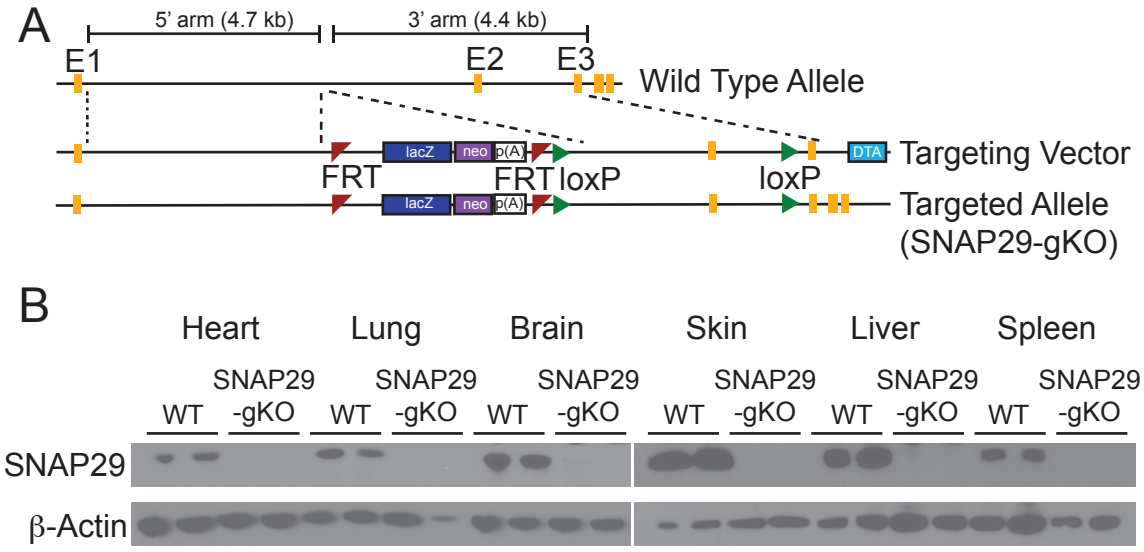


Figure 17. SNAP29 is ablated in global SNAP29 knockout (SNAP29-gKO) neonatal mice. (A) Genetic construct used to globally knockout SNAP29 in mouse. (B) Western blot analysis of organs from SNAP29-gKO P1 mice. β-actin is used as a loading control.

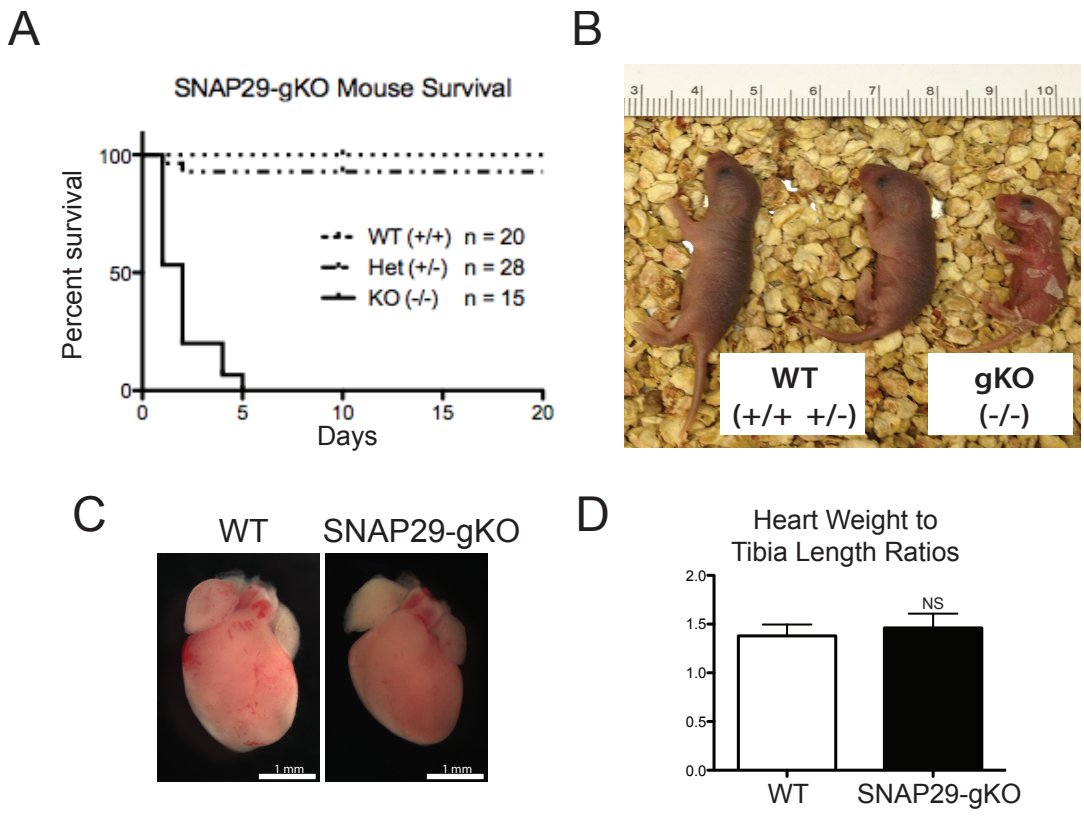


Figure 18. SNAP29-gKO mice exhibit perinatal lethality, growth retardation, and skin peeling without changes in cardiac morphology. (A) Kaplan-Meier survival curve of SNAP29-gKO mice. (B) Gross morphology of SNAP29-gKO pups at P2. (C) Gross morphology of SNAP29-gKO hearts at P0. (D) Heart weight to tibia length ratios of SNAP29-gKO hearts at P0.

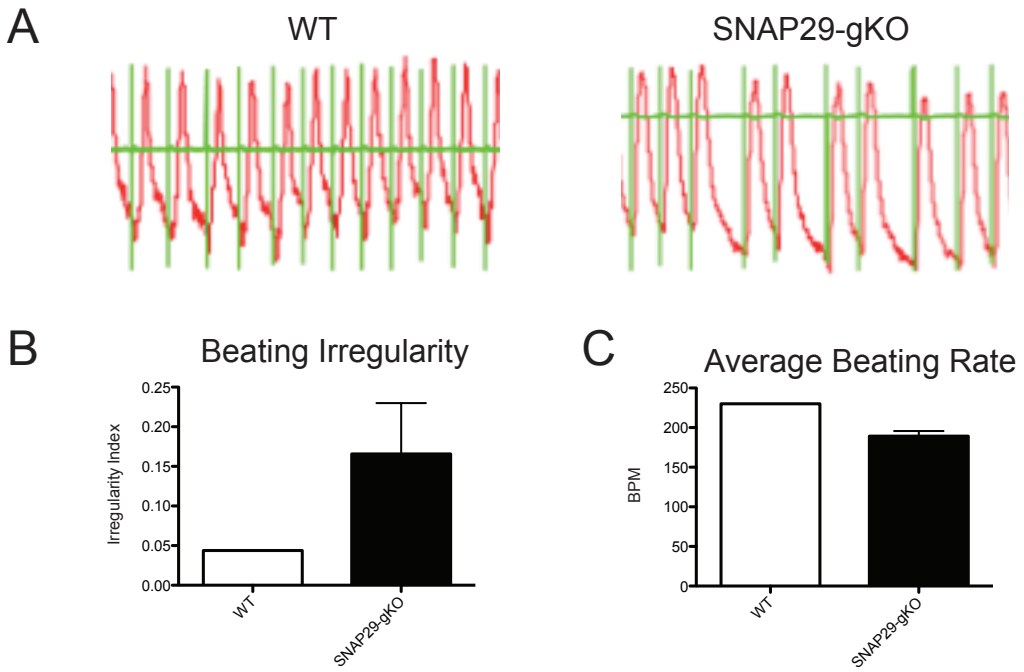


Figure 19. Electrophysiological function in SNAP29-gKO cardiomyocytes. (A) Representative contraction and electrical potential tracings from SNAP29-gKO and littermate control neonatal mouse cardiomyocytes. (B) Analysis of beating rate variability via coefficient of variability in SNAP29-gKO and littermate control neonatal mouse cardiomyocytes. (C) Average beating rates in SNAP29-gKO and littermate control neonatal mouse cardiomyocytes neonatal mouse cardiomyocytes (mean ± SEM).

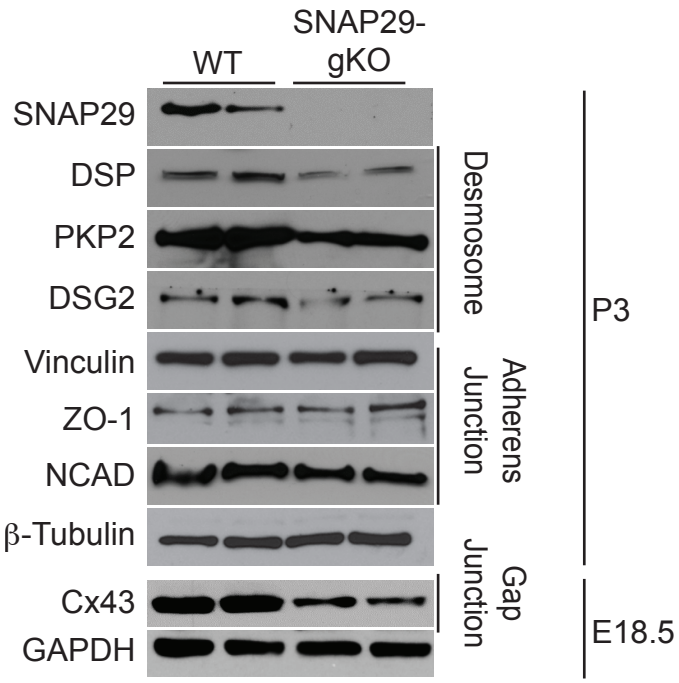


Figure 20. Expression levels of ICD proteins in SNAP29-gKO mouse hearts. Western blot analysis of desmosomal, gap junction, and FAJ proteins in P3 or E18.5 SNAP29-gKO hearts. β-tubulin and GAPDH were used as a loading control.

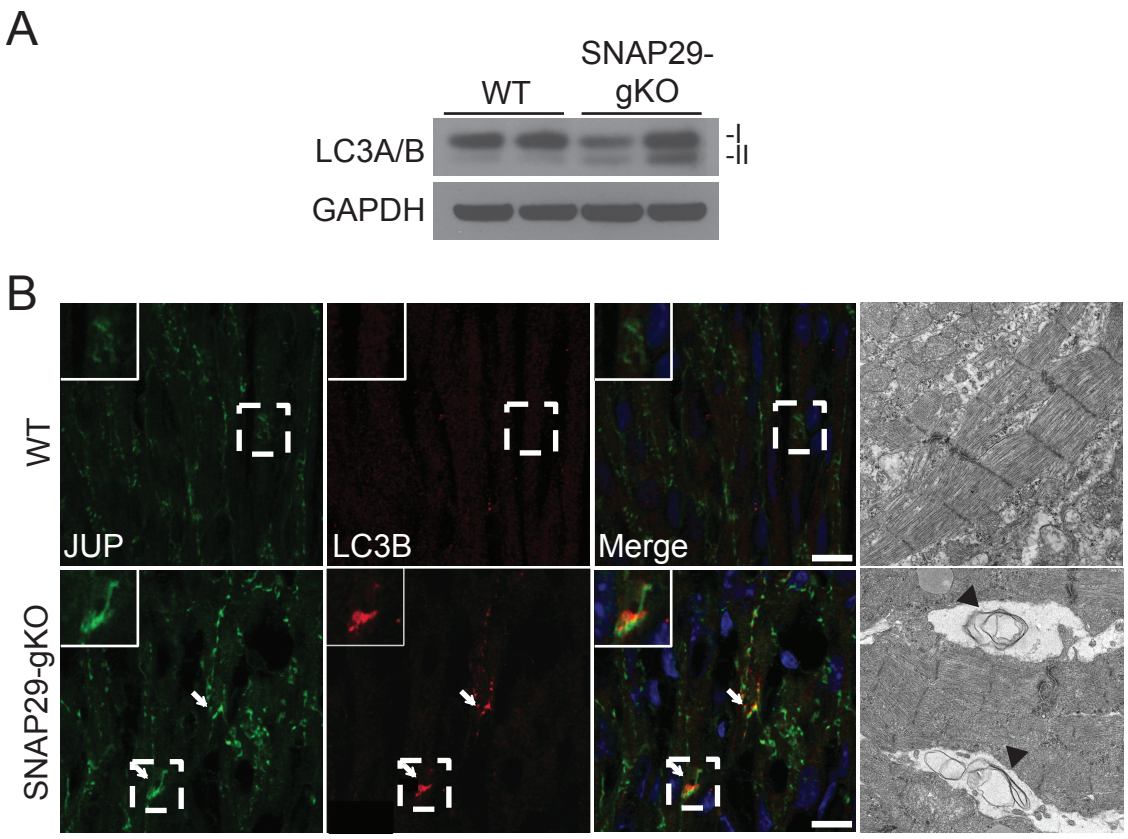


Figure 21. Autophagy defects in SNAP29-gKO mouse hearts. (A) Western blot analysis of P2 SNAP29-gKO mouse hearts for LC3B and p62. GAPDH was used as a loading control. (B) Immunofluorescence staining of P2 hearts from SNAP29-gKO mice for LC3B (red), DSP (green), and JUP (white) and counterstained with DAPI (blue). Scale bar = 10 μm. At right, transmission electron micrographs of intercalated discs of P2 SNAP29-gKO hearts. Multi-membrane structures are marked by black arrowheads. Scale bar = 500 nm.

Chapter 7

Discussion of the Dissertation

7.1 SNAP29 is a novel desmosomal interacting protein

The desmosome is classically thought to primarily have a structural function in the cell, however more recently non-structural roles of desmosomal proteins have begun to be described. This dissertation provides evidence for the SNARE protein SNAP29 as a novel cardiac desmosomal protein through its newly identified interaction with the N-terminus of DSP. The function of SNAP29 in the heart has not been investigated; however, previous studies have proposed a role for SNAP29 in protein degradation via autophagy (Itakura, Kishi-Itakura et al. 2012, Morelli, Ginefra et al. 2014). SNAP29 is a 29 kDa SNARE protein of the SNAP25 family, which are generally though to mediate membrane fusion processes as part of a complex with syntaxin and VAMP family SNAREs (Wong, Xu et al. 1999, Su, Mochida et al. 2001). The studies in this dissertation provide evidence for a novel protein that directly links the desmosome to protein degradation mechanisms, which is required for homeostatic cardiac rhythm and lipid control.

7.2 SNAP29 is a negative regulator of autophagy

In vitro studies in SNAP29 deficient neonatal cardiomyocytes demonstrate that SNAP29 may act to limit autophagosome production in cardiomyocytes, based on the observations of (i) increased number of LC3 puncta (autophagosomes and autolysosomes) in SNAP29 deficient versus control cardiomyocytes and (ii) similar ratios of autophagosome to autolyosomes (no change in autophagic flux) in SNAP29 deficient versus control cardiomyocytes. These findings suggested that cardiomyocyte SNAP29 functions as a negative regulator of autophagy and is not required for autophagosome-lysosome fusion. These findings are in contrast to previous studies in the field that suggested a role for SNAP29 as a positive regulator of autophagy and a blocker of

autophagosome-lysosome fusion (Itakura, Kishi-Itakura et al. 2012, Morelli, Ginefra et al. 2014). Specifically, siRNA knockdown of SNAP29 in HeLa cells and *Drosophila* lead to an increase in LC3 positive puncta; however, in these systems loss of SNAP29 also caused an increase in the ratio of autophagosomes to autolyosomes, and thus, blockade of autophagic flux suggestive of its requirement in autophagosome-lysosome fusion (Itakura, Kishi-Itakura et al. 2012, Morelli, Ginefra et al. 2014). It is possible that SNAP29 may have different effects on autophagy according to cell type, as autophagy signaling is different across cell lines (Klionsky, Abdelmohsen et al. 2016). Furthermore, a study comparing autophagic response in cardiomyocytes and skin fibroblasts revealed strikingly different responses to autophagic stress (Hashem, Perry et al. 2015). Interestingly, SNAP29 localization is found in the cytoplasm in cell lines and Drosophila; however, in cardiomyocytes SNAP29 presents at a unique localization associated with ICD, thus its differential compartmentalized expression pattern and thus, targets, may result in distinct protein degradation functions in different cell types.

7.3 Desmosomal proteins are targeted by SNAP29-mediated autophagy

In vitro and *in vivo* studies in SNAP29 deficient cardiomyocytes demonstrate that SNAP29 deficiency specifically targets desmosomal protein loss/degradation via autophagy-mediated mechanisms. *In vivo* studies in SNAP29 deficient hearts suggest that SNAP29 may impact a hierarchy of proteins associated with ICD, as specific loss of DSP, PKP2 and Cx43 protein levels were observed. *In vitro* studies in SNAP29 deficient cardiomyocytes also confirm that ICD defects are primary to SNAP29 loss. Data from our previous mouse models of DSP deficiency supports the theme of hierarchical organization of ICD proteins. DSP deficient mouse hearts similarly exhibit specific loss of desmosomal and gap junction proteins without affecting FAJ proteins (Lyon, Mezzano et

al. 2014). In vitro studies in DSP deficient cardiomyocytes have also demonstrated that these effects are primary to loss of DSP and independent of cardiac structural defects (Lyon, Mezzano et al. 2014), suggesting that desmosome and gap junction regulation is directly linked. The effects on a subset of desmosomal proteins in SNAP29 deficient hearts suggest that complex organization within the desmosome itself may also be hierarchical. Previous studies on mouse models deficient in other desmosomal proteins have also shown varying effects on other desmosomal protein. For example our DSP deficient mouse model exhibits loss of DSP, PKP2, DSC2, and DSG2 with no change in JUP (Lyon, Mezzano et al. 2014). Meanwhile, in hearts from DSG2 cardiac specific knockout mice, neither DSP nor JUP are reduced, though other desmosomal proteins were not analyzed (Kant, Holthofer et al. 2015). In mice expressing mutant iASSP, a recently identified ICD protein and DSP interactor, DSP levels are unaffected, though localization at the ICD is reduced (Notari, Hu et al. 2015). All together these studies suggest that the desmosome is regulated such that primary loss of a protein from the desmosome may have effects only its most closely associated interactors, e.g. loss of SNAP29 leads to loss of DSP, while leaving the rest of the complex relatively unaffected.

In vitro studies in SNAP29 deficient cardiomyocytes suggest that DSP is targeted by autophagy as a result of loss of SNAP29. Autophagy inhibition in SNAP29 deficient cardiomyocytes *in vitro* with the lysosomal inhibitor chloroquine was sufficient to restore DSP protein levels. The role of autophagy is corroborated by in vivo ultrastructural data revealing accumulation of autophagosome-like and autolysosome-like structures specifically at the ICD of SNAP29 deficient mouse hearts. The autophagosome marker LC3 also appears specifically at the ICD in these hearts, suggesting that autophagy is active at the ICD. These findings are in line with previous studies suggesting that the ICD may an active site of autophagy (Hilenski, Terracio et al. 1992, Nepomnyashchikh,

Lushnikova et al. 2000, Lange, Xiang et al. 2005, Balasubramanian, Mani et al. 2006, Hirschy, Croquelois et al. 2010). These studies altogether establish that DSP can be targeted and degraded by autophagy protein degradation mechanisms in cardiomyoctes.

7.4 SNAP29-mediated autophagy protects cardiomyocytes from arrhythmias

In vivo studies utilizing cardiac specific SNAP29 knockout mice (SNAP29-cKO) demonstrates a role for SNAP29 loss in predisposing mice to premature and inducible ventricular arrhythmias. Premature and inducible ventricular arrhythmias have also been observed in DSP-cKO mice and PKP2 heterozygous knockout mice (Cerrone, Noorman et al. 2012, Lyon, Mezzano et al. 2014), supporting these data support shared functional consequences associated with loss of these protein interactions. In PKP2 global heterozygous knockout mice, ventricular arrhythmias are the primary disease feature observed (Cerrone, Noorman et al. 2012). This parallels features of SNAP29-cKO mice which exhibit reduced PKP2 in the context of ventricular arrhythmias. In DSP-cKO mice which have now been shown to express reduced levels of SNAP29 at the ICD, premature ventricular contractions and inducible ventricular arrhythmias are both electrical defects in this model (Lyon, Mezzano et al. 2014). Previous studies in DSP-cKO mice and DSP deficient cardiomyocytes suggest that Cx43 loss may trigger the cardiac arrhythmias underlying ARVC. Our studies also show that Cx43 levels are reduced with loss of SNAP29 and that this is associated with arrhythmias *in vivo* and *in vitro,* suggesting that loss of Cx43 may be a common underlying mechanism in development of these ventricular arrhythmias. This supported by findings in Cx43 cardiac specific knockout models that show ventricular arrhythmias as the major disease feature in these mice (Jansen, Noorman et al. 2012). Furthermore, both SNAP29-cKO and DSP-cKO models exhibit consistent loss of DSP, Cx43 and SNAP29 underlying

ventricular arrhythmias which reveal the possibility that SNAP29 may mediate the previously observed functional interaction between DSP and Cx43. Both of these mouse models also feature elevated autophagy levels. Previous studies on Cx43 turnover *in vitro* support a role for autophagy in Cx43 degradation in cardiomyocytes (Su and Lau 2012, Basheer, Harris et al. 2015), suggesting that changes in SNAP29-mediated autophagy may alter Cx43 levels.

7.5 SNAP29-mediated autophagy is required for cardiomyocyte lipid droplet homeostasis

In vivo studies on SNAP29 deficient hearts suggest a role for SNAP29 in lipid droplet homeostasis as evidenced by accumulation of lipid droplets in cardiomyocytes of the right ventricles of these hearts. Lipid defects are also present in DSP-cKO hearts as observed by fatty deposition (Lyon, Mezzano et al. 2014). Lipid droplets have also been reported in ultrastructural studies on hearts for ARVC patients, who harbor underlying desmosomal defects (Masani, Aizawa et al. 1990, Basso, Czarnowska et al. 2006). Similarly, human induced pluripotent stem cell-derived cardiomyocytes (hiPSC-CMs) from ARVC patients with PKP2 mutations also accumulate lipid droplets (Kim, Wong et al. 2013, Ma, Wei et al. 2013), suggesting that this may be a common underlying feature of desmosomal disease. The selective accumulation of lipid droplets in the right ventricle of SNAP29 deficient hearts may arise from right vs. left metabolic differences in the heart. Cardiomyocytes from the right heart have been shown to be sufficient for development of fatty accumulation in mice specifically lacking DSP in the second heart field which developmentally forms the right heart (Lombardi, Dong et al. 2009). Studies in hiPSC-CMs from ARVC patients with PKP2 mutations have previously identified activation of peroxisome proliferator-activated receptor gamma (PPARγ), a

proadipogenic transcription factor (Ma, Wei et al. 2013). Interestingly, analysis of cardiac biopsies from ARVC patients have revealed increased levels of PPARγ in RV compared to LV tissue, suggesting that differences in adipogenic signaling may underlie the increased propensity for RV lipid accumulation.

Lipid droplet homeostasis has previously been shown to be regulated by autophagy mechanisms . LC3 has been observed on starvation induced lipid droplets in the mouse heart (Shibata, Yoshimura et al. 2009). Additional studies in cell lines have revealed that knockdown of LC3 leads to reduced lipid droplet numbers (Shibata, Yoshimura et al. 2010), suggesting that autophagy may be required for lipid droplet production. The role of SNAP29 in autophagy suggest that these mechanisms may be at play in SNAP29 deficient hearts. While there is no previously described relationship between SNAP29 and lipid droplet homeostasis, another SNAP25 protein family member has been shown *in vitro* to regulate lipid droplet size in 3T3 cells and also localize to lipid droplets in HL-1 cells (Bostrom, Andersson et al. 2007). It remains to be determined if SNAP29 has direct effects on lipid droplet formation or turnover in the heart.

7.6 SNAP29-mediated autophagy defects may underlie a subset of early ARVC disease features

Previous studies using mouse models and human biopsies have proposed various pathways underlying ARVC including Wnt/b-catenin signaling and the Hippo pathway (Garcia-Gras, Lombardi et al. 2006, Chen, Gurha et al. 2014). For the first time through this dissertation, our data demonstrates that loss of SNAP29 expression, localization and functions associated with autophagy are defective in a mouse model of ARVC as evidenced by the loss of SNAP29 from the ICD and accumulation of

autophagosome-like and autolysosome-like vesicles at the ICD in DSP deficient mouse hearts. The loss of SNAP29 is also been demonstrated in hiPSC-CMs derived from ARVC patients, suggesting that loss of SNAP29 may also be a feature of human ARVC. As shown in SNAP29 deficient mouse hearts, these molecular and ultrastructural features are associated with ventricular arrhythmias and lipid accumulation. This suggests that loss of SNAP29 and SNAP29-mediated autophagy mechanisms may contribute to development of a subset of disease features ARVC. Some evidence of vesicular defects at the ICD has been observed in DSG2 deficient mouse hearts as well as in ARVC patient biopsies (Basso, Czarnowska et al. 2006, Kant, Krull et al. 2012), therefore autophagic defects may represent an underappreciated feature underlying ARVC. These mechanisms may be especially relevant during the “concealed” phase of ARVC, during which electrical disease features are the only cardiac defects (Dalal, Nasir et al. 2005, Basso, Czarnowska et al. 2006). SNAP29 deficient hearts exhibit predominantly electrical disease features; therefore SNAP29-mediated autophagy defects may be particularly important for development of these features of ARVC. Analysis of electrical forms of ARVC may reveal whether these molecular and ultrastructural defects are present and contribute to this specific disease feature development.

7.7 Cardiac desmosomal and autophagy defects underlie a SNAP29-deficient mouse model of CEDNIK syndrome

In vivo and *in vitro* studies in SNAP29 deficient heart and cardiomyocytes suggest a potential role for SNAP29 at the desmosome in other human diseases. SNAP29 mutations in humans are associated with the neurocutaneous syndrome called CEDNIK syndrome (cerebral dysgenesis, neuropathy, ichthyosis, and keratoderma) that

ultimately results in sudden death of pediatric patients between 6-11 years of age, though the hearts of these patients have not been examined in detail (Sprecher, Ishida-Yamamoto et al. 2005, Fuchs-Telem, Stewart et al. 2011). Global loss of SNAP29 in mouse has previously been shown to lead to skin defects and early lethality at postnatal day one (Schiller, Seebode et al. 2016). Skin specific knockout of SNAP29 in mouse also leads to the same skin defects and lethality (Schiller, Seebode et al. 2016), suggesting that cause of death in mice originates from the skin. However, human patients live for years before death and do not appear to die of skin-related causes (Sprecher, Ishida-Yamamoto et al. 2005, Fuchs-Telem, Stewart et al. 2011), therefore there may be previously unappreciated disease features underlying CEDNIK.

Analysis of hearts from SNAP29-gKO mice which model CEDNIK have revealed striking early cardiac desmosomal and gap junction defects by E18.5. In vitro studies in cardiomyocytes reveal electrical defects in the form of cardiomyocyte arrhythmias. These findings recapitulate features from cardiomyocyte specific SNAP29 deficient models and early electrical disease features of ARVC. ARVC has more recently been observed in pediatric populations ranging from infants to children in their teens, though diagnosis is more difficult (Daliento, Turrini et al. 1995, Nishikawa, Ishiyama et al. 1999, Garcia-Gras, Lombardi et al. 2006, Rey, Rodriguez-Nunez et al. 2007, Wong, AbdurRazak et al. 2008). Altogether, this suggests the possibility that cardiac defects may underlie CEDNIK syndrome and may contribute to sudden death in CEDNIK patients.

SNAP29 mediated desmosomal targeted autophagy defects could also potentially underlie the brain defects in CEDNIK syndrome. Both neurons and cardiomyocytes rely on cell-cell communication to drive the electrical activity. A major feature of the cardiomyocytes from SNAP29-gKO mice is arrhythmia with underlying loss

of Cx43. It is interesting to note that electrical defects are also present in CEDNIK patients in the nervous system, observed as neuropathy (Sprecher, Ishida-Yamamoto et al. 2005, Fuchs-Telem, Stewart et al. 2011). A role for Cx43 in neurons has been investigated in a model of glaucoma induced neuropathy, wherein Cx43 loss appears to contribute to development of neuropathy features (Malone, Miao et al. 2007). These studies altogether suggest that SNAP29-mediated loss of Cx43 may potentially contribute to nervous system defects in CEDNIK. Furthermore, the role of the desmosome of the brain is unclear. There is some evidence of desmosomes in the nervous system. For example the desmosomal protein DSG1 has been observed in the brain, specifically in the corpus callosum, though other desmosomal proteins have not been examined (Miyata, Yoshikawa et al. 2015). Interestingly, this region of the brain is also dysmorphic in CEDNIK patients (Sprecher, Ishida-Yamamoto et al. 2005, Fuchs-Telem, Stewart et al. 2011), opening up the possibility of desmosomal-related mechanisms in disease pathogenesis in the brain.

Desmosomal targeted autophagy defects may also underlie the skin defects in CEDNIK syndrome as CEDNIK patients and mice exhibiting SNAP29 loss also display similar skin defects as patients with Carvajal syndrome, which is associated with recessive DSP loss (Carvajal-Huerta 1998, Norgett, Hatsell et al. 2000). It has also been reported that markers of autophagy are increased in skin from SNAP29 global knockout mice (Schiller, Seebode et al. 2016). Based on the connection between SNAP29-mediated autophagy and desmosomal protein loss as well as the presence of desmosomal proteins in the affected organs, CEDNIK may be a disease of the desmosome. Furthermore, yeast-2-hybrid studies on DSP mutations associated with the heart and skin disease erythrokeratodermia-cardiomyopathy syndrome (Boyden, Kam et

al. 2016) revealed a loss of interaction with SNAP29, suggesting that disruption of the DSP-SNAP29 interaction may underlie diseases of both the heart and skin.

7.8 Conclusions

In conclusion, SNAP29 is a novel desmosomal protein whose function in autophagy is required for maintenance of desmosomal and gap junction protein levels in the heart. SNAP29 appears to maintain DSP levels in cardiomyocytes through its role as a negative regulator of autophagy in cardiomyocytes. Loss of SNAP29 in the heart triggers a reduction in desmosomal and gap junction proteins and accumulation of autophagy markers leading to lipid accumulation and ventricular arrhythmias characteristic of ARVC. Loss of SNAP29 levels, localization and function are also observed in a DSP-deficient mouse model of ARVC and loss of SNAP29 levels are observed in hiPSC-CMs from ARVC patents, suggesting that disrupted autophagy function may be a molecular feature of ARVC. In a mouse model of CEDNIK syndrome, cardiac desmosomal defects are present in the context of cardiomyocyte electrical and autophagy defects reminiscent of SNAP29-deficient and DSP-deficient hearts. Altogether, these findings suggest that SNAP29 protects desmosomes from targeted protein degradation to restrict cardiac arrhythmias.

7.9 Future Studies

These studies have identified a role for SNAP29 in autophagy. SNAP29 appears to be a negative regulator of autophagy based on the increase in autophagic vesicles without a change in flux in the absence of SNAP29. To more precisely determine how SNAP29 exerts control on autophagy, additional biochemical studies are required.

Based on the potential role of SNAP29 as an inhibitor of SNARE complex disassembly, examination of mechanisms at various steps of autophagy, especially at the termination of autophagy, may reveal whether complex disassembly is affected. Based on the maintenance of autophagic flux in SNAP29-deficient cardiomyocytes, it is unlikely that SNAP29 is required for autophagosome-lysosome fusion. SNAP29 has previously been described as a promiscuous SNARE due to proposed interactions with numerous SNARE complexes (Hohenstein and Roche 2001), however none of these have been examined in the heart. The localization of SNAP29 at the desmosome in cardiomyocytes and the appearance of autophagosomes at the ICD under disease conditions suggest that it may participate locally in autophagy at the ICD. Interestingly, VAMP5 has previously identified at the ICD (Takahashi, Tajika et al. 2013), however it has not been determined whether it can complex with SNAP29. A previously proposed SNAP29 interacting protein Rab24 (Schardt, Brinkmann et al. 2009) is thought to be required for the final steps in autophagy that are responsible for clearance of autolysosomes (Yla-Anttila, Mikkonen et al. 2015), therefore it is possible that autophagy clearance mechanisms are also affected in a SNAP29-deficient setting. Identification and characterization of a cardiomyocyte SNAP29-containing SNARE complex may shed light on the unique protein degradation mechanisms at play at the ICD.

These studies have identified a potential role for autophagy in ARVC. Loss of desmosomal proteins is a common molecular hallmark of ARVC, though the mechanisms responsible are not established. Disruption of autophagy underlies our DSP-deficient mouse model of ARVC, however the extent to which it is responsible for development of disease features has yet to be determined. Recent studies have implicated protein degradation mechanisms in ischemia induced loss of Cx43 (Martins-Marques, Catarino et al. 2015), a key protein thought to be involved in the ventricular

arrhythmias in ARVC (Lyon, Mezzano et al. 2014), however the these mechanisms have not been assessed in the context of ARVC. Future studies that take advantage of the DSP-cKO mouse line would be able to test the effects of pharmacological or genetic inhibition of autophagy in the mouse *in vivo* by treating mice with autophagy inhibitors (3-MA or chloroquine) or crossing the line with the autophagy deficient beclin-1 heterozygous knockout mouse. This can also be addressed *in vitro* by similarly inhibiting autophagy in DSP-deficient cardiomyocytes. These studies would have the potential to provide insight on whether there are therapeutic benefits to targeting protein degradation pathways in ARVC.

Cardiac desmosomal turnover mechanisms remain poorly understood, though they have the potential to impact cardiac function and disease. These studies have identified a link between DSP degradation and SNAP29 mediated degradation via autophagy. However, the mechanisms responsible for the targeting of DSP and other ICD proteins for degradation in the absence of SNAP29 remain unclear. Studies utilizing the SNAP29-cKO and DSP-cKO mouse lines could identify the protein complexes involved in loading of desmosomal protein into the autophagosome. Both of these models feature accumulation of autophagosomes at the ICD, making them ideal systems to detect the molecular complexes associating with them.

Mutation analysis of DSP has revealed the existence of DSP mutants associated with an array of heart and skin disease features (Boyden, Kam et al. 2016), however it remains unclear what regulatory mechanisms are shared between the two organs. Based on the studies in this dissertation, SNAP29 may be a downstream regulator of desmosome function that can impact both heart and skin. The interaction between SNAP29 and the desmosome may be disrupted by disease associated mutation and lead to defects in the heart and skin. Interaction analysis between SNAP29 and

desmosomal mutations may reveal the importance of this interaction in development of desmosome-based disease. Protein interaction studies focused on these mutations may reveal disrupted interactions with SNAP29 that could contribute to development of disease.

References

Ahmad, F., D. Li, A. Karibe, O. Gonzalez, T. Tapscott, R. Hill, D. Weilbaecher, P. Blackie, M. Furey, M. Gardner, L. L. Bachinski and R. Roberts (1998). "Localization of a gene responsible for arrhythmogenic right ventricular dysplasia to chromosome 3p23." Circulation **98**(25): 2791-2795.

Al-Owain, M., S. Wakil, F. Shareef, A. Al-Fatani, E. Hamadah, M. Haider, H. Al-Hindi, A. Awaji, O. Khalifa, B. Baz, R. Ramadhan and B. Meyer (2011). "Novel homozygous mutation in DSP causing skin fragility-woolly hair syndrome: report of a large family and review of the desmoplakin-related phenotypes." Clin Genet **80**(1): 50-58.

Alcalai, R., S. Metzger, S. Rosenheck, V. Meiner and T. Chajek-Shaul (2003). "A recessive mutation in desmoplakin causes arrhythmogenic right ventricular dysplasia, skin disorder, and woolly hair." J Am Coll Cardiol **42**(2): 319-327.

Asimaki, A., S. Kapoor, E. Plovie, A. Karin Arndt, E. Adams, Z. Liu, C. A. James, D. P. Judge, H. Calkins, J. Churko, J. C. Wu, C. A. MacRae, A. G. Kleber and J. E. Saffitz (2014). "Identification of a new modulator of the intercalated disc in a zebrafish model of arrhythmogenic cardiomyopathy." Sci Transl Med **6**(240): 240ra274.

Azzimato, V., N. Genneback, A. M. Tabish, B. Buyandelger and R. Knoll (2016). "Desmin, desminopathy and the complexity of genetics." J Mol Cell Cardiol **92**: 93-95.

Balasubramanian, S., S. Mani, H. Shiraishi, R. K. Johnston, K. Yamane, C. D. Willey, G. t. Cooper, W. J. Tuxworth and D. Kuppuswamy (2006). "Enhanced ubiquitination of cytoskeletal proteins in pressure overloaded myocardium is accompanied by changes in specific E3 ligases." J Mol Cell Cardiol **41**(4): 669-679.

Bao, J., J. Wang, Y. Yao, Y. Wang, X. Fan, K. Sun, D. S. He, F. I. Marcus, S. Zhang, R. Hui and L. Song (2013). "Correlation of ventricular arrhythmias with genotype in arrhythmogenic right ventricular cardiomyopathy." Circ Cardiovasc Genet **6**(6): 552-556.

Basheer, W. A., B. S. Harris, H. L. Mentrup, M. Abreha, E. L. Thames, J. B. Lea, D. A. Swing, N. G. Copeland, N. A. Jenkins, R. L. Price and L. E. Matesic (2015). "Cardiomyocyte-specific overexpression of the ubiquitin ligase Wwp1 contributes to reduction in Connexin 43 and arrhythmogenesis." J Mol Cell Cardiol **88**: 1-13.

Basso, C., D. Corrado, F. I. Marcus, A. Nava and G. Thiene (2009). "Arrhythmogenic right ventricular cardiomyopathy." Lancet **373**(9671): 1289-1300.

Basso, C., E. Czarnowska, M. Della Barbera, B. Bauce, G. Beffagna, E. K. Wlodarska, K. Pilichou, A. Ramondo, A. Lorenzon, O. Wozniek, D. Corrado, L. Daliento, G. A.

Danieli, M. Valente, A. Nava, G. Thiene and A. Rampazzo (2006). "Ultrastructural evidence of intercalated disc remodelling in arrhythmogenic right ventricular cardiomyopathy: an electron microscopy investigation on endomyocardial biopsies." Eur Heart J **27**(15): 1847-1854.

Basso, C., G. Thiene, D. Corrado, A. Angelini, A. Nava and M. Valente (1996). "Arrhythmogenic right ventricular cardiomyopathy. Dysplasia, dystrophy, or myocarditis?" Circulation **94**(5): 983-991.

Beffagna, G., M. De Bortoli, A. Nava, M. Salamon, A. Lorenzon, M. Zaccolo, L. Mancuso, L. Sigalotti, B. Bauce, G. Occhi, C. Basso, G. Lanfranchi, J. A. Towbin, G. Thiene, G. A. Danieli and A. Rampazzo (2007). "Missense mutations in desmocollin-2 N-terminus, associated with arrhythmogenic right ventricular cardiomyopathy, affect intracellular localization of desmocollin-2 in vitro." BMC Med Genet **8**: 65.

Beffagna, G., G. Occhi, A. Nava, L. Vitiello, A. Ditadi, C. Basso, B. Bauce, G. Carraro, G. Thiene, J. A. Towbin, G. A. Danieli and A. Rampazzo (2005). "Regulatory mutations in transforming growth factor-beta3 gene cause arrhythmogenic right ventricular cardiomyopathy type 1." Cardiovasc Res **65**(2): 366-373.

Bhuiyan, M. S., J. S. Pattison, H. Osinska, J. James, J. Gulick, P. M. McLendon, J. A. Hill, J. Sadoshima and J. Robbins (2013). "Enhanced autophagy ameliorates cardiac proteinopathy." J Clin Invest **123**(12): 5284-5297.

Bhuiyan, Z. A., J. D. Jongbloed, J. van der Smagt, P. M. Lombardi, A. C. Wiesfeld, M. Nelen, M. Schouten, R. Jongbloed, M. G. Cox, M. van Wolferen, L. M. Rodriguez, I. C. van Gelder, H. Bikker, A. J. Suurmeijer, M. P. van den Berg, M. M. Mannens, R. N. Hauer, A. A. Wilde and J. P. van Tintelen (2009). "Desmoglein-2 and desmocollin-2 mutations in dutch arrhythmogenic right ventricular dysplasia/cardiomypathy patients: results from a multicenter study." Circ Cardiovasc Genet **2**(5): 418-427.

Bierkamp, C., K. J. McLaughlin, H. Schwarz, O. Huber and R. Kemler (1996). "Embryonic heart and skin defects in mice lacking plakoglobin." Dev Biol **180**(2): 780-785.

Birks, E. J., N. Latif, K. Enesa, T. Folkvang, A. Luong le, P. Sarathchandra, M. Khan, H. Ovaa, C. M. Terracciano, P. J. Barton, M. H. Yacoub and P. C. Evans (2008). "Elevated p53 expression is associated with dysregulation of the ubiquitin-proteasome system in dilated cardiomyopathy." Cardiovasc Res **79**(3): 472-480.

Bogomolovas, J., J. R. Fleming, B. R. Anderson, R. Williams, S. Lange, B. Simon, M. M. Khan, R. Rudolf, B. Franke, B. Bullard, D. J. Rigden, H. Granzier, S. Labeit and O.

Mayans (2016). "Exploration of pathomechanisms triggered by a single-nucleotide polymorphism in titin's I-band: the cardiomyopathy-linked mutation T2580I." Open Biol **6**(9).

Bonne, G., M. R. Di Barletta, S. Varnous, H. M. Becane, E. H. Hammouda, L. Merlini, F. Muntoni, C. R. Greenberg, F. Gary, J. A. Urtizberea, D. Duboc, M. Fardeau, D. Toniolo and K. Schwartz (1999). "Mutations in the gene encoding lamin A/C cause autosomal dominant Emery-Dreifuss muscular dystrophy." Nat Genet **21**(3): 285-288.

Borrmann, C. M., C. Grund, C. Kuhn, I. Hofmann, S. Pieperhoff and W. W. Franke (2006). "The area composita of adhering junctions connecting heart muscle cells of vertebrates. II. Colocalizations of desmosomal and fascia adhaerens molecules in the intercalated disk." Eur J Cell Biol **85**(6): 469-485.

Bostrom, P., L. Andersson, M. Rutberg, J. Perman, U. Lidberg, B. R. Johansson, J. Fernandez-Rodriguez, J. Ericson, T. Nilsson, J. Boren and S. O. Olofsson (2007). "SNARE proteins mediate fusion between cytosolic lipid droplets and are implicated in insulin sensitivity." Nat Cell Biol **9**(11): 1286-1293.

Boyden, L. M., C. Y. Kam, A. Hernandez-Martin, J. Zhou, B. G. Craiglow, R. Sidbury, E. F. Mathes, S. M. Maguiness, D. A. Crumrine, M. L. Williams, R. Hu, R. P. Lifton, P. M. Elias, K. J. Green and K. A. Choate (2016). "Dominant de novo DSP mutations cause erythrokeratodermia-cardiomyopathy syndrome." Hum Mol Genet **25**(2): 348-357.

Breckenridge, R., S. Kotecha, N. Towers, M. Bennett and T. Mohun (2007). "Pan-myocardial expression of Cre recombinase throughout mouse development." Genesis **45**(3): 135-144.

Cao, D. J., N. Jiang, A. Blagg, J. L. Johnstone, R. Gondalia, M. Oh, X. Luo, K. C. Yang, J. M. Shelton, B. A. Rothermel, T. G. Gillette, G. W. Dorn and J. A. Hill (2013). "Mechanical unloading activates FoxO3 to trigger Bnip3-dependent cardiomyocyte atrophy." J Am Heart Assoc **2**(2): e000016.

Carmosino, M., S. Torretta, G. Procino, A. Gerbino, C. Forleo, S. Favale and M. Svelto (2014). "Role of nuclear Lamin A/C in cardiomyocyte functions." Biol Cell **106**(10): 346-358.

Carvajal-Huerta, L. (1998). "Epidermolytic palmoplantar keratoderma with woolly hair and dilated cardiomyopathy." J Am Acad Dermatol **39**(3): 418-421.

Centner, T., J. Yano, E. Kimura, A. S. McElhinny, K. Pelin, C. C. Witt, M. L. Bang, K. Trombitas, H. Granzier, C. C. Gregorio, H. Sorimachi and S. Labeit (2001). "Identification of muscle specific ring finger proteins as potential regulators of the titin kinase domain." J Mol Biol **306**(4): 717-726.

Cerrone, M., C. Napolitano and S. G. Priori (2009). "Catecholaminergic polymorphic ventricular tachycardia: A paradigm to understand mechanisms of arrhythmias associated to impaired Ca(2+) regulation." Heart Rhythm **6**(11): 1652-1659.

Cerrone, M., M. Noorman, X. Lin, H. Chkourko, F. X. Liang, R. van der Nagel, T. Hund, W. Birchmeier, P. Mohler, T. A. van Veen, H. V. van Rijen and M. Delmar (2012). "Sodium current deficit and arrhythmogenesis in a murine model of plakophilin-2 haploinsufficiency." Cardiovasc Res **95**(4): 460-468.

Cetin, N., B. Balci-Hayta, H. Gundesli, P. Korkusuz, N. Purali, B. Talim, E. Tan, D. Selcen, S. Erdem-Ozdamar and P. Dincer (2013). "A novel desmin mutation leading to autosomal recessive limb-girdle muscular dystrophy: distinct histopathological outcomes compared with desminopathies." J Med Genet **50**(7): 437-443.

Chelko, S. P., A. Asimaki, P. Andersen, D. Bedja, N. Amat-Alarcon, D. DeMazumder, R. Jasti, C. A. MacRae, R. Leber, A. G. Kleber, J. E. Saffitz and D. P. Judge (2016). "Central role for GSK3beta in the pathogenesis of arrhythmogenic cardiomyopathy." JCI Insight **1**(5).

Chen, B., Y. Ma, R. Meng, Z. Xiong, C. Zhang, G. Chen, A. Zhang and Y. Dong (2010). "MG132, a proteasome inhibitor, attenuates pressure-overload-induced cardiac hypertrophy in rats by modulation of mitogen-activated protein kinase signals." Acta Biochim Biophys Sin (Shanghai) **42**(4): 253-258.

Chen, S. N., P. Gurha, R. Lombardi, A. Ruggiero, J. T. Willerson and A. J. Marian (2014). "The hippo pathway is activated and is a causal mechanism for adipogenesis in arrhythmogenic cardiomyopathy." Circ Res **114**(3): 454-468.

Cheng, Z. and Q. Fang (2012). "Danon disease: focusing on heart." J Hum Genet **57**(7): 407-410.

Comelli, I., G. Gonzi, G. Mossini, G. Lippi, T. Meschi, L. Borghi and G. Cervellin (2014). "Dizziness and syncope in young people: keep your mind open! Case report of the challenging differentiation between arrhythmogenic right ventricular cardiomyopathy/dysplasia (ARVC/D) and catecholaminergic polymorphic ventricular tachycardia (CPVT)." Acta Biomed **85**(1): 73-80.

Corrado, D., C. Basso, G. Rizzoli, M. Schiavon and G. Thiene (2003). "Does sports activity enhance the risk of sudden death in adolescents and young adults?" J Am Coll Cardiol **42**(11): 1959-1963.

Corrado, D. and G. Thiene (2006). "Arrhythmogenic right ventricular cardiomyopathy/dysplasia: clinical impact of molecular genetic studies." Circulation **113**(13): 1634-1637.

Cruz, F. M., D. Sanz-Rosa, M. Roche-Molina, J. Garcia-Prieto, J. M. Garcia-Ruiz, G. Pizarro, L. J. Jimenez-Borreguero, M. Torres, A. Bernad, J. Ruiz-Cabello, V. Fuster, B. Ibanez and J. A. Bernal (2015). "Exercise triggers ARVC phenotype in mice expressing a disease-causing mutated version of human plakophilin-2." J Am Coll Cardiol **65**(14): 1438-1450.

Curran, M. E., I. Splawski, K. W. Timothy, G. M. Vincent, E. D. Green and M. T. Keating (1995). "A molecular basis for cardiac arrhythmia: HERG mutations cause long QT syndrome." Cell **80**(5): 795-803.

Dalal, D., K. Nasir, C. Bomma, K. Prakasa, H. Tandri, J. Piccini, A. Roguin, C. Tichnell, C. James, S. D. Russell, D. P. Judge, T. Abraham, P. J. Spevak, D. A. Bluemke and H. Calkins (2005). "Arrhythmogenic right ventricular dysplasia: a United States experience." Circulation **112**(25): 3823-3832.

Daliento, L., P. Turrini, A. Nava, G. Rizzoli, A. Angelini, G. Buja, R. Scognamiglio and G. Thiene (1995). "Arrhythmogenic right ventricular cardiomyopathy in young versus adult patients: similarities and differences." J Am Coll Cardiol **25**(3): 655-664.

Danon, M. J., S. J. Oh, S. DiMauro, J. R. Manaligod, A. Eastwood, S. Naidu and L. H. Schliselfeld (1981). "Lysosomal glycogen storage disease with normal acid maltase." Neurology **31**(1): 51-57.

Day, S. M. (2013). "The ubiquitin proteasome system in human cardiomyopathies and heart failure." Am J Physiol Heart Circ Physiol **304**(10): H1283-1293.

De Sandre-Giovannoli, A., R. Bernard, P. Cau, C. Navarro, J. Amiel, I. Boccaccio, S. Lyonnet, C. L. Stewart, A. Munnich, M. Le Merrer and N. Levy (2003). "Lamin a truncation in Hutchinson-Gilford progeria." Science **300**(5628): 2055.

den Haan, A. D., B. Y. Tan, M. N. Zikusoka, L. I. Llado, R. Jain, A. Daly, C. Tichnell, C. James, N. Amat-Alarcon, T. Abraham, S. D. Russell, D. A. Bluemke, H. Calkins, D. Dalal and D. P. Judge (2009). "Comprehensive desmosome mutation analysis in north

americans with arrhythmogenic right ventricular dysplasia/cardiomyopathy." Circ Cardiovasc Genet **2**(5): 428-435.

Deo, M., P. Y. Sato, H. Musa, X. Lin, S. V. Pandit, M. Delmar and O. Berenfeld (2011). "Relative contribution of changes in sodium current versus intercellular coupling on reentry initiation in 2-dimensional preparations of plakophilin-2-deficient cardiac cells." Heart Rhythm **8**(11): 1740-1748.

Dubash, A. D., C. Y. Kam, B. A. Aguado, D. M. Patel, M. Delmar, L. D. Shea and K. J. Green (2016). "Plakophilin-2 loss promotes TGF-beta1/p38 MAPK-dependent fibrotic gene expression in cardiomyocytes." J Cell Biol **212**(4): 425-438.

Ellawindy, A., K. Satoh, S. Sunamura, N. Kikuchi, K. Suzuki, T. Minami, S. Ikeda, S. Tanaka, T. Shimizu, B. Enkhjargal, S. Miyata, Y. Taguchi, T. Handoh, K. Kobayashi, K. Kobayashi, K. Nakayama, M. Miura and H. Shimokawa (2015). "Rho-Kinase Inhibition During Early Cardiac Development Causes Arrhythmogenic Right Ventricular Cardiomyopathy in Mice." Arterioscler Thromb Vasc Biol **35**(10): 2172-2184.

Elsasser, A., A. M. Vogt, H. Nef, S. Kostin, H. Mollmann, W. Skwara, C. Bode, C. Hamm and J. Schaper (2004). "Human hibernating myocardium is jeopardized by apoptotic and autophagic cell death." J Am Coll Cardiol **43**(12): 2191-2199.

Erkapic, D., T. Neumann, J. Schmitt, J. Sperzel, A. Berkowitsch, M. Kuniss, C. W. Hamm and H. F. Pitschner (2008). "Electrical storm in a patient with arrhythmogenic right ventricular cardiomyopathy and SCN5A mutation." Europace **10**(7): 884-887.

Fabritz, L., M. G. Hoogendijk, B. P. Scicluna, S. C. van Amersfoorth, L. Fortmueller, S. Wolf, S. Laakmann, N. Kreienkamp, I. Piccini, G. Breithardt, P. R. Noppinger, H. Witt, K. Ebnet, T. Wichter, B. Levkau, W. W. Franke, S. Pieperhoff, J. M. de Bakker, R. Coronel and P. Kirchhof (2011). "Load-reducing therapy prevents development of arrhythmogenic right ventricular cardiomyopathy in plakoglobin-deficient mice." J Am Coll Cardiol **57**(6): 740-750.

Fatkin, D., C. MacRae, T. Sasaki, M. R. Wolff, M. Porcu, M. Frenneaux, J. Atherton, H. J. Vidaillet, Jr., S. Spudich, U. De Girolami, J. G. Seidman, C. Seidman, F. Muntoni, G. Muehle, W. Johnson and B. McDonough (1999). "Missense mutations in the rod domain of the lamin A/C gene as causes of dilated cardiomyopathy and conduction-system disease." N Engl J Med **341**(23): 1715-1724.

Fielitz, J., E. van Rooij, J. A. Spencer, J. M. Shelton, S. Latif, R. van der Nagel, S. Bezprozvannaya, L. de Windt, J. A. Richardson, R. Bassel-Duby and E. N. Olson (2007).

"Loss of muscle-specific RING-finger 3 predisposes the heart to cardiac rupture after myocardial infarction." Proc Natl Acad Sci U S A **104**(11): 4377-4382.

Fontaine, G., R. Frank, G. Guiraudon, A. Pavie, Y. Tereau, G. Chomette and Y. Grosgogeat (1984). "[Significance of intraventricular conduction disorders observed in arrhythmogenic right ventricular dysplasia]." Arch Mal Coeur Vaiss **77**(8): 872-879.

Franke, W. W., C. M. Borrmann, C. Grund and S. Pieperhoff (2006). "The area composita of adhering junctions connecting heart muscle cells of vertebrates. I. Molecular definition in intercalated disks of cardiomyocytes by immunoelectron microscopy of desmosomal proteins." Eur J Cell Biol **85**(2): 69-82.

Fuchs-Telem, D., H. Stewart, D. Rapaport, J. Nousbeck, A. Gat, M. Gini, Y. Lugassy, S. Emmert, K. Eckl, H. C. Hennies, O. Sarig, D. Goldsher, B. Meilik, A. Ishida-Yamamoto, M. Horowitz and E. Sprecher (2011). "CEDNIK syndrome results from loss-of-function mutations in SNAP29." Br J Dermatol **164**(3): 610-616.

Fujita, S., F. Terasaki, K. Otsuka, T. Katashima, Y. Kanzaki, K. Kawamura, T. Tanaka and Y. Kitaura (2008). "Markedly increased intracellular lipid droplets and disruption of intercellular junctions in biopsied myocardium from a patient with arrhythmogenic right ventricular cardiomyopathy." Heart Vessels **23**(6): 440-444.

Furlanello, F., A. Bertoldi, M. Dallago, C. Furlanello, F. Fernando, G. Inama, C. Pappone and S. Chierchia (1998). "Cardiac arrest and sudden death in competitive athletes with arrhythmogenic right ventricular dysplasia." Pacing Clin Electrophysiol **21**(1 Pt 2): 331-335.

Garcia-Gras, E., R. Lombardi, M. J. Giocondo, J. T. Willerson, M. D. Schneider, D. S. Khoury and A. J. Marian (2006). "Suppression of canonical Wnt/beta-catenin signaling by nuclear plakoglobin recapitulates phenotype of arrhythmogenic right ventricular cardiomyopathy." J Clin Invest **116**(7): 2012-2021.

Garg, V., I. S. Kathiriya, R. Barnes, M. K. Schluterman, I. N. King, C. A. Butler, C. R. Rothrock, R. S. Eapen, K. Hirayama-Yamada, K. Joo, R. Matsuoka, J. C. Cohen and D. Srivastava (2003). "GATA4 mutations cause human congenital heart defects and reveal an interaction with TBX5." Nature **424**(6947): 443-447.

Garg, V., A. N. Muth, J. F. Ransom, M. K. Schluterman, R. Barnes, I. N. King, P. D. Grossfeld and D. Srivastava (2005). "Mutations in NOTCH1 cause aortic valve disease." Nature **437**(7056): 270-274.

Garrod, D. and M. Chidgey (2008). "Desmosome structure, composition and function." Biochim Biophys Acta **1778**(3): 572-587.

Gehmlich, K., P. Syrris, E. Peskett, A. Evans, E. Ehler, A. Asimaki, A. Anastasakis, A. Tsatsopoulou, A. I. Vouliotis, C. Stefanadis, J. E. Saffitz, N. Protonotarios and W. J. McKenna (2011). "Mechanistic insights into arrhythmogenic right ventricular cardiomyopathy caused by desmocollin-2 mutations." Cardiovasc Res **90**(1): 77-87.

Geisterfer-Lowrance, A. A., S. Kass, G. Tanigawa, H. P. Vosberg, W. McKenna, C. E. Seidman and J. G. Seidman (1990). "A molecular basis for familial hypertrophic cardiomyopathy: a beta cardiac myosin heavy chain gene missense mutation." Cell **62**(5): 999-1006.

Giepmans, B. N. and W. H. Moolenaar (1998). "The gap junction protein connexin43 interacts with the second PDZ domain of the zona occludens-1 protein." Curr Biol **8**(16): 931-934.

Goldfarb, L. G., K. Y. Park, L. Cervenakova, S. Gorokhova, H. S. Lee, O. Vasconcelos, J. W. Nagle, C. Semino-Mora, K. Sivakumar and M. C. Dalakas (1998). "Missense mutations in desmin associated with familial cardiac and skeletal myopathy." Nat Genet **19**(4): 402-403.

Gomes, J., M. Finlay, A. K. Ahmed, E. J. Ciaccio, A. Asimaki, J. E. Saffitz, G. Quarta, M. Nobles, P. Syrris, S. Chaubey, W. J. McKenna, A. Tinker and P. D. Lambiase (2012). "Electrophysiological abnormalities precede overt structural changes in arrhythmogenic right ventricular cardiomyopathy due to mutations in desmoplakin-A combined murine and human study." Eur Heart J **33**(15): 1942-1953.

Goossens, S., B. Janssens, S. Bonne, R. De Rycke, F. Braet, J. van Hengel and F. van Roy (2007). "A unique and specific interaction between alphaT-catenin and plakophilin-2 in the area composita, the mixed-type junctional structure of cardiac intercalated discs." J Cell Sci **120**(Pt 12): 2126-2136.

Grossmann, K. S., C. Grund, J. Huelsken, M. Behrend, B. Erdmann, W. W. Franke and W. Birchmeier (2004). "Requirement of plakophilin 2 for heart morphogenesis and cardiac junction formation." J Cell Biol **167**(1): 149-160.

Hager, S., H. Mahrholdt, L. G. Goldfarb, H. H. Goebel and U. Sechtem (2006). "Images in cardiovascular medicine. Giant right atrium in the setting of desmin-related restrictive cardiomyopathy." Circulation **113**(4): e53-55.

Hariharan, N., Y. Ikeda, C. Hong, R. R. Alcendor, S. Usui, S. Gao, Y. Maejima and J. Sadoshima (2013). "Autophagy plays an essential role in mediating regression of hypertrophy during unloading of the heart." PLoS One **8**(1): e51632.

Hashem, S. I., C. N. Perry, M. Bauer, S. Han, S. D. Clegg, K. Ouyang, D. C. Deacon, M. Spinharney, A. D. Panopoulos, J. C. Izpisua Belmonte, K. A. Frazer, J. Chen, Q. Gong, Z. Zhou, N. C. Chi and E. D. Adler (2015). "Brief Report: Oxidative Stress Mediates Cardiomyocyte Apoptosis in a Human Model of Danon Disease and Heart Failure." Stem Cells **33**(7): 2343-2350.

Haugaa, K. H., T. F. Haland, I. S. Leren, J. Saberniak and T. Edvardsen (2016). "Arrhythmogenic right ventricular cardiomyopathy, clinical manifestations, and diagnosis." Europace **18**(7): 965-972.

Heidbuchel, H., J. Hoogsteen, R. Fagard, L. Vanhees, H. Ector, R. Willems and J. Van Lierde (2003). "High prevalence of right ventricular involvement in endurance athletes with ventricular arrhythmias. Role of an electrophysiologic study in risk stratification." Eur Heart J **24**(16): 1473-1480.

Herman, D. S., L. Lam, M. R. Taylor, L. Wang, P. Teekakirikul, D. Christodoulou, L. Conner, S. R. DePalma, B. McDonough, E. Sparks, D. L. Teodorescu, A. L. Cirino, N. R. Banner, D. J. Pennell, S. Graw, M. Merlo, A. Di Lenarda, G. Sinagra, J. M. Bos, M. J. Ackerman, R. N. Mitchell, C. E. Murry, N. K. Lakdawala, C. Y. Ho, P. J. Barton, S. A. Cook, L. Mestroni, J. G. Seidman and C. E. Seidman (2012). "Truncations of titin causing dilated cardiomyopathy." N Engl J Med **366**(7): 619-628.

Heuser, A., E. R. Plovie, P. T. Ellinor, K. S. Grossmann, J. T. Shin, T. Wichter, C. T. Basson, B. B. Lerman, S. Sasse-Klaassen, L. Thierfelder, C. A. MacRae and B. Gerull (2006). "Mutant desmocollin-2 causes arrhythmogenic right ventricular cardiomyopathy." Am J Hum Genet **79**(6): 1081-1088.

Hilenski, L. L., L. Terracio, A. L. Haas and T. K. Borg (1992). "Immunolocalization of ubiquitin conjugates at Z-bands and intercalated discs of rat cardiomyocytes in vitro and in vivo." J Histochem Cytochem **40**(7): 1037-1042.

Hirschy, A., A. Croquelois, E. Perriard, R. Schoenauer, I. Agarkova, S. P. Hoerstrup, M. M. Taketo, T. Pedrazzini, J. C. Perriard and E. Ehler (2010). "Stabilised beta-catenin in postnatal ventricular myocardium leads to dilated cardiomyopathy and premature death." Basic Res Cardiol **105**(5): 597-608.

Hohenstein, A. C. and P. A. Roche (2001). "SNAP-29 is a promiscuous syntaxin-binding SNARE." Biochem Biophys Res Commun **285**(2): 167-171.

Honda, S., S. Arakawa, Y. Nishida, H. Yamaguchi, E. Ishii and S. Shimizu (2014). "Ulk1-mediated Atg5-independent macroautophagy mediates elimination of mitochondria from embryonic reticulocytes." Nat Commun **5**: 4004.

Hong, M., L. Bao, E. Kefaloyianni, E. Agullo-Pascual, H. Chkourko, M. Foster, E. Taskin, M. Zhandre, D. A. Reid, E. Rothenberg, M. Delmar and W. A. Coetzee (2012). "Heterogeneity of ATP-sensitive K+ channels in cardiac myocytes: enrichment at the intercalated disk." J Biol Chem **287**(49): 41258-41267.

Hong, T., H. Yang, S. S. Zhang, H. C. Cho, M. Kalashnikova, B. Sun, H. Zhang, A. Bhargava, M. Grabe, J. Olgin, J. Gorelik, E. Marban, L. Y. Jan and R. M. Shaw (2014). "Cardiac BIN1 folds T-tubule membrane, controlling ion flux and limiting arrhythmia." Nat Med **20**(6): 624-632.

Itakura, E., C. Kishi-Itakura and N. Mizushima (2012). "The hairpin-type tail-anchored SNARE syntaxin 17 targets to autophagosomes for fusion with endosomes/lysosomes." Cell **151**(6): 1256-1269.

Itoh-Satoh, M., T. Hayashi, H. Nishi, Y. Koga, T. Arimura, T. Koyanagi, M. Takahashi, S. Hohda, K. Ueda, T. Nouchi, M. Hiroe, F. Marumo, T. Imaizumi, M. Yasunami and A. Kimura (2002). "Titin mutations as the molecular basis for dilated cardiomyopathy." Biochem Biophys Res Commun **291**(2): 385-393.

Jansen, J. A., M. Noorman, H. Musa, M. Stein, S. de Jong, R. van der Nagel, T. J. Hund, P. J. Mohler, M. A. Vos, T. A. van Veen, J. M. de Bakker, M. Delmar and H. V. van Rijen (2012). "Reduced heterogeneous expression of Cx43 results in decreased Nav1.5 expression and reduced sodium current that accounts for arrhythmia vulnerability in conditional Cx43 knockout mice." Heart Rhythm **9**(4): 600-607.

Johansen, T. and T. Lamark (2011). "Selective autophagy mediated by autophagic adapter proteins." Autophagy **7**(3): 279-296.

Kant, S., B. Holthofer, T. M. Magin, C. A. Krusche and R. E. Leube (2015). "Desmoglein 2-Dependent Arrhythmogenic Cardiomyopathy Is Caused by a Loss of Adhesive Function." Circ Cardiovasc Genet **8**(4): 553-563.

Kant, S., P. Krull, S. Eisner, R. E. Leube and C. A. Krusche (2012). "Histological and ultrastructural abnormalities in murine desmoglein 2-mutant hearts." Cell Tissue Res **348**(2): 249-259.

Karakikes, I., F. Stillitano, M. Nonnenmacher, C. Tzimas, D. Sanoudou, V. Termglinchan, C. W. Kong, S. Rushing, J. Hansen, D. Ceholski, F. Kolokathis, D. Kremastinos, A. Katoulis, L. Ren, N. Cohen, J. M. Gho, D. Tsiapras, A. Vink, J. C. Wu, F. W. Asselbergs, R. A. Li, J. S. Hulot, E. G. Kranias and R. J. Hajjar (2015). "Correction of human phospholamban R14del mutation associated with cardiomyopathy using targeted nucleases and combination therapy." Nat Commun **6**: 6955.

Kathiresan, S. and D. Srivastava (2012). "Genetics of human cardiovascular disease." Cell **148**(6): 1242-1257.

Kato, K., N. Takahashi, Y. Fujii, A. Umehara, S. Nishiuchi, T. Makiyama, S. Ohno and M. Horie (2016). "LMNA cardiomyopathy detected in Japanese arrhythmogenic right ventricular cardiomyopathy cohort." J Cardiol **68**(4): 346-351.

Kedar, V., H. McDonough, R. Arya, H. H. Li, H. A. Rockman and C. Patterson (2004). "Muscle-specific RING finger 1 is a bona fide ubiquitin ligase that degrades cardiac troponin I." Proc Natl Acad Sci U S A **101**(52): 18135-18140.

Kim, C., J. Wong, J. Wen, S. Wang, C. Wang, S. Spiering, N. G. Kan, S. Forcales, P. L. Puri, T. C. Leone, J. E. Marine, H. Calkins, D. P. Kelly, D. P. Judge and H. S. Chen (2013). "Studying arrhythmogenic right ventricular dysplasia with patient-specific iPSCs." Nature **494**(7435): 105-110.

Kirchhof, P., L. Fabritz, M. Zwiener, H. Witt, M. Schafers, S. Zellerhoff, M. Paul, T. Athai, K. H. Hiller, H. A. Baba, G. Breithardt, P. Ruiz, T. Wichter and B. Levkau (2006). "Age- and training-dependent development of arrhythmogenic right ventricular cardiomyopathy in heterozygous plakoglobin-deficient mice." Circulation **114**(17): 1799-1806.

Kirkin, V., D. G. McEwan, I. Novak and I. Dikic (2009). "A role for ubiquitin in selective autophagy." Mol Cell **34**(3): 259-269.

Klauke, B., S. Kossmann, A. Gaertner, K. Brand, I. Stork, A. Brodehl, M. Dieding, V. Walhorn, D. Anselmetti, D. Gerdes, B. Bohms, U. Schulz, E. Zu Knyphausen, M. Vorgerd, J. Gummert and H. Milting (2010). "De novo desmin-mutation N116S is associated with arrhythmogenic right ventricular cardiomyopathy." Hum Mol Genet **19**(23): 4595-4607.

Klionsky, D. J., K. Abdelmohsen, A. Abe, M. J. Abedin, H. Abeliovich, A. Acevedo Arozena, H. Adachi, C. M. Adams, P. D. Adams, K. Adeli, P. J. Adhihetty, S. G. Adler, G. Agam, R. Agarwal, M. K. Aghi, M. Agnello, P. Agostinis, P. V. Aguilar, J. Aguirre-Ghiso, E. M. Airoldi, S. Ait-Si-Ali, T. Akematsu, E. T. Akporiaye, M. Al-Rubeai, G. M. Albaiceta, C. Albanese, D. Albani, M. L. Albert, J. Aldudo, H. Algul, M. Alirezaei, I. Alloza, A.

Almasan, M. Almonte-Beceril, E. S. Alnemri, C. Alonso, N. Altan-Bonnet, D. C. Altieri, S. Alvarez, L. Alvarez-Erviti, S. Alves, G. Amadoro, A. Amano, C. Amantini, S. Ambrosio, I. Amelio, A. O. Amer, M. Amessou, A. Amon, Z. An, F. A. Anania, S. U. Andersen, U. P. Andley, C. K. Andreadi, N. Andrieu-Abadie, A. Anel, D. K. Ann, S. Anoopkumar-Dukie, M. Antonioli, H. Aoki, N. Apostolova, S. Aquila, K. Aquilano, K. Araki, E. Arama, A. Aranda, J. Araya, A. Arcaro, E. Arias, H. Arimoto, A. R. Ariosa, J. L. Armstrong, T. Arnould, I. Arsov, K. Asanuma, V. Askanas, E. Asselin, R. Atarashi, S. S. Atherton, J. D. Atkin, L. D. Attardi, P. Auberger, G. Auburger, L. Aurelian, R. Autelli, L. Avagliano, M. L. Avantaggiati, L. Avrahami, S. Awale, N. Azad, T. Bachetti, J. M. Backer, D. H. Bae, J. S. Bae, O. N. Bae, S. H. Bae, E. H. Baehrecke, S. H. Baek, S. Baghdiguian, A. Bagniewska-Zadworna, H. Bai, J. Bai, X. Y. Bai, Y. Bailly, K. N. Balaji, W. Balduini, A. Ballabio, R. Balzan, R. Banerjee, G. Banhegyi, H. Bao, B. Barbeau, M. D. Barrachina, E. Barreiro, B. Bartel, A. Bartolome, D. C. Bassham, M. T. Bassi, R. C. Bast, Jr., A. Basu, M. T. Batista, H. Batoko, M. Battino, K. Bauckman, B. L. Baumgarner, K. U. Bayer, R. Beale, J. F. Beaulieu, G. R. Beck, Jr., C. Becker, J. D. Beckham, P. A. Bedard, P. J. Bednarski, T. J. Begley, C. Behl, C. Behrends, G. M. Behrens, K. E. Behrns, E. Bejarano, A. Belaid, F. Belleudi, G. Benard, G. Berchem, D. Bergamaschi, M. Bergami, B. Berkhout, L. Berliocchi, A. Bernard, M. Bernard, F. Bernassola, A. Bertolotti, A. S. Bess, S. Besteiro, S. Bettuzzi, S. Bhalla, S. Bhattacharyya, S. K. Bhutia, C. Biagosch, M. W. Bianchi, M. Biard-Piechaczyk, V. Billes, C. Bincoletto, B. Bingol, S. W. Bird, M. Bitoun, I. Bjedov, C. Blackstone, L. Blanc, G. A. Blanco, H. K. Blomhoff, E. Boada-Romero, S. Bockler, M. Boes, K. Boesze-Battaglia, L. H. Boise, A. Bolino, A. Boman, P. Bonaldo, M. Bordi, J. Bosch, L. M. Botana, J. Botti, G. Bou, M. Bouche, M. Bouchecareilh, M. J. Boucher, M. E. Boulton, S. G. Bouret, P. Boya, M. Boyer-Guittaut, P. V. Bozhkov, N. Brady, V. M. Braga, C. Brancolini, G. H. Braus, J. M. Bravo-San Pedro, L. A. Brennan, E. H. Bresnick, P. Brest, D. Bridges, M. A. Bringer, M. Brini, G. C. Brito, B. Brodin, P. S. Brookes, E. J. Brown, K. Brown, H. E. Broxmeyer, A. Bruhat, P. C. Brum, J. H. Brumell, N. Brunetti-Pierri, R. J. Bryson-Richardson, S. Buch, A. M. Buchan, H. Budak, D. V. Bulavin, S. J. Bultman, G. Bultynck, V. Bumbasirevic, Y. Burelle, R. E. Burke, M. Burmeister, P. Butikofer, L. Caberlotto, K. Cadwell, M. Cahova, D. Cai, J. Cai, Q. Cai, S. Calatayud, N. Camougrand, M. Campanella, G. R. Campbell, M. Campbell, S. Campello, R. Candau, I. Caniggia, L. Cantoni, L. Cao, A. B. Caplan, M. Caraglia, C. Cardinali, S. M. Cardoso, J. S. Carew, L. A. Carleton, C. R. Carlin, S. Carloni, S. R. Carlsson, D. Carmona-Gutierrez, L. A. Carneiro, O. Carnevali, S. Carra, A. Carrier, B. Carroll, C. Casas, J. Casas, G. Cassinelli, P. Castets, S. Castro-Obregon, G. Cavallini, I. Ceccherini, F. Cecconi, A. I. Cederbaum, V. Cena, S. Cenci, C. Cerella, D. Cervia, S. Cetrullo, H. Chaachouay, H. J. Chae, A. S. Chagin, C. Y. Chai, G. Chakrabarti, G. Chamilos, E. Y. Chan, M. T. Chan, D. Chandra, P. Chandra, C. P. Chang, R. C. Chang, T. Y. Chang, J. C. Chatham, S. Chatterjee, S. Chauhan, Y. Che, M. E. Cheetham, R. Cheluvappa, C. J. Chen, G. Chen, G. C. Chen, G. Chen, H. Chen, J. W. Chen, J. K. Chen, M. Chen, M. Chen, P. Chen, Q. Chen, Q. Chen, S. D. Chen, S. Chen, S. S. Chen, W. Chen, W. J. Chen, W. Q. Chen, W. Chen, X. Chen, Y. H. Chen, Y. G. Chen, Y. Chen, Y. Chen, Y. Chen, Y. J. Chen, Y. Q. Chen, Y. Chen, Z. Chen, Z. Chen, A. Cheng, C. H. Cheng, H. Cheng, H. Cheong, S. Cherry, J. Chesney, C. H. Cheung, E. Chevet, H. C. Chi, S. G. Chi, F. Chiacchiera, H. L. Chiang, R. Chiarelli, M. Chiariello, M. Chieppa, L. S. Chin, M. Chiong, G. N. Chiu, D. H. Cho, S. G. Cho, W. C. Cho, Y. Y. Cho, Y. S. Cho, A. M. Choi, E. J. Choi, E. K. Choi, J. Choi, M. E. Choi, S. I. Choi, T. F. Chou, S. Chouaib, D. Choubey, V. Choubey, K. C. Chow, K. Chowdhury, C. T. Chu, T. H. Chuang, T. Chun, H. Chung, T. Chung, Y. L. Chung, Y. J. Chwae, V. Cianfanelli, R. Ciarcia, I. A.

Ciechomska, M. R. Ciriolo, M. Cirone, S. Claerhout, M. J. Clague, J. Claria, P. G. Clarke, R. Clarke, E. Clementi, C. Cleyrat, M. Cnop, E. M. Coccia, T. Cocco, P. Codogno, J. Coers, E. E. Cohen, D. Colecchia, L. Coletto, N. S. Coll, E. Colucci-Guyon, S. Comincini, M. Condello, K. L. Cook, G. H. Coombs, C. D. Cooper, J. M. Cooper, I. Coppens, M. T. Corasaniti, M. Corazzari, R. Corbalan, E. Corcelle-Termeau, M. D. Cordero, C. Corral-Ramos, O. Corti, A. Cossarizza, P. Costelli, S. Costes, S. L. Cotman, A. Coto-Montes, S. Cottet, E. Couve, L. R. Covey, L. A. Cowart, J. S. Cox, F. P. Coxon, C. B. Coyne, M. S. Cragg, R. J. Craven, T. Crepaldi, J. L. Crespo, A. Criollo, V. Crippa, M. T. Cruz, A. M. Cuervo, J. M. Cuezva, T. Cui, P. R. Cutillas, M. J. Czaja, M. F. Czyzyk-Krzeska, R. K. Dagda, U. Dahmen, C. Dai, W. Dai, Y. Dai, K. N. Dalby, L. Dalla Valle, G. Dalmasso, M. D'Amelio, M. Damme, A. Darfeuille-Michaud, C. Dargemont, V. M. Darley-Usmar, S. Dasarathy, B. Dasgupta, S. Dash, C. R. Dass, H. M. Davey, L. M. Davids, D. Davila, R. J. Davis, T. M. Dawson, V. L. Dawson, P. Daza, J. de Belleroche, P. de Figueiredo, R. C. de Figueiredo, J. de la Fuente, L. De Martino, A. De Matteis, G. R. De Meyer, A. De Milito, M. De Santi, W. de Souza, V. De Tata, D. De Zio, J. Debnath, R. Dechant, J. P. Decuypere, S. Deegan, B. Dehay, B. Del Bello, D. P. Del Re, R. Delage-Mourroux, L. M. Delbridge, L. Deldicque, E. Delorme-Axford, Y. Deng, J. Dengjel, M. Denizot, P. Dent, C. J. Der, V. Deretic, B. Derrien, E. Deutsch, T. P. Devarenne, R. J. Devenish, S. Di Bartolomeo, N. Di Daniele, F. Di Domenico, A. Di Nardo, S. Di Paola, A. Di Pietro, L. Di Renzo, A. DiAntonio, G. Diaz-Araya, I. Diaz-Laviada, M. T. Diaz-Meco, J. Diaz-Nido, C. A. Dickey, R. C. Dickson, M. Diederich, P. Digard, I. Dikic, S. P. Dinesh-Kumar, C. Ding, W. X. Ding, Z. Ding, L. Dini, J. H. Distler, A. Diwan, M. Djavaheri-Mergny, K. Dmytruk, R. C. Dobson, V. Doetsch, K. Dokladny, S. Dokudovskaya, M. Donadelli, X. C. Dong, X. Dong, Z. Dong, T. M. Donohue, Jr., K. S. Doran, G. D'Orazi, G. W. Dorn, 2nd, V. Dosenko, S. Dridi, L. Drucker, J. Du, L. L. Du, L. Du, A. du Toit, P. Dua, L. Duan, P. Duann, V. K. Dubey, M. R. Duchen, M. A. Duchosal, H. Duez, I. Dugail, V. I. Dumit, M. C. Duncan, E. A. Dunlop, W. A. Dunn, Jr., N. Dupont, L. Dupuis, R. V. Duran, T. M. Durcan, S. Duvezin-Caubet, U. Duvvuri, V. Eapen, D. Ebrahimi-Fakhari, A. Echard, L. Eckhart, C. L. Edelstein, A. L. Edinger, L. Eichinger, T. Eisenberg, A. Eisenberg-Lerner, N. T. Eissa, W. S. El-Deiry, V. El-Khoury, Z. Elazar, H. Eldar-Finkelman, C. J. Elliott, E. Emanuele, U. Emmenegger, N. Engedal, A. M. Engelbrecht, S. Engelender, J. M. Enserink, R. Erdmann, J. Erenpreisa, R. Eri, J. L. Eriksen, A. Erman, R. Escalante, E. L. Eskelinen, L. Espert, L. Esteban-Martinez, T. J. Evans, M. Fabri, G. Fabrias, C. Fabrizi, A. Facchiano, N. J. Faergeman, A. Faggioni, W. D. Fairlie, C. Fan, D. Fan, J. Fan, S. Fang, M. Fanto, A. Fanzani, T. Farkas, M. Faure, F. B. Favier, H. Fearnhead, M. Federici, E. Fei, T. C. Felizardo, H. Feng, Y. Feng, Y. Feng, T. A. Ferguson, A. F. Fernandez, M. G. Fernandez-Barrena, J. C. Fernandez-Checa, A. Fernandez-Lopez, M. E. Fernandez-Zapico, O. Feron, E. Ferraro, C. V. Ferreira-Halder, L. Fesus, R. Feuer, F. C. Fiesel, E. C. Filippi-Chiela, G. Filomeni, G. M. Fimia, J. H. Fingert, S. Finkbeiner, T. Finkel, F. Fiorito, P. B. Fisher, M. Flajolet, F. Flamigni, O. Florey, S. Florio, R. A. Floto, M. Folini, C. Follo, E. A. Fon, F. Fornai, F. Fortunato, A. Fraldi, R. Franco, A. Francois, A. Francois, L. B. Frankel, I. D. Fraser, N. Frey, D. G. Freyssenet, C. Frezza, S. L. Friedman, D. E. Frigo, D. Fu, J. M. Fuentes, J. Fueyo, Y. Fujitani, Y. Fujiwara, M. Fujiya, M. Fukuda, S. Fulda, C. Fusco, B. Gabryel, M. Gaestel, P. Gailly, M. Gajewska, S. Galadari, G. Galili, I. Galindo, M. F. Galindo, G. Galliciotti, L. Galluzzi, L. Galluzzi, V. Galy, N. Gammoh, S. Gandy, A. K. Ganesan, S. Ganesan, I. G. Ganley, M. Gannage, F. B. Gao, F. Gao, J. X. Gao, L. Garcia Nannig, E. Garcia Vescovi, M. Garcia-Macia, C. Garcia-Ruiz, A. D. Garg, P. K. Garg, R. Gargini, N. C. Gassen, D. Gatica, E. Gatti, J. Gavard, E. Gavathiotis, L. Ge, P. Ge, S. Ge, P. W. Gean, V. Gelmetti, A. A. Genazzani,

J. Geng, P. Genschik, L. Gerner, J. E. Gestwicki, D. A. Gewirtz, S. Ghavami, E. Ghigo, D. Ghosh, A. M. Giammarioli, F. Giampieri, C. Giampietri, A. Giatromanolaki, D. J. Gibbings, L. Gibellini, S. B. Gibson, V. Ginet, A. Giordano, F. Giorgini, E. Giovannetti, S. E. Girardin, S. Gispert, S. Giuliano, C. L. Gladson, A. Glavic, M. Gleave, N. Godefroy, R. M. Gogal, Jr., K. Gokulan, G. H. Goldman, D. Goletti, M. S. Goligorsky, A. V. Gomes, L. C. Gomes, H. Gomez, C. Gomez-Manzano, R. Gomez-Sanchez, D. A. Goncalves, E. Goncu, Q. Gong, C. Gongora, C. B. Gonzalez, P. Gonzalez-Alegre, P. Gonzalez-Cabo, R. A. Gonzalez-Polo, I. S. Goping, C. Gorbea, N. V. Gorbunov, D. R. Goring, A. M. Gorman, S. M. Gorski, S. Goruppi, S. Goto-Yamada, C. Gotor, R. A. Gottlieb, I. Gozes, D. Gozuacik, Y. Graba, M. Graef, G. E. Granato, G. D. Grant, S. Grant, G. L. Gravina, D. R. Green, A. Greenhough, M. T. Greenwood, B. Grimaldi, F. Gros, C. Grose, J. F. Groulx, F. Gruber, P. Grumati, T. Grune, J. L. Guan, K. L. Guan, B. Guerra, C. Guillen, K. Gulshan, J. Gunst, C. Guo, L. Guo, M. Guo, W. Guo, X. G. Guo, A. A. Gust, A. B. Gustafsson, E. Gutierrez, M. G. Gutierrez, H. S. Gwak, A. Haas, J. E. Haber, S. Hadano, M. Hagedorn, D. R. Hahn, A. J. Halayko, A. Hamacher-Brady, K. Hamada, A. Hamai, A. Hamann, M. Hamasaki, I. Hamer, Q. Hamid, E. M. Hammond, F. Han, W. Han, J. T. Handa, J. A. Hanover, M. Hansen, M. Harada, L. Harhaji-Trajkovic, J. W. Harper, A. H. Harrath, A. L. Harris, J. Harris, U. Hasler, P. Hasselblatt, K. Hasui, R. G. Hawley, T. S. Hawley, C. He, C. Y. He, F. He, G. He, R. R. He, X. H. He, Y. W. He, Y. Y. He, J. K. Heath, M. J. Hebert, R. A. Heinzen, G. V. Helgason, M. Hensel, E. P. Henske, C. Her, P. K. Herman, A. Hernandez, C. Hernandez, S. Hernandez-Tiedra, C. Hetz, P. R. Hiesinger, K. Higaki, S. Hilfiker, B. G. Hill, J. A. Hill, W. D. Hill, K. Hino, D. Hofius, P. Hofman, G. U. Hoglinger, J. Hohfeld, M. K. Holz, Y. Hong, D. A. Hood, J. J. Hoozemans, T. Hoppe, C. Hsu, C. Y. Hsu, L. C. Hsu, D. Hu, G. Hu, H. M. Hu, H. Hu, M. C. Hu, Y. C. Hu, Z. W. Hu, F. Hua, Y. Hua, C. Huang, H. L. Huang, K. H. Huang, K. Y. Huang, S. Huang, S. Huang, W. P. Huang, Y. R. Huang, Y. Huang, Y. Huang, T. B. Huber, P. Huebbe, W. K. Huh, J. J. Hulmi, G. M. Hur, J. H. Hurley, Z. Husak, S. N. Hussain, S. Hussain, J. J. Hwang, S. Hwang, T. I. Hwang, A. Ichihara, Y. Imai, C. Imbriano, M. Inomata, T. Into, V. Iovane, J. L. Iovanna, R. V. Iozzo, N. Y. Ip, J. E. Irazoqui, P. Iribarren, Y. Isaka, A. J. Isakovic, H. Ischiropoulos, J. S. Isenberg, M. Ishaq, H. Ishida, I. Ishii, J. E. Ishmael, C. Isidoro, K. Isobe, E. Isono, S. Issazadeh-Navikas, K. Itahana, E. Itakura, A. I. Ivanov, A. K. Iyer, J. M. Izquierdo, Y. Izumi, V. Izzo, M. Jaattela, N. Jaber, D. J. Jackson, W. T. Jackson, T. G. Jacob, T. S. Jacques, C. Jagannath, A. Jain, N. R. Jana, B. K. Jang, A. Jani, B. Janji, P. R. Jannig, P. J. Jansson, S. Jean, M. Jendrach, J. H. Jeon, N. Jessen, E. B. Jeung, K. Jia, L. Jia, H. Jiang, H. Jiang, L. Jiang, T. Jiang, X. Jiang, X. Jiang, X. Jiang, Y. Jiang, Y. Jiang, A. Jimenez, C. Jin, H. Jin, L. Jin, M. Jin, S. Jin, U. K. Jinwal, E. K. Jo, T. Johansen, D. E. Johnson, G. V. Johnson, J. D. Johnson, E. Jonasch, C. Jones, L. A. Joosten, J. Jordan, A. M. Joseph, B. Joseph, A. M. Joubert, D. Ju, J. Ju, H. F. Juan, K. Juenemann, G. Juhasz, H. S. Jung, J. U. Jung, Y. K. Jung, H. Jungbluth, M. J. Justice, B. Jutten, N. O. Kaakoush, K. Kaarniranta, A. Kaasik, T. Kabuta, B. Kaeffer, K. Kagedal, A. Kahana, S. Kajimura, O. Kakhlon, M. Kalia, D. V. Kalvakolanu, Y. Kamada, K. Kambas, V. O. Kaminskyy, H. H. Kampinga, M. Kandouz, C. Kang, R. Kang, T. C. Kang, T. Kanki, T. D. Kanneganti, H. Kanno, A. G. Kanthasamy, M. Kantorow, M. Kaparakis-Liaskos, O. Kapuy, V. Karantza, M. R. Karim, P. Karmakar, A. Kaser, S. Kaushik, T. Kawula, A. M. Kaynar, P. Y. Ke, Z. J. Ke, J. H. Kehrl, K. E. Keller, J. K. Kemper, A. K. Kenworthy, O. Kepp, A. Kern, S. Kesari, D. Kessel, R. Ketteler, C. Kettelhut Ido, B. Khambu, M. M. Khan, V. K. Khandelwal, S. Khare, J. G. Kiang, A. A. Kiger, A. Kihara, A. L. Kim, C. H. Kim, D. R. Kim, D. H. Kim, E. K. Kim, H. Y. Kim, H. R. Kim, J. S. Kim, J. H. Kim, J. C. Kim, J. H. Kim, K. W. Kim, M. D. Kim, M. M.

Kim, P. K. Kim, S. W. Kim, S. Y. Kim, Y. S. Kim, Y. Kim, A. Kimchi, A. C. Kimmelman, T. Kimura, J. S. King, K. Kirkegaard, V. Kirkin, L. A. Kirshenbaum, S. Kishi, Y. Kitajima, K. Kitamoto, Y. Kitaoka, K. Kitazato, R. A. Kley, W. T. Klimecki, M. Klinkenberg, J. Klucken, H. Knaevelsrud, E. Knecht, L. Knuppertz, J. L. Ko, S. Kobayashi, J. C. Koch, C. Koechlin-Ramonatxo, U. Koenig, Y. H. Koh, K. Kohler, S. D. Kohlwein, M. Koike, M. Komatsu, E. Kominami, D. Kong, H. J. Kong, E. G. Konstantakou, B. T. Kopp, T. Korcsmaros, L. Korhonen, V. I. Korolchuk, N. V. Koshkina, Y. Kou, M. I. Koukourakis, C. Koumenis, A. L. Kovacs, T. Kovacs, W. J. Kovacs, D. Koya, C. Kraft, D. Krainc, H. Kramer, T. Kravic-Stevovic, W. Krek, C. Kretz-Remy, R. Krick, M. Krishnamurthy, J. Kriston-Vizi, G. Kroemer, M. C. Kruer, R. Kruger, N. T. Ktistakis, K. Kuchitsu, C. Kuhn, A. P. Kumar, A. Kumar, A. Kumar, D. Kumar, D. Kumar, R. Kumar, S. Kumar, M. Kundu, H. J. Kung, A. Kuno, S. H. Kuo, J. Kuret, T. Kurz, T. Kwok, T. K. Kwon, Y. T. Kwon, I. Kyrmizi, A. R. La Spada, F. Lafont, T. Lahm, A. Lakkaraju, T. Lam, T. Lamark, S. Lancel, T. H. Landowski, D. J. Lane, J. D. Lane, C. Lanzi, P. Lapaquette, L. R. Lapierre, J. Laporte, J. Laukkarinen, G. W. Laurie, S. Lavandero, L. Lavie, M. J. LaVoie, B. Y. Law, H. K. Law, K. B. Law, R. Layfield, P. A. Lazo, L. Le Cam, K. G. Le Roch, H. Le Stunff, V. Leardkamolkarn, M. Lecuit, B. H. Lee, C. H. Lee, E. F. Lee, G. M. Lee, H. J. Lee, H. Lee, J. K. Lee, J. Lee, J. H. Lee, J. H. Lee, M. Lee, M. S. Lee, P. J. Lee, S. W. Lee, S. J. Lee, S. J. Lee, S. Y. Lee, S. H. Lee, S. S. Lee, S. J. Lee, S. Lee, Y. R. Lee, Y. J. Lee, Y. H. Lee, C. Leeuwenburgh, S. Lefort, R. Legouis, J. Lei, Q. Y. Lei, D. A. Leib, G. Leibowitz, I. Lekli, S. D. Lemaire, J. J. Lemasters, M. K. Lemberg, A. Lemoine, S. Leng, G. Lenz, P. Lenzi, L. O. Lerman, D. Lettieri Barbato, J. I. Leu, H. Y. Leung, B. Levine, P. A. Lewis, F. Lezoualc'h, C. Li, F. Li, F. J. Li, J. Li, K. Li, L. Li, M. Li, M. Li, Q. Li, R. Li, S. Li, W. Li, W. Li, X. Li, Y. Li, J. Lian, C. Liang, Q. Liang, Y. Liao, J. Liberal, P. P. Liberski, P. Lie, A. P. Lieberman, H. J. Lim, K. L. Lim, K. Lim, R. T. Lima, C. S. Lin, C. F. Lin, F. Lin, F. Lin, F. C. Lin, K. Lin, K. H. Lin, P. H. Lin, T. Lin, W. W. Lin, Y. S. Lin, Y. Lin, R. Linden, D. Lindholm, L. M. Lindqvist, P. Lingor, A. Linkermann, L. A. Liotta, M. M. Lipinski, V. A. Lira, M. P. Lisanti, P. B. Liton, B. Liu, C. Liu, C. F. Liu, F. Liu, H. J. Liu, J. Liu, J. J. Liu, J. L. Liu, K. Liu, L. Liu, L. Liu, Q. Liu, R. Y. Liu, S. Liu, S. Liu, W. Liu, X. D. Liu, X. Liu, X. H. Liu, X. Liu, X. Liu, X. Liu, Y. Liu, Y. Liu, Z. Liu, Z. Liu, J. P. Liuzzi, G. Lizard, M. Ljujic, I. J. Lodhi, S. E. Logue, B. L. Lokeshwar, Y. C. Long, S. Lonial, B. Loos, C. Lopez-Otin, C. Lopez-Vicario, M. Lorente, P. L. Lorenzi, P. Lorincz, M. Los, M. T. Lotze, P. E. Lovat, B. Lu, B. Lu, J. Lu, Q. Lu, S. M. Lu, S. Lu, Y. Lu, F. Luciano, S. Luckhart, J. M. Lucocq, P. Ludovico, A. Lugea, N. W. Lukacs, J. J. Lum, A. H. Lund, H. Luo, J. Luo, S. Luo, C. Luparello, T. Lyons, J. Ma, Y. Ma, Y. Ma, Z. Ma, J. Machado, G. M. Machado-Santelli, F. Macian, G. C. MacIntosh, J. P. MacKeigan, K. F. Macleod, J. D. MacMicking, L. A. MacMillan-Crow, F. Madeo, M. Madesh, J. Madrigal-Matute, A. Maeda, T. Maeda, G. Maegawa, E. Maellaro, H. Maes, M. Magarinos, K. Maiese, T. K. Maiti, L. Maiuri, M. C. Maiuri, C. G. Maki, R. Malli, W. Malorni, A. Maloyan, F. Mami-Chouaib, N. Man, J. D. Mancias, E. M. Mandelkow, M. A. Mandell, A. A. Manfredi, S. N. Manie, C. Manzoni, K. Mao, Z. Mao, Z. W. Mao, P. Marambaud, A. M. Marconi, Z. Marelja, G. Marfe, M. Margeta, E. Margittai, M. Mari, F. V. Mariani, C. Marin, S. Marinelli, G. Marino, I. Markovic, R. Marquez, A. M. Martelli, S. Martens, K. R. Martin, S. J. Martin, S. Martin, M. A. Martin-Acebes, P. Martin-Sanz, C. Martinand-Mari, W. Martinet, J. Martinez, N. Martinez-Lopez, U. Martinez-Outschoorn, M. Martinez-Velazquez, M. Martinez-Vicente, W. K. Martins, H. Mashima, J. A. Mastrianni, G. Matarese, P. Matarrese, R. Mateo, S. Matoba, N. Matsumoto, T. Matsushita, A. Matsuura, T. Matsuzawa, M. P. Mattson, S. Matus, N. Maugeri, C. Mauvezin, A. Mayer, D. Maysinger, G. D. Mazzolini, M. K. McBrayer, K. McCall, C. McCormick, G. M. McInerney, S. C. McIver, S. McKenna, J. J.

McMahon, I. A. McNeish, F. Mechta-Grigoriou, J. P. Medema, D. L. Medina, K. Megyeri, M. Mehrpour, J. L. Mehta, Y. Mei, U. C. Meier, A. J. Meijer, A. Melendez, G. Melino, S. Melino, E. J. de Melo, M. A. Mena, M. D. Meneghini, J. A. Menendez, R. Menezes, L. Meng, L. H. Meng, S. Meng, R. Menghini, A. S. Menko, R. F. Menna-Barreto, M. B. Menon, M. A. Meraz-Rios, G. Merla, L. Merlini, A. M. Merlot, A. Meryk, S. Meschini, J. N. Meyer, M. T. Mi, C. Y. Miao, L. Micale, S. Michaeli, C. Michiels, A. R. Migliaccio, A. S. Mihailidou, D. Mijaljica, K. Mikoshiba, E. Milan, L. Miller-Fleming, G. B. Mills, I. G. Mills, G. Minakaki, B. A. Minassian, X. F. Ming, F. Minibayeva, E. A. Minina, J. D. Mintern, S. Minucci, A. Miranda-Vizuete, C. H. Mitchell, S. Miyamoto, K. Miyazawa, N. Mizushima, K. Mnich, B. Mograbi, S. Mohseni, L. F. Moita, M. Molinari, M. Molinari, A. B. Moller, B. Mollereau, F. Mollinedo, M. Mongillo, M. M. Monick, S. Montagnaro, C. Montell, D. J. Moore, M. N. Moore, R. Mora-Rodriguez, P. I. Moreira, E. Morel, M. B. Morelli, S. Moreno, M. J. Morgan, A. Moris, Y. Moriyasu, J. L. Morrison, L. A. Morrison, E. Morselli, J. Moscat, P. L. Moseley, S. Mostowy, E. Motori, D. Mottet, J. C. Mottram, C. E. Moussa, V. E. Mpakou, H. Mukhtar, J. M. Mulcahy Levy, S. Muller, R. Munoz-Moreno, C. Munoz-Pinedo, C. Munz, M. E. Murphy, J. T. Murray, A. Murthy, I. U. Mysorekar, I. R. Nabi, M. Nabissi, G. A. Nader, Y. Nagahara, Y. Nagai, K. Nagata, A. Nagelkerke, P. Nagy, S. R. Naidu, S. Nair, H. Nakano, H. Nakatogawa, M. Nanjundan, G. Napolitano, N. I. Naqvi, R. Nardacci, D. P. Narendra, M. Narita, A. C. Nascimbeni, R. Natarajan, L. C. Navegantes, S. T. Nawrocki, T. Y. Nazarko, V. Y. Nazarko, T. Neill, L. M. Neri, M. G. Netea, R. T. Netea-Maier, B. M. Neves, P. A. Ney, I. P. Nezis, H. T. Nguyen, H. P. Nguyen, A. S. Nicot, H. Nilsen, P. Nilsson, M. Nishimura, I. Nishino, M. Niso-Santano, H. Niu, R. A. Nixon, V. C. Njar, T. Noda, A. A. Noegel, E. M. Nolte, E. Norberg, K. K. Norga, S. K. Noureini, S. Notomi, L. Notterpek, K. Nowikovsky, N. Nukina, T. Nurnberger, V. B. O'Donnell, T. O'Donovan, P. J. O'Dwyer, I. Oehme, C. L. Oeste, M. Ogawa, B. Ogretmen, Y. Ogura, Y. J. Oh, M. Ohmuraya, T. Ohshima, R. Ojha, K. Okamoto, T. Okazaki, F. J. Oliver, K. Ollinger, S. Olsson, D. P. Orban, P. Ordonez, I. Orhon, L. Orosz, E. J. O'Rourke, H. Orozco, A. L. Ortega, E. Ortona, L. D. Osellame, J. Oshima, S. Oshima, H. D. Osiewacz, T. Otomo, K. Otsu, J. H. Ou, T. F. Outeiro, D. Y. Ouyang, H. Ouyang, M. Overholtzer, M. A. Ozbun, P. H. Ozdinler, B. Ozpolat, C. Pacelli, P. Paganetti, G. Page, G. Pages, U. Pagnini, B. Pajak, S. C. Pak, K. Pakos-Zebrucka, N. Pakpour, Z. Palkova, F. Palladino, K. Pallauf, N. Pallet, M. Palmieri, S. R. Paludan, C. Palumbo, S. Palumbo, O. Pampliega, H. Pan, W. Pan, T. Panaretakis, A. Pandey, A. Pantazopoulou, Z. Papackova, D. L. Papademetrio, I. Papassideri, A. Papini, N. Parajuli, J. Pardo, V. V. Parekh, G. Parenti, J. I. Park, J. Park, O. K. Park, R. Parker, R. Parlato, J. B. Parys, K. R. Parzych, J. M. Pasquet, B. Pasquier, K. B. Pasumarthi, D. Patschan, C. Patterson, S. Pattingre, S. Pattison, A. Pause, H. Pavenstadt, F. Pavone, Z. Pedrozo, F. J. Pena, M. A. Penalva, M. Pende, J. Peng, F. Penna, J. M. Penninger, A. Pensalfini, S. Pepe, G. J. Pereira, P. C. Pereira, V. Perez-de la Cruz, M. E. Perez-Perez, D. Perez-Rodriguez, D. Perez-Sala, C. Perier, A. Perl, D. H. Perlmutter, I. Perrotta, S. Pervaiz, M. Pesonen, J. E. Pessin, G. J. Peters, M. Petersen, I. Petrache, B. J. Petrof, G. Petrovski, J. M. Phang, M. Piacentini, M. Pierdominici, P. Pierre, V. Pierrefite-Carle, F. Pietrocola, F. X. Pimentel-Muinos, M. Pinar, B. Pineda, R. Pinkas-Kramarski, M. Pinti, P. Pinton, B. Piperdi, J. M. Piret, L. C. Platanias, H. W. Platta, E. D. Plowey, S. Poggeler, M. Poirot, P. Polcic, A. Poletti, A. H. Poon, H. Popelka, B. Popova, I. Poprawa, S. M. Poulose, J. Poulton, S. K. Powers, T. Powers, M. Pozuelo-Rubio, K. Prak, R. Prange, M. Prescott, M. Priault, S. Prince, R. L. Proia, T. Proikas-Cezanne, H. Prokisch, V. J. Promponas, K. Przyklenk, R. Puertollano, S. Pugazhenthi, L. Puglielli, A. Pujol, J. Puyal, D. Pyeon, X. Qi, W. B. Qian, Z. H. Qin, Y. Qiu, Z. Qu, J. Quadrilatero, F. Quinn, N. Raben, H.

Rabinowich, F. Radogna, M. J. Ragusa, M. Rahmani, K. Raina, S. Ramanadham, R. Ramesh, A. Rami, S. Randall-Demllo, F. Randow, H. Rao, V. A. Rao, B. B. Rasmussen, T. M. Rasse, E. A. Ratovitski, P. E. Rautou, S. K. Ray, B. Razani, B. H. Reed, F. Reggiori, M. Rehm, A. S. Reichert, T. Rein, D. J. Reiner, E. Reits, J. Ren, X. Ren, M. Renna, J. E. Reusch, J. L. Revuelta, L. Reyes, A. R. Rezaie, R. I. Richards, D. R. Richardson, C. Richetta, M. A. Riehle, B. H. Rihn, Y. Rikihisa, B. E. Riley, G. Rimbach, M. R. Rippo, K. Ritis, F. Rizzi, E. Rizzo, P. J. Roach, J. Robbins, M. Roberge, G. Roca, M. C. Roccheri, S. Rocha, C. M. Rodrigues, C. I. Rodriguez, S. R. de Cordoba, N. Rodriguez-Muela, J. Roelofs, V. V. Rogov, T. T. Rohn, B. Rohrer, D. Romanelli, L. Romani, P. S. Romano, M. I. Roncero, J. L. Rosa, A. Rosello, K. V. Rosen, P. Rosenstiel, M. Rost-Roszkowska, K. A. Roth, G. Roue, M. Rouis, K. M. Rouschop, D. T. Ruan, D. Ruano, D. C. Rubinsztein, E. B. Rucker, 3rd, A. Rudich, E. Rudolf, R. Rudolf, M. A. Ruegg, C. Ruiz-Roldan, A. A. Ruparelia, P. Rusmini, D. W. Russ, G. L. Russo, G. Russo, R. Russo, T. E. Rusten, V. Ryabovol, K. M. Ryan, S. W. Ryter, D. M. Sabatini, M. Sacher, C. Sachse, M. N. Sack, J. Sadoshima, P. Saftig, R. Sagi-Eisenberg, S. Sahni, P. Saikumar, T. Saito, T. Saitoh, K. Sakakura, M. Sakoh-Nakatogawa, Y. Sakuraba, M. Salazar-Roa, P. Salomoni, A. K. Saluja, P. M. Salvaterra, R. Salvioli, A. Samali, A. M. Sanchez, J. A. Sanchez-Alcazar, R. Sanchez-Prieto, M. Sandri, M. A. Sanjuan, S. Santaguida, L. Santambrogio, G. Santoni, C. N. Dos Santos, S. Saran, M. Sardiello, G. Sargent, P. Sarkar, S. Sarkar, M. R. Sarrias, M. M. Sarwal, C. Sasakawa, M. Sasaki, M. Sass, K. Sato, M. Sato, J. Satriano, N. Savaraj, S. Saveljeva, L. Schaefer, U. E. Schaible, M. Scharl, H. M. Schatzl, R. Schekman, W. Scheper, A. Schiavi, H. M. Schipper, H. Schmeisser, J. Schmidt, I. Schmitz, B. E. Schneider, E. M. Schneider, J. L. Schneider, E. A. Schon, M. J. Schonenberger, A. H. Schonthal, D. F. Schorderet, B. Schroder, S. Schuck, R. J. Schulze, M. Schwarten, T. L. Schwarz, S. Sciarretta, K. Scotto, A. I. Scovassi, R. A. Screaton, M. Screen, H. Seca, S. Sedej, L. Segatori, N. Segev, P. O. Seglen, J. M. Segui-Simarro, J. Segura-Aguilar, E. Seki, C. Sell, I. Seiliez, C. F. Semenkovich, G. L. Semenza, U. Sen, A. L. Serra, A. Serrano-Puebla, H. Sesaki, T. Setoguchi, C. Settembre, J. J. Shacka, A. N. Shajahan-Haq, I. M. Shapiro, S. Sharma, H. She, C. K. Shen, C. C. Shen, H. M. Shen, S. Shen, W. Shen, R. Sheng, X. Sheng, Z. H. Sheng, T. G. Shepherd, J. Shi, Q. Shi, Q. Shi, Y. Shi, S. Shibutani, K. Shibuya, Y. Shidoji, J. J. Shieh, C. M. Shih, Y. Shimada, S. Shimizu, D. W. Shin, M. L. Shinohara, M. Shintani, T. Shintani, T. Shioi, K. Shirabe, R. Shiri-Sverdlov, O. Shirihai, G. C. Shore, C. W. Shu, D. Shukla, A. A. Sibirny, V. Sica, C. J. Sigurdson, E. M. Sigurdsson, P. S. Sijwali, B. Sikorska, W. A. Silveira, S. Silvente-Poirot, G. A. Silverman, J. Simak, T. Simmet, A. K. Simon, H. U. Simon, C. Simone, M. Simons, A. Simonsen, R. Singh, S. V. Singh, S. K. Singh, D. Sinha, S. Sinha, F. A. Sinicrope, A. Sirko, K. Sirohi, B. J. Sishi, A. Sittler, P. M. Siu, E. Sivridis, A. Skwarska, R. Slack, I. Slaninova, N. Slavov, S. S. Smaili, K. S. Smalley, D. R. Smith, S. J. Soenen, S. A. Soleimanpour, A. Solhaug, K. Somasundaram, J. H. Son, A. Sonawane, C. Song, F. Song, H. K. Song, J. X. Song, W. Song, K. Y. Soo, A. K. Sood, T. W. Soong, V. Soontornniyomkij, M. Sorice, F. Sotgia, D. R. Soto-Pantoja, A. Sotthibundhu, M. J. Sousa, H. P. Spaink, P. N. Span, A. Spang, J. D. Sparks, P. G. Speck, S. A. Spector, C. D. Spies, W. Springer, D. S. Clair, A. Stacchiotti, B. Staels, M. T. Stang, D. T. Starczynowski, P. Starokadomskyy, C. Steegborn, J. W. Steele, L. Stefanis, J. Steffan, C. M. Stellrecht, H. Stenmark, T. M. Stepkowski, S. T. Stern, C. Stevens, B. R. Stockwell, V. Stoka, Z. Storchova, B. Stork, V. Stratoulias, D. J. Stravopodis, P. Strnad, A. M. Strohecker, A. L. Strom, P. Stromhaug, J. Stulik, Y. X. Su, Z. Su, C. S. Subauste, S. Subramaniam, C. M. Sue, S. W. Suh, X. Sui, S. Sukseree, D. Sulzer, F. L. Sun, J. Sun, J. Sun, S. Y. Sun, Y. Sun, Y.

Sun, Y. Sun, V. Sundaramoorthy, J. Sung, H. Suzuki, K. Suzuki, N. Suzuki, T. Suzuki, Y. J. Suzuki, M. S. Swanson, C. Swanton, K. Sward, G. Swarup, S. T. Sweeney, P. W. Sylvester, Z. Szatmari, E. Szegezdi, P. W. Szlosarek, H. Taegtmeyer, M. Tafani, E. Taillebourg, S. W. Tait, K. Takacs-Vellai, Y. Takahashi, S. Takats, G. Takemura, N. Takigawa, N. J. Talbot, E. Tamagno, J. Tamburini, C. P. Tan, L. Tan, M. L. Tan, M. Tan, Y. J. Tan, K. Tanaka, M. Tanaka, D. Tang, D. Tang, G. Tang, I. Tanida, K. Tanji, B. A. Tannous, J. A. Tapia, I. Tasset-Cuevas, M. Tatar, I. Tavassoly, N. Tavernarakis, A. Taylor, G. S. Taylor, G. A. Taylor, J. P. Taylor, M. J. Taylor, E. V. Tchetina, A. R. Tee, F. Teixeira-Clerc, S. Telang, T. Tencomnao, B. B. Teng, R. J. Teng, F. Terro, G. Tettamanti, A. L. Theiss, A. E. Theron, K. J. Thomas, M. P. Thome, P. G. Thomes, A. Thorburn, J. Thorner, T. Thum, M. Thumm, T. L. Thurston, L. Tian, A. Till, J. P. Ting, V. I. Titorenko, L. Toker, S. Toldo, S. A. Tooze, I. Topisirovic, M. L. Torgersen, L. Torosantucci, A. Torriglia, M. R. Torrisi, C. Tournier, R. Towns, V. Trajkovic, L. H. Travassos, G. Triola, D. N. Tripathi, D. Trisciuoglio, R. Troncoso, I. P. Trougakos, A. C. Truttmann, K. J. Tsai, M. P. Tschan, Y. H. Tseng, T. Tsukuba, A. Tsung, A. S. Tsvetkov, S. Tu, H. Y. Tuan, M. Tucci, D. A. Tumbarello, B. Turk, V. Turk, R. F. Turner, A. A. Tveita, S. C. Tyagi, M. Ubukata, Y. Uchiyama, A. Udelnow, T. Ueno, M. Umekawa, R. Umemiya-Shirafuji, B. R. Underwood, C. Ungermann, R. P. Ureshino, R. Ushioda, V. N. Uversky, N. L. Uzcategui, T. Vaccari, M. I. Vaccaro, L. Vachova, H. Vakifahmetoglu-Norberg, R. Valdor, E. M. Valente, F. Vallette, A. M. Valverde, G. Van den Berghe, L. Van Den Bosch, G. R. van den Brink, F. G. van der Goot, I. J. van der Klei, L. J. van der Laan, W. G. van Doorn, M. van Egmond, K. L. van Golen, L. Van Kaer, M. van Lookeren Campagne, P. Vandenabeele, W. Vandenberghe, I. Vanhorebeek, I. Varela-Nieto, M. H. Vasconcelos, R. Vasko, D. G. Vavvas, I. Vega-Naredo, G. Velasco, A. D. Velentzas, P. D. Velentzas, T. Vellai, E. Vellenga, M. H. Vendelbo, K. Venkatachalam, N. Ventura, S. Ventura, P. S. Veras, M. Verdier, B. G. Vertessy, A. Viale, M. Vidal, H. L. Vieira, R. D. Vierstra, N. Vigneswaran, N. Vij, M. Vila, M. Villar, V. H. Villar, J. Villarroya, C. Vindis, G. Viola, M. T. Viscomi, G. Vitale, D. T. Vogl, O. V. Voitsekhovskaja, C. von Haefen, K. von Schwarzenberg, D. E. Voth, V. Vouret-Craviari, K. Vuori, J. M. Vyas, C. Waeber, C. L. Walker, M. J. Walker, J. Walter, L. Wan, X. Wan, B. Wang, C. Wang, C. Y. Wang, C. Wang, C. Wang, C. Wang, D. Wang, F. Wang, F. Wang, G. Wang, H. J. Wang, H. Wang, H. G. Wang, H. Wang, H. D. Wang, J. Wang, J. Wang, M. Wang, M. Q. Wang, P. Y. Wang, P. Wang, R. C. Wang, S. Wang, T. F. Wang, X. Wang, X. J. Wang, X. W. Wang, X. Wang, X. Wang, Y. Wang, Y. Wang, Y. Wang, Y. J. Wang, Y. Wang, Y. Wang, Y. T. Wang, Y. Wang, Z. N. Wang, P. Wappner, C. Ward, D. M. Ward, G. Warnes, H. Watada, Y. Watanabe, K. Watase, T. E. Weaver, C. D. Weekes, J. Wei, T. Weide, C. C. Weihl, G. Weindl, S. N. Weis, L. Wen, X. Wen, Y. Wen, B. Westermann, C. M. Weyand, A. R. White, E. White, J. L. Whitton, A. J. Whitworth, J. Wiels, F. Wild, M. E. Wildenberg, T. Wileman, D. S. Wilkinson, S. Wilkinson, D. Willbold, C. Williams, K. Williams, P. R. Williamson, K. F. Winklhofer, S. S. Witkin, S. E. Wohlgemuth, T. Wollert, E. J. Wolvetang, E. Wong, G. W. Wong, R. W. Wong, V. K. Wong, E. A. Woodcock, K. L. Wright, C. Wu, D. Wu, G. S. Wu, J. Wu, J. Wu, M. Wu, M. Wu, S. Wu, W. K. Wu, Y. Wu, Z. Wu, C. P. Xavier, R. J. Xavier, G. X. Xia, T. Xia, W. Xia, Y. Xia, H. Xiao, J. Xiao, S. Xiao, W. Xiao, C. M. Xie, Z. Xie, Z. Xie, M. Xilouri, Y. Xiong, C. Xu, C. Xu, F. Xu, H. Xu, H. Xu, J. Xu, J. Xu, J. Xu, L. Xu, X. Xu, Y. Xu, Y. Xu, Z. X. Xu, Z. Xu, Y. Xue, T. Yamada, A. Yamamoto, K. Yamanaka, S. Yamashina, S. Yamashiro, B. Yan, B. Yan, X. Yan, Z. Yan, Y. Yanagi, D. S. Yang, J. M. Yang, L. Yang, M. Yang, P. M. Yang, P. Yang, Q. Yang, W. Yang, W. Y. Yang, X. Yang, Y. Yang, Y. Yang, Z. Yang, Z. Yang, M. C. Yao, P. J. Yao, X. Yao, Z. Yao, Z. Yao, L. S. Yasui, M. Ye, B. Yedvobnick, B. Yeganeh,

E. S. Yeh, P. L. Yeyati, F. Yi, L. Yi, X. M. Yin, C. K. Yip, Y. M. Yoo, Y. H. Yoo, S. Y. Yoon, K. Yoshida, T. Yoshimori, K. H. Young, H. Yu, J. J. Yu, J. T. Yu, J. Yu, L. Yu, W. H. Yu, X. F. Yu, Z. Yu, J. Yuan, Z. M. Yuan, B. Y. Yue, J. Yue, Z. Yue, D. N. Zacks, E. Zacksenhaus, N. Zaffaroni, T. Zaglia, Z. Zakeri, V. Zecchini, J. Zeng, M. Zeng, Q. Zeng, A. S. Zervos, D. D. Zhang, F. Zhang, G. Zhang, G. C. Zhang, H. Zhang, H. Zhang, H. Zhang, H. Zhang, J. Zhang, J. Zhang, J. Zhang, J. Zhang, J. P. Zhang, L. Zhang, L. Zhang, L. Zhang, L. Zhang, M. Y. Zhang, X. Zhang, X. D. Zhang, Y. Zhang, Y. Zhang, Y. Zhang, Y. Zhang, Y. Zhang, M. Zhao, W. L. Zhao, X. Zhao, Y. G. Zhao, Y. Zhao, Y. Zhao, Y. X. Zhao, Z. Zhao, Z. J. Zhao, D. Zheng, X. L. Zheng, X. Zheng, B. Zhivotovsky, Q. Zhong, G. Z. Zhou, G. Zhou, H. Zhou, S. F. Zhou, X. J. Zhou, H. Zhu, H. Zhu, W. G. Zhu, W. Zhu, X. F. Zhu, Y. Zhu, S. M. Zhuang, X. Zhuang, E. Ziparo, C. E. Zois, T. Zoladek, W. X. Zong, A. Zorzano and S. M. Zughaier (2016). "Guidelines for the use and interpretation of assays for monitoring autophagy (3rd edition)." Autophagy **12**(1): 1-222.

Koop, A., P. Goldmann, S. R. Chen, R. Thieleczek and M. Varsanyi (2008). "ARVC-related mutations in divergent region 3 alter functional properties of the cardiac ryanodine receptor." Biophys J **94**(12): 4668-4677.

Krusche, C. A., B. Holthofer, V. Hofe, A. M. van de Sandt, L. Eshkind, E. Bockamp, M. W. Merx, S. Kant, R. Windoffer and R. E. Leube (2011). "Desmoglein 2 mutant mice develop cardiac fibrosis and dilation." Basic Res Cardiol **106**(4): 617-633.

Lammerding, J., P. C. Schulze, T. Takahashi, S. Kozlov, T. Sullivan, R. D. Kamm, C. L. Stewart and R. T. Lee (2004). "Lamin A/C deficiency causes defective nuclear mechanics and mechanotransduction." J Clin Invest **113**(3): 370-378.

Lange, S., F. Xiang, A. Yakovenko, A. Vihola, P. Hackman, E. Rostkova, J. Kristensen, B. Brandmeier, G. Franzen, B. Hedberg, L. G. Gunnarsson, S. M. Hughes, S. Marchand, T. Sejersen, I. Richard, L. Edstrom, E. Ehler, B. Udd and M. Gautel (2005). "The kinase domain of titin controls muscle gene expression and protein turnover." Science **308**(5728): 1599-1603.

Leask, A. and D. J. Abraham (2004). "TGF-beta signaling and the fibrotic response." FASEB J **18**(7): 816-827.

LeWinter, M. M. and H. Granzier (2010). "Cardiac titin: a multifunctional giant." Circulation **121**(19): 2137-2145.

Li, D., Y. Liu, M. Maruyama, W. Zhu, H. Chen, W. Zhang, S. Reuter, S. F. Lin, L. S. Haneline, L. J. Field, P. S. Chen and W. Shou (2011). "Restrictive loss of plakoglobin in cardiomyocytes leads to arrhythmogenic cardiomyopathy." Hum Mol Genet **20**(23): 4582-4596.

Li, D., T. Tapscoft, O. Gonzalez, P. E. Burch, M. A. Quinones, W. A. Zoghbi, R. Hill, L. L. Bachinski, D. L. Mann and R. Roberts (1999). "Desmin mutation responsible for idiopathic dilated cardiomyopathy." Circulation **100**(5): 461-464.

Li, J., S. Goossens, J. van Hengel, E. Gao, L. Cheng, K. Tyberghein, X. Shang, R. De Rycke, F. van Roy and G. L. Radice (2012). "Loss of alphaT-catenin alters the hybrid adhering junctions in the heart and leads to dilated cardiomyopathy and ventricular arrhythmia following acute ischemia." J Cell Sci **125**(Pt 4): 1058-1067.

Li, J., K. M. Horak, H. Su, A. Sanbe, J. Robbins and X. Wang (2011). "Enhancement of proteasomal function protects against cardiac proteinopathy and ischemia/reperfusion injury in mice." J Clin Invest **121**(9): 3689-3700.

Li, J., D. Swope, N. Raess, L. Cheng, E. J. Muller and G. L. Radice (2011). "Cardiac tissue-restricted deletion of plakoglobin results in progressive cardiomyopathy and activation of {beta}-catenin signaling." Mol Cell Biol **31**(6): 1134-1144.

Lian, X., J. Zhang, S. M. Azarin, K. Zhu, L. B. Hazeltine, X. Bao, C. Hsiao, T. J. Kamp and S. P. Palecek (2013). "Directed cardiomyocyte differentiation from human pluripotent stem cells by modulating Wnt/beta-catenin signaling under fully defined conditions." Nat Protoc **8**(1): 162-175.

Liang, W. C., H. Mitsuhashi, E. Keduka, I. Nonaka, S. Noguchi, I. Nishino and Y. K. Hayashi (2011). "TMEM43 mutations in Emery-Dreifuss muscular dystrophy-related myopathy." Ann Neurol **69**(6): 1005-1013.

Lim, B. K., D. Xiong, A. Dorner, T. J. Youn, A. Yung, T. I. Liu, Y. Gu, N. D. Dalton, A. T. Wright, S. M. Evans, J. Chen, K. L. Peterson, A. D. McCulloch, T. Yajima and K. U. Knowlton (2008). "Coxsackievirus and adenovirus receptor (CAR) mediates atrioventricular-node function and connexin 45 localization in the murine heart." J Clin Invest **118**(8): 2758-2770.

Lim, G. B. (2017). "Heart failure: Phase II trial results of omecamtiv mecarbil." Nat Rev Cardiol **14**(2): 66.

Lombardi, R., M. da Graca Cabreira-Hansen, A. Bell, R. R. Fromm, J. T. Willerson and A. J. Marian (2011). "Nuclear plakoglobin is essential for differentiation of cardiac progenitor cells to adipocytes in arrhythmogenic right ventricular cardiomyopathy." Circ Res **109**(12): 1342-1353.

Lombardi, R., J. Dong, G. Rodriguez, A. Bell, T. K. Leung, R. J. Schwartz, J. T. Willerson, R. Brugada and A. J. Marian (2009). "Genetic fate mapping identifies second heart field progenitor cells as a source of adipocytes in arrhythmogenic right ventricular cardiomyopathy." Circ Res **104**(9): 1076-1084.

Lusis, A. J. (2003). "Genetic factors in cardiovascular disease. 10 questions." Trends Cardiovasc Med **13**(8): 309-316.

Lyon, R. C., S. Lange and F. Sheikh (2013). "Breaking down protein degradation mechanisms in cardiac muscle." Trends Mol Med **19**(4): 239-249.

Lyon, R. C., V. Mezzano, A. T. Wright, E. Pfeiffer, J. Chuang, K. Banares, A. Castaneda, K. Ouyang, L. Cui, R. Contu, Y. Gu, S. M. Evans, J. H. Omens, K. L. Peterson, A. D. McCulloch and F. Sheikh (2014). "Connexin defects underlie arrhythmogenic right ventricular cardiomyopathy in a novel mouse model." Hum Mol Genet **23**(5): 1134-1150.

Ma, D., H. Wei, J. Lu, S. Ho, G. Zhang, X. Sun, Y. Oh, S. H. Tan, M. L. Ng, W. Shim, P. Wong and R. Liew (2013). "Generation of patient-specific induced pluripotent stem cell-derived cardiomyocytes as a cellular model of arrhythmogenic right ventricular cardiomyopathy." Eur Heart J **34**(15): 1122-1133.

MacLennan, D. H. and E. G. Kranias (2003). "Phospholamban: a crucial regulator of cardiac contractility." Nat Rev Mol Cell Biol **4**(7): 566-577.

MacLeod, H. M., M. R. Culley, J. M. Huber and E. M. McNally (2003). "Lamin A/C truncation in dilated cardiomyopathy with conduction disease." BMC Med Genet **4**: 4.

Malik, F. I., J. J. Hartman, K. A. Elias, B. P. Morgan, H. Rodriguez, K. Brejc, R. L. Anderson, S. H. Sueoka, K. H. Lee, J. T. Finer, R. Sakowicz, R. Baliga, D. R. Cox, M. Garard, G. Godinez, R. Kawas, E. Kraynack, D. Lenzi, P. P. Lu, A. Muci, C. Niu, X. Qian, D. W. Pierce, M. Pokrovskii, I. Suehiro, S. Sylvester, T. Tochimoto, C. Valdez, W. Wang, T. Katori, D. A. Kass, Y. T. Shen, S. F. Vatner and D. J. Morgans (2011). "Cardiac myosin activation: a potential therapeutic approach for systolic heart failure." Science **331**(6023): 1439-1443.

Malone, P., H. Miao, A. Parker, S. Juarez and M. R. Hernandez (2007). "Pressure induces loss of gap junction communication and redistribution of connexin 43 in astrocytes." Glia **55**(10): 1085-1098.

Martins-Marques, T., S. Catarino, C. Marques, P. Matafome, T. Ribeiro-Rodrigues, R. Baptista, P. Pereira and H. Girao (2015). "Heart ischemia results in connexin43 ubiquitination localized at the intercalated discs." Biochimie **112**: 196-201.

Martins-Marques, T., S. Catarino, M. Zuzarte, C. Marques, P. Matafome, P. Pereira and H. Girao (2015). "Ischaemia-induced autophagy leads to degradation of gap junction protein connexin43 in cardiomyocytes." Biochem J **467**(2): 231-245.

Marx, S. O. and A. R. Marks (2013). "Dysfunctional ryanodine receptors in the heart: new insights into complex cardiovascular diseases." J Mol Cell Cardiol **58**: 225-231.

Masani, F., Y. Aizawa, T. Izumi and A. Shibata (1990). "An ultrastructural study on arrhythmogenic right ventricular dysplasia with special reference to lipid droplets." Heart Vessels Suppl **5**: 55-58.

McNally, E. M., J. R. Golbus and M. J. Puckelwartz (2013). "Genetic mutations and mechanisms in dilated cardiomyopathy." J Clin Invest **123**(1): 19-26.

Meinke, P., T. D. Nguyen and M. S. Wehnert (2011). "The LINC complex and human disease." Biochem Soc Trans **39**(6): 1693-1697.

Melberg, A., A. Oldfors, C. Blomstrom-Lundqvist, E. Stalberg, B. Carlsson, E. Larrson, C. Lidell, K. E. Eeg-Olofsson, G. Wikstrom, G. Henriksson and N. Dahl (1999). "Autosomal dominant myofibrillar myopathy with arrhythmogenic right ventricular cardiomyopathy linked to chromosome 10q." Ann Neurol **46**(5): 684-692.

Merner, N. D., K. A. Hodgkinson, A. F. Haywood, S. Connors, V. M. French, J. D. Drenckhahn, C. Kupprion, K. Ramadanova, L. Thierfelder, W. McKenna, B. Gallagher, L. Morris-Larkin, A. S. Bassett, P. S. Parfrey and T. L. Young (2008). "Arrhythmogenic right ventricular cardiomyopathy type 5 is a fully penetrant, lethal arrhythmic disorder caused by a missense mutation in the TMEM43 gene." Am J Hum Genet **82**(4): 809-821.

Mezzano, V., J. Pellman and F. Sheikh (2014). "Cell junctions in the specialized conduction system of the heart." Cell Commun Adhes **21**(3): 149-159.

Michalodimitrakis, M., A. Papadomanolakis, J. Stiakakis and K. Kanaki (2002). "Left side right ventricular cardiomyopathy." Med Sci Law **42**(4): 313-317.

Miller, D., L. Wang and J. Zhong (2014). "Sodium channels, cardiac arrhythmia, and therapeutic strategy." Adv Pharmacol **70**: 367-392.

Milting, H., B. Klauke, A. H. Christensen, J. Musebeck, V. Walhorn, S. Grannemann, T. Munnich, T. Saric, T. B. Rasmussen, H. K. Jensen, J. Mogensen, C. Baecker, E. Romaker, K. T. Laser, E. zu Knyphausen, A. Kassner, J. Gummert, D. P. Judge, S. Connors, K. Hodgkinson, T. L. Young, P. A. van der Zwaag, J. P. van Tintelen and D. Anselmetti (2015). "The TMEM43 Newfoundland mutation p.S358L causing ARVC-5 was imported from Europe and increases the stiffness of the cell nucleus." Eur Heart J **36**(14): 872-881.

Miyata, S., K. Yoshikawa, M. Taniguchi, T. Ishikawa, T. Tanaka, S. Shimizu and M. Tohyama (2015). "Sgk1 regulates desmoglein 1 expression levels in oligodendrocytes in the mouse corpus callosum after chronic stress exposure." Biochem Biophys Res Commun **464**(1): 76-82.

Moncayo-Arlandi, J., E. Guasch, M. Sanz-de la Garza, M. Casado, N. A. Garcia, L. Mont, M. Sitges, R. Knoll, B. Buyandelger, O. Campuzano, A. Diez-Juan and R. Brugada (2016). "Molecular disturbance underlies to arrhythmogenic cardiomyopathy induced by transgene content, age and exercise in a truncated PKP2 mouse model." Hum Mol Genet **25**(17): 3676-3688.

Montonen, O., M. Aho, J. Uitto and S. Aho (2001). "Tissue distribution and cell type-specific expression of p120ctn isoforms." J Histochem Cytochem **49**(12): 1487-1496.

Morelli, E., P. Ginefra, V. Mastrodonato, G. V. Beznoussenko, T. E. Rusten, D. Bilder, H. Stenmark, A. A. Mironov and T. Vaccari (2014). "Multiple functions of the SNARE protein Snap29 in autophagy, endocytic, and exocytic trafficking during epithelial formation in Drosophila." Autophagy **10**(12): 2251-2268.

Nakai, A., O. Yamaguchi, T. Takeda, Y. Higuchi, S. Hikoso, M. Taniike, S. Omiya, I. Mizote, Y. Matsumura, M. Asahi, K. Nishida, M. Hori, N. Mizushima and K. Otsu (2007). "The role of autophagy in cardiomyocytes in the basal state and in response to hemodynamic stress." Nat Med **13**(5): 619-624.

Nepomnyashchikh, L. M., E. L. Lushnikova and D. E. Semenov (2000). "Focal degradation of cytoplasmic organelles in cardiomyocytes during regenerative and plastic myocardial insufficiency." Bull Exp Biol Med **130**(12): 1190-1195.

Nishida, K., S. Kyoi, O. Yamaguchi, J. Sadoshima and K. Otsu (2009). "The role of autophagy in the heart." Cell Death Differ **16**(1): 31-38.

Nishida, Y., S. Arakawa, K. Fujitani, H. Yamaguchi, T. Mizuta, T. Kanaseki, M. Komatsu, K. Otsu, Y. Tsujimoto and S. Shimizu (2009). "Discovery of Atg5/Atg7-independent alternative macroautophagy." Nature **461**(7264): 654-658.

Nishikawa, T., S. Ishiyama, M. Nagata, Y. Sakomura, M. Nakazawa, K. Momma, M. Hiroe and T. Kasajima (1999). "Programmed cell death in the myocardium of arrhythmogenic right ventricular cardiomyopathy in children and adults." Cardiovasc Pathol **8**(4): 185-189.

Nishino, I., J. Fu, K. Tanji, T. Yamada, S. Shimojo, T. Koori, M. Mora, J. E. Riggs, S. J. Oh, Y. Koga, C. M. Sue, A. Yamamoto, N. Murakami, S. Shanske, E. Byrne, E. Bonilla, I. Nonaka, S. DiMauro and M. Hirano (2000). "Primary LAMP-2 deficiency causes X-linked vacuolar cardiomyopathy and myopathy (Danon disease)." Nature **406**(6798): 906-910.

Norgett, E. E., S. J. Hatsell, L. Carvajal-Huerta, J. C. Cabezas, J. Common, P. E. Purkis, N. Whittock, I. M. Leigh, H. P. Stevens and D. P. Kelsell (2000). "Recessive mutation in desmoplakin disrupts desmoplakin-intermediate filament interactions and causes dilated cardiomyopathy, woolly hair and keratoderma." Hum Mol Genet **9**(18): 2761-2766.

Norman, M., M. Simpson, J. Mogensen, A. Shaw, S. Hughes, P. Syrris, S. Sen-Chowdhry, E. Rowland, A. Crosby and W. J. McKenna (2005). "Novel mutation in desmoplakin causes arrhythmogenic left ventricular cardiomyopathy." Circulation **112**(5): 636-642.

Notari, M., Y. Hu, G. Sutendra, Z. Dedeic, M. Lu, L. Dupays, A. Yavari, C. A. Carr, S. Zhong, A. Opel, A. Tinker, K. Clarke, H. Watkins, D. J. Ferguson, D. P. Kelsell, S. de Noronha, M. N. Sheppard, M. Hollinshead, T. J. Mohun and X. Lu (2015). "iASPP, a previously unidentified regulator of desmosomes, prevents arrhythmogenic right ventricular cardiomyopathy (ARVC)-induced sudden death." Proc Natl Acad Sci U S A **112**(9): E973-981.

Olive, M., J. Armstrong, F. Miralles, A. Pou, M. Fardeau, L. Gonzalez, F. Martinez, D. Fischer, J. A. Martinez Matos, A. Shatunov, L. Goldfarb and I. Ferrer (2007). "Phenotypic patterns of desminopathy associated with three novel mutations in the desmin gene." Neuromuscul Disord **17**(6): 443-450.

Otten, E., A. Asimaki, A. Maass, I. M. van Langen, A. van der Wal, N. de Jonge, M. P. van den Berg, J. E. Saffitz, A. A. Wilde, J. D. Jongbloed and J. P. van Tintelen (2010). "Desmin mutations as a cause of right ventricular heart failure affect the intercalated disks." Heart Rhythm **7**(8): 1058-1064.

Oyabu, J., O. Yamaguchi, S. Hikoso, T. Takeda, T. Oka, T. Murakawa, H. Yasui, H. Ueda, H. Nakayama, M. Taneike, S. Omiya, A. M. Shah, K. Nishida and K. Otsu (2013). "Autophagy-mediated degradation is necessary for regression of cardiac hypertrophy during ventricular unloading." Biochem Biophys Res Commun **441**(4): 787-792.

Patel, H., P. Shah, U. Rampal, F. Shamoon and S. Tiyyagura (2015). "Arrythmogenic right ventricular dysplasia/cardiomyopathy (ARVD/C) and cathecholaminergic polymorphic ventricular tachycardia (CPVT): A phenotypic spectrum seen in same patient." J Electrocardiol **48**(5): 874-878.

Peters, S., M. Trummel and W. Meyners (2004). "Prevalence of right ventricular dysplasia-cardiomyopathy in a non-referral hospital." Int J Cardiol **97**(3): 499-501.

Pilichou, K., C. A. Remme, C. Basso, M. E. Campian, S. Rizzo, P. Barnett, B. P. Scicluna, B. Bauce, M. J. van den Hoff, J. M. de Bakker, H. L. Tan, M. Valente, A. Nava, A. A. Wilde, A. F. Moorman, G. Thiene and C. R. Bezzina (2009). "Myocyte necrosis underlies progressive myocardial dystrophy in mouse dsg2-related arrhythmogenic right ventricular cardiomyopathy." J Exp Med **206**(8): 1787-1802.

Portbury, A. L., M. S. Willis and C. Patterson (2011). "Tearin' up my heart: proteolysis in the cardiac sarcomere." J Biol Chem **286**(12): 9929-9934.

Predmore, J. M., P. Wang, F. Davis, S. Bartolone, M. V. Westfall, D. B. Dyke, F. Pagani, S. R. Powell and S. M. Day (2010). "Ubiquitin proteasome dysfunction in human hypertrophic and dilated cardiomyopathies." Circulation **121**(8): 997-1004.

Protonotarios, N. and A. Tsatsopoulou (2004). "Naxos disease and Carvajal syndrome: cardiocutaneous disorders that highlight the pathogenesis and broaden the spectrum of arrhythmogenic right ventricular cardiomyopathy." Cardiovasc Pathol **13**(4): 185-194.

Protonotarios, N., A. Tsatsopoulou, P. Patsourakos, D. Alexopoulos, P. Gezerlis, S. Simitsis and G. Scampardonis (1986). "Cardiac abnormalities in familial palmoplantar keratosis." Br Heart J **56**(4): 321-326.

Quarta, G., P. Syrris, M. Ashworth, S. Jenkins, K. Zuborne Alapi, J. Morgan, A. Muir, A. Pantazis, W. J. McKenna and P. M. Elliott (2012). "Mutations in the Lamin A/C gene mimic arrhythmogenic right ventricular cardiomyopathy." Eur Heart J **33**(9): 1128-1136.

Rafiq, K., J. Guo, L. Vlasenko, X. Guo, M. A. Kolpakov, A. Sanjay, S. R. Houser and A. Sabri (2012). "c-Cbl ubiquitin ligase regulates focal adhesion protein turnover and myofibril degeneration induced by neutrophil protease cathepsin G." J Biol Chem **287**(8): 5327-5339.

Rampazzo, A., A. Nava, G. A. Danieli, G. Buja, L. Daliento, G. Fasoli, R. Scognamiglio, D. Corrado and G. Thiene (1994). "The gene for arrhythmogenic right ventricular cardiomyopathy maps to chromosome 14q23-q24." Hum Mol Genet **3**(6): 959-962.

Rampazzo, A., A. Nava, P. Erne, M. Eberhard, E. Vian, P. Slomp, N. Tiso, G. Thiene and G. A. Danieli (1995). "A new locus for arrhythmogenic right ventricular cardiomyopathy (ARVD2) maps to chromosome 1q42-q43." Hum Mol Genet **4**(11): 2151-2154.

Rampazzo, A., A. Nava, S. Malacrida, G. Beffagna, B. Bauce, V. Rossi, R. Zimbello, B. Simionati, C. Basso, G. Thiene, J. A. Towbin and G. A. Danieli (2002). "Mutation in human desmoplakin domain binding to plakoglobin causes a dominant form of arrhythmogenic right ventricular cardiomyopathy." Am J Hum Genet **71**(5): 1200-1206.

Rampazzo, A., A. Nava, M. Miorin, P. Fonderico, B. Pope, N. Tiso, B. Livolsi, R. Zimbello, G. Thiene and G. A. Danieli (1997). "ARVD4, a new locus for arrhythmogenic right ventricular cardiomyopathy, maps to chromosome 2 long arm." Genomics **45**(2): 259-263.

Rasmussen, T. B., P. H. Nissen, J. Palmfeldt, K. Gehmlich, S. Dalager, U. B. Jensen, W. Y. Kim, L. Heickendorff, H. Molgaard, H. K. Jensen, U. T. Baandrup, P. Bross and J. Mogensen (2014). "Truncating plakophilin-2 mutations in arrhythmogenic cardiomyopathy are associated with protein haploinsufficiency in both myocardium and epidermis." Circ Cardiovasc Genet **7**(3): 230-240.

Remme, C. A. (2013). "Cardiac sodium channelopathy associated with SCN5A mutations: electrophysiological, molecular and genetic aspects." J Physiol **591**(17): 4099-4116.

Rey, C., A. Rodriguez-Nunez, A. Medina and J. Mayordomo (2007). "Life-saving automated external defibrillation in a teenager: a case report." J Med Case Rep **1**: 76.

Rhett, J. M., J. Jourdan and R. G. Gourdie (2011). "Connexin 43 connexon to gap junction transition is regulated by zonula occludens-1." Mol Biol Cell **22**(9): 1516-1528.

Rizzo, S., E. M. Lodder, A. O. Verkerk, R. Wolswinkel, L. Beekman, K. Pilichou, C. Basso, C. A. Remme, G. Thiene and C. R. Bezzina (2012). "Intercalated disc abnormalities, reduced Na(+) current density, and conduction slowing in desmoglein-2 mutant mice prior to cardiomyopathic changes." Cardiovasc Res **95**(4): 409-418.

Ruiz, P., V. Brinkmann, B. Ledermann, M. Behrend, C. Grund, C. Thalhammer, F. Vogel, C. Birchmeier, U. Gunthert, W. W. Franke and W. Birchmeier (1996). "Targeted mutation of plakoglobin in mice reveals essential functions of desmosomes in the embryonic heart." J Cell Biol **135**(1): 215-225.

Saffitz, J. E., A. Asimaki and H. Huang (2009). "Arrhythmogenic right ventricular cardiomyopathy: new insights into disease mechanisms and diagnosis." J Investig Med **57**(8): 861-864.

Saguner, A. M., A. Medeiros-Domingo, M. A. Schwyzer, C. J. On, L. M. Haegeli, T. Wolber, D. Hurlimann, J. Steffel, N. Krasniqi, S. Rueger, L. Held, T. F. Luscher, C. Brunckhorst and F. Duru (2013). "Usefulness of inducible ventricular tachycardia to predict long-term adverse outcomes in arrhythmogenic right ventricular cardiomyopathy." Am J Cardiol **111**(2): 250-257.

Sato, P. Y., W. Coombs, X. Lin, O. Nekrasova, K. J. Green, L. L. Isom, S. M. Taffet and M. Delmar (2011). "Interactions between ankyrin-G, Plakophilin-2, and Connexin43 at the cardiac intercalated disc." Circ Res **109**(2): 193-201.

Sato, P. Y., H. Musa, W. Coombs, G. Guerrero-Serna, G. A. Patino, S. M. Taffet, L. L. Isom and M. Delmar (2009). "Loss of plakophilin-2 expression leads to decreased sodium current and slower conduction velocity in cultured cardiac myocytes." Circ Res **105**(6): 523-526.

Satoh, M., M. Takahashi, T. Sakamoto, M. Hiroe, F. Marumo and A. Kimura (1999). "Structural analysis of the titin gene in hypertrophic cardiomyopathy: identification of a novel disease gene." Biochem Biophys Res Commun **262**(2): 411-417.

Schardt, A., B. G. Brinkmann, M. Mitkovski, M. W. Sereda, H. B. Werner and K. A. Nave (2009). "The SNARE protein SNAP-29 interacts with the GTPase Rab3A: Implications for membrane trafficking in myelinating glia." J Neurosci Res **87**(15): 3465-3479.

Schiller, S. A., C. Seebode, G. L. Wieser, S. Goebbels, W. Mobius, M. Horowitz, O. Sarig, E. Sprecher and S. Emmert (2016). "Establishment of Two Mouse Models for CEDNIK Syndrome Reveals the Pivotal Role of SNAP29 in Epidermal Differentiation." J Invest Dermatol **136**(3): 672-679.

Seeger, T. S., D. Frank, C. Rohr, R. Will, S. Just, C. Grund, R. Lyon, M. Luedde, M. Koegl, F. Sheikh, W. Rottbauer, W. W. Franke, H. A. Katus, E. N. Olson and N. Frey (2010). "Myozap, a novel intercalated disc protein, activates serum response factor-dependent signaling and is required to maintain cardiac function in vivo." Circ Res **106**(5): 880-890.

Sen-Chowdhry, S., R. D. Morgan, J. C. Chambers and W. J. McKenna (2010). "Arrhythmogenic cardiomyopathy: etiology, diagnosis, and treatment." Annu Rev Med **61**: 233-253.

Sen-Chowdhry, S., P. Syrris, D. Ward, A. Asimaki, E. Sevdalis and W. J. McKenna (2007). "Clinical and genetic characterization of families with arrhythmogenic right ventricular dysplasia/cardiomyopathy provides novel insights into patterns of disease expression." Circulation **115**(13): 1710-1720.

Sheikh, F., R. S. Ross and J. Chen (2009). "Cell-cell connection to cardiac disease." Trends Cardiovasc Med **19**(6): 182-190.

Shibata, M., K. Yoshimura, N. Furuya, M. Koike, T. Ueno, M. Komatsu, H. Arai, K. Tanaka, E. Kominami and Y. Uchiyama (2009). "The MAP1-LC3 conjugation system is involved in lipid droplet formation." Biochem Biophys Res Commun **382**(2): 419-423.

Shibata, M., K. Yoshimura, H. Tamura, T. Ueno, T. Nishimura, T. Inoue, M. Sasaki, M. Koike, H. Arai, E. Kominami and Y. Uchiyama (2010). "LC3, a microtubule-associated protein1A/B light chain3, is involved in cytoplasmic lipid droplet formation." Biochem Biophys Res Commun **393**(2): 274-279.

Shimokawa, H. and A. Takeshita (2005). "Rho-kinase is an important therapeutic target in cardiovascular medicine." Arterioscler Thromb Vasc Biol **25**(9): 1767-1775.

Shimomura, H., F. Terasaki, T. Hayashi, Y. Kitaura, T. Isomura and H. Suma (2001). "Autophagic degeneration as a possible mechanism of myocardial cell death in dilated cardiomyopathy." Jpn Circ J **65**(11): 965-968.

Simpson, M. A., S. Mansour, D. Ahnood, K. Kalidas, M. A. Patton, W. J. McKenna, E. R. Behr and A. H. Crosby (2009). "Homozygous mutation of desmocollin-2 in arrhythmogenic right ventricular cardiomyopathy with mild palmoplantar keratoderma and woolly hair." Cardiology **113**(1): 28-34.

Siragam, V., X. Cui, S. Masse, C. Ackerley, S. Aafaqi, L. Strandberg, M. Tropak, M. D. Fridman, K. Nanthakumar, J. Liu, Y. Sun, B. Su, C. Wang, X. Liu, Y. Yan, A. Mendlowitz and R. M. Hamilton (2014). "TMEM43 mutation p.S358L alters intercalated disc protein expression and reduces conduction velocity in arrhythmogenic right ventricular cardiomyopathy." PLoS One **9**(10): e109128.

Smith, E. A. and E. Fuchs (1998). "Defining the interactions between intermediate filaments and desmosomes." J Cell Biol **141**(5): 1229-1241.

Sommariva, E., S. Brambilla, C. Carbucicchio, E. Gambini, V. Meraviglia, A. Dello Russo, F. M. Farina, M. Casella, V. Catto, G. Pontone, M. Chiesa, I. Stadiotti, E. Cogliati, A. Paolin, N. Ouali Alami, C. Preziuso, G. d'Amati, G. I. Colombo, A. Rossini, M.

C. Capogrossi, C. Tondo and G. Pompilio (2016). "Cardiac mesenchymal stromal cells are a source of adipocytes in arrhythmogenic cardiomyopathy." Eur Heart J **37**(23): 1835-1846.

Spencer, J. A., S. Eliazer, R. L. Ilaria, Jr., J. A. Richardson and E. N. Olson (2000). "Regulation of microtubule dynamics and myogenic differentiation by MURF, a striated muscle RING-finger protein." J Cell Biol **150**(4): 771-784.

Sprecher, E., A. Ishida-Yamamoto, M. Mizrahi-Koren, D. Rapaport, D. Goldsher, M. Indelman, O. Topaz, I. Chefetz, H. Keren, J. O'Brien T, D. Bercovich, S. Shalev, D. Geiger, R. Bergman, M. Horowitz and H. Mandel (2005). "A mutation in SNAP29, coding for a SNARE protein involved in intracellular trafficking, causes a novel neurocutaneous syndrome characterized by cerebral dysgenesis, neuropathy, ichthyosis, and palmoplantar keratoderma." Am J Hum Genet **77**(2): 242-251.

Su, H. and X. Wang (2010). "The ubiquitin-proteasome system in cardiac proteinopathy: a quality control perspective." Cardiovasc Res **85**(2): 253-262.

Su, Q., S. Mochida, J. H. Tian, R. Mehta and Z. H. Sheng (2001). "SNAP-29: a general SNARE protein that inhibits SNARE disassembly and is implicated in synaptic transmission." Proc Natl Acad Sci U S A **98**(24): 14038-14043.

Su, V. and A. F. Lau (2012). "Ubiquitination, intracellular trafficking, and degradation of connexins." Arch Biochem Biophys **524**(1): 16-22.

Tabib, A., R. Loire, L. Chalabreysse, D. Meyronnet, A. Miras, D. Malicier, F. Thivolet, P. Chevalier and P. Bouvagnet (2003). "Circumstances of death and gross and microscopic observations in a series of 200 cases of sudden death associated with arrhythmogenic right ventricular cardiomyopathy and/or dysplasia." Circulation **108**(24): 3000-3005.

Tabib, A., A. Miras, P. Taniere and R. Loire (1999). "Undetected cardiac lesions cause unexpected sudden cardiac death during occasional sport activity. A report of 80 cases." Eur Heart J **20**(12): 900-903.

Takahashi, M., Y. Tajika, A. F. Khairani, H. Ueno, T. Murakami and H. Yorifuji (2013). "The localization of VAMP5 in skeletal and cardiac muscle." Histochem Cell Biol **139**(4): 573-582.

Takats, S., P. Nagy, A. Varga, K. Pircs, M. Karpati, K. Varga, A. L. Kovacs, K. Hegedus and G. Juhasz (2013). "Autophagosomal Syntaxin17-dependent lysosomal degradation maintains neuronal function in Drosophila." J Cell Biol **201**(4): 531-539.

Tanaka, Y., G. Guhde, A. Suter, E. L. Eskelinen, D. Hartmann, R. Lullmann-Rauch, P. M. Janssen, J. Blanz, K. von Figura and P. Saftig (2000). "Accumulation of autophagic vacuoles and cardiomyopathy in LAMP-2-deficient mice." Nature **406**(6798): 902-906.

Tannous, P., H. Zhu, J. L. Johnstone, J. M. Shelton, N. S. Rajasekaran, I. J. Benjamin, L. Nguyen, R. D. Gerard, B. Levine, B. A. Rothermel and J. A. Hill (2008). "Autophagy is an adaptive response in desmin-related cardiomyopathy." Proc Natl Acad Sci U S A **105**(28): 9745-9750.

Taylor, M., S. Graw, G. Sinagra, C. Barnes, D. Slavov, F. Brun, B. Pinamonti, E. E. Salcedo, W. Sauer, S. Pyxaras, B. Anderson, B. Simon, J. Bogomolovas, S. Labeit, H. Granzier and L. Mestroni (2011). "Genetic variation in titin in arrhythmogenic right ventricular cardiomyopathy-overlap syndromes." Circulation **124**(8): 876-885.

Te Riele, A. S., E. Agullo-Pascual, C. A. James, A. Leo-Macias, M. Cerrone, M. Zhang, X. Lin, B. Lin, N. L. Sobreira, N. Amat-Alarcon, R. F. Marsman, B. Murray, C. Tichnell, J. F. van der Heijden, D. Dooijes, T. A. van Veen, H. Tandri, S. J. Fowler, R. N. Hauer, G. Tomaselli, M. P. van den Berg, M. R. Taylor, F. Brun, G. Sinagra, A. A. Wilde, L. Mestroni, C. R. Bezzina, H. Calkins, J. Peter van Tintelen, L. Bu, M. Delmar and D. P. Judge (2017). "Multilevel analyses of SCN5A mutations in arrhythmogenic right ventricular dysplasia/cardiomyopathy suggest non-canonical mechanisms for disease pathogenesis." Cardiovasc Res **113**(1): 102-111.

Te Riele, A. S., A. Bhonsale, J. R. Burt, S. L. Zimmerman and H. Tandri (2012). "Genotype-specific pattern of LV involvement in ARVD/C." JACC Cardiovasc Imaging **5**(8): 849-851.

Thiene, G., D. Corrado and C. Basso (2007). "Arrhythmogenic right ventricular cardiomyopathy/dysplasia." Orphanet J Rare Dis **2**: 45.

Tian, Z., H. Zheng, J. Li, Y. Li, H. Su and X. Wang (2012). "Genetically induced moderate inhibition of the proteasome in cardiomyocytes exacerbates myocardial ischemia-reperfusion injury in mice." Circ Res **111**(5): 532-542.

Tiso, N., D. A. Stephan, A. Nava, A. Bagattin, J. M. Devaney, F. Stanchi, G. Larderet, B. Brahmbhatt, K. Brown, B. Bauce, M. Muriago, C. Basso, G. Thiene, G. A. Danieli and A. Rampazzo (2001). "Identification of mutations in the cardiac ryanodine receptor gene in families affected with arrhythmogenic right ventricular cardiomyopathy type 2 (ARVD2)." Hum Mol Genet **10**(3): 189-194.

Toyofuku, T., M. Yabuki, K. Otsu, T. Kuzuya, M. Hori and M. Tada (1998). "Direct association of the gap junction protein connexin-43 with ZO-1 in cardiac myocytes." J Biol Chem **273**(21): 12725-12731.

Uzumcu, A., E. E. Norgett, A. Dindar, O. Uyguner, K. Nisli, H. Kayserili, S. E. Sahin, E. Dupont, N. J. Severs, I. M. Leigh, M. Yuksel-Apak, D. P. Kelsell and B. Wollnik (2006). "Loss of desmoplakin isoform I causes early onset cardiomyopathy and heart failure in a Naxos-like syndrome." J Med Genet **43**(2): e5.

van der Zwaag, P. A., I. A. van Rijsingen, A. Asimaki, J. D. Jongbloed, D. J. van Veldhuisen, A. C. Wiesfeld, M. G. Cox, L. T. van Lochem, R. A. de Boer, R. M. Hofstra, I. Christiaans, K. Y. van Spaendonck-Zwarts, R. H. Lekanne dit Deprez, D. P. Judge, H. Calkins, A. J. Suurmeijer, R. N. Hauer, J. E. Saffitz, A. A. Wilde, M. P. van den Berg and J. P. van Tintelen (2012). "Phospholamban R14del mutation in patients diagnosed with dilated cardiomyopathy or arrhythmogenic right ventricular cardiomyopathy: evidence supporting the concept of arrhythmogenic cardiomyopathy." Eur J Heart Fail **14**(11): 1199-1207.

van Hengel, J., M. Calore, B. Bauce, E. Dazzo, E. Mazzotti, M. De Bortoli, A. Lorenzon, I. E. Li Mura, G. Beffagna, I. Rigato, M. Vleeschouwers, K. Tyberghein, P. Hulpiau, E. van Hamme, T. Zaglia, D. Corrado, C. Basso, G. Thiene, L. Daliento, A. Nava, F. van Roy and A. Rampazzo (2013). "Mutations in the area composita protein alphaT-catenin are associated with arrhythmogenic right ventricular cardiomyopathy." Eur Heart J **34**(3): 201-210.

van Opbergen, C. J., M. Delmar and T. A. van Veen (2017). "Potential new mechanisms of pro-arrhythmia in arrhythmogenic cardiomyopathy: focus on calcium sensitive pathways." Neth Heart J **25**(3): 157-169.

Walter, M. C., P. Reilich, A. Huebner, D. Fischer, R. Schroder, M. Vorgerd, W. Kress, C. Born, B. G. Schoser, K. H. Krause, U. Klutzny, S. Bulst, J. R. Frey and H. Lochmuller (2007). "Scapuloperoneal syndrome type Kaeser and a wide phenotypic spectrum of adult-onset, dominant myopathies are associated with the desmin mutation R350P." Brain **130**(Pt 6): 1485-1496.

Wang, Q., T. L. Lu, E. Adams, J. L. Lin and J. J. Lin (2013). "Intercalated disc protein, mXinalpha, suppresses p120-catenin-induced branching phenotype via its interactions with p120-catenin and cortactin." Arch Biochem Biophys **535**(1): 91-100.

Wang, Y., W. Sun, B. Du, X. Miao, Y. Bai, Y. Xin, Y. Tan, W. Cui, B. Liu, T. Cui, P. N. Epstein, Y. Fu and L. Cai (2013). "Therapeutic effect of MG-132 on diabetic cardiomyopathy is associated with its suppression of proteasomal activities: roles of Nrf2 and NF-kappaB." Am J Physiol Heart Circ Physiol **304**(4): H567-578.

Witt, C. C., S. H. Witt, S. Lerche, D. Labeit, W. Back and S. Labeit (2008). "Cooperative control of striated muscle mass and metabolism by MuRF1 and MuRF2." EMBO J **27**(2): 350-360.

Witt, S. H., H. Granzier, C. C. Witt and S. Labeit (2005). "MURF-1 and MURF-2 target a specific subset of myofibrillar proteins redundantly: towards understanding MURF-dependent muscle ubiquitination." J Mol Biol **350**(4): 713-722.

Wong, A. R., N. AbdurRazak, S. M. Al-Hadlaq and A. S. Al-Jarallah (2008). "Arrhythmogenic right ventricular cardiomyopathy in an 11-year-old girl and typical echocardiographic features." Pediatr Cardiol **29**(2): 427-430.

Wong, S. H., Y. Xu, T. Zhang, G. Griffiths, S. L. Lowe, V. N. Subramaniam, K. T. Seow and W. Hong (1999). "GS32, a novel Golgi SNARE of 32 kDa, interacts preferentially with syntaxin 6." Mol Biol Cell **10**(1): 119-134.

Wu, G., G. Xu, B. A. Schulman, P. D. Jeffrey, J. W. Harper and N. P. Pavletich (2003). "Structure of a beta-TrCP1-Skp1-beta-catenin complex: destruction motif binding and lysine specificity of the SCF(beta-TrCP1) ubiquitin ligase." Mol Cell **11**(6): 1445-1456.

Yan, L., D. E. Vatner, S. J. Kim, H. Ge, M. Masurekar, W. H. Massover, G. Yang, Y. Matsui, J. Sadoshima and S. F. Vatner (2005). "Autophagy in chronically ischemic myocardium." Proc Natl Acad Sci U S A **102**(39): 13807-13812.

Yang, Z., N. E. Bowles, S. E. Scherer, M. D. Taylor, D. L. Kearney, S. Ge, V. V. Nadvoretskiy, G. DeFreitas, B. Carabello, L. I. Brandon, L. M. Godsel, K. J. Green, J. E. Saffitz, H. Li, G. A. Danieli, H. Calkins, F. Marcus and J. A. Towbin (2006). "Desmosomal dysfunction due to mutations in desmoplakin causes arrhythmogenic right ventricular dysplasia/cardiomyopathy." Circ Res **99**(6): 646-655.

Yano, M., T. Yamamoto, S. Kobayashi and M. Matsuzaki (2009). "Role of ryanodine receptor as a Ca(2)(+) regulatory center in normal and failing hearts." J Cardiol **53**(1): 1-7.

Yla-Anttila, P., E. Mikkonen, K. E. Happonen, P. Holland, T. Ueno, A. Simonsen and E. L. Eskelinen (2015). "RAB24 facilitates clearance of autophagic compartments during basal conditions." Autophagy **11**(10): 1833-1848.

Zanella, F. and F. Sheikh (2016). "Patient-Specific Induced Pluripotent Stem Cell Models: Generation and Characterization of Cardiac Cells." Methods Mol Biol **1353**: 147-162.

Zhang, Z., M. J. Stroud, J. Zhang, X. Fang, K. Ouyang, K. Kimura, Y. Mu, N. D. Dalton, Y. Gu, W. H. Bradford, K. L. Peterson, H. Cheng, X. Zhou and J. Chen (2015). "Normalization of Naxos plakoglobin levels restores cardiac function in mice." J Clin Invest **125**(4): 1708-1712.

Zhou, X., M. Chen, H. Song, B. Wang, H. Chen, J. Wang, W. Wang, S. Feng, F. Zhang, W. Ju, M. Li, K. Gu, K. Cao, D. W. Wang and B. Yang (2015). "Comprehensive analysis of desmosomal gene mutations in Han Chinese patients with arrhythmogenic right ventricular cardiomyopathy." Eur J Med Genet **58**(4): 258-265.

Zhu, H., P. Tannous, J. L. Johnstone, Y. Kong, J. M. Shelton, J. A. Richardson, V. Le, B. Levine, B. A. Rothermel and J. A. Hill (2007). "Cardiac autophagy is a maladaptive response to hemodynamic stress." J Clin Invest **117**(7): 1782-1793.